Role of atmospheric teleconnection processes in the observed relationship between the Atlantic Multidecadal Oscillation and Indian summer monsoon

A thesis

submitted in partial fulfilment of

the requirements for

the Degree of

Doctor of Philosophy

By

Arijeet Dutta

(ID: 20173542)

Department of Earth and Climate Science

Indian Institute of Science Education and Research (IISER),

Pune, India – 411008

Dedicated to
my late parents

CERTIFICATE

This is to certify that the work incorporated in the thesis entitled "Role of atmospheric teleconnection process in the observed relationship between the Atlantic Multidecadal Oscillation and Indian summer monsoon" submitted by Arijeet Dutta has been carried out by the candidate under the supervision of Dr. Neena Joseph Mani, Assistant Professor, Department of Earth and Climate Science, IISER Pune during the academic year 2017-2023. The work presented here or any part of it has not been included in any other thesis submitted previously for the award of any degree or diploma from any other university or institution.

Signature of Thesis Supervisor
Dr. Neena J Mani
Assistant Professor
Department of Earth and Climate Science
IISER Pune – 411008

Dated: 24th July 2023

DECLARATION

I hereby declare that the work embodied in the thesis entitled "Role of atmospheric teleconnection process in the observed relationship between the Atlantic Multidecadal Oscillation and Indian summer monsoon" represents my ideas in my own words and the experimental results carried out by me and where others' ideas have been included, I have adequately cited and referenced the sources. I also declare that I have adhered to all academic honesty and integrity principles and have not misrepresented, fabricated, or falsified any idea/data/fact/source in my submission. I understand that violation of the above will cause disciplinary action by the Institute and can also evoke penal action from the sources which have thus not been appropriately cited or from whom proper permission has not been taken when needed.

Signature of the student

Dated: 24th July 2023

Mr. Arijeet Dutta
Department of Earth and Climate Science
ID no. – 20173542
IISER Pune – 411008

Acknowledgment

First, I would like to convey my heartfelt gratitude to my supervisor Dr. Neena Joseph Mani. Her scientific temperament and ethical values will always inspire me. I was given complete freedom to develop and execute my own ideas, for which I am grateful to her. Apart from our scientific discussions, I learned a great deal about life in general and I thank her for that. I must also thank Dr. Suhas Ettammal for his constant support, insightful suggestions, and scholarly criticisms throughout the course of my Ph.D. I should also mention my lab mates Daniel and Pratiksha who cheerfully took the pain to listen to my mock talks and always helped me to improve. I must thank Dr Rahul Sivankutty who helped me a lot during my early days at IISER. I would like to thank my RAC member, Prof. Chandrasekar, for providing constructive feedback and suggestions during annual meetings. I would like to convey my regards to the present and past directors of IISER Pune, for providing world-class facilities. I wish to thank the academic staff of IISER. I am thankful to everyone in the ECS department at IISER. I made a lot of good friends in ECS and I will forever cherish the time spent with them. I am also grateful to my funding agency DST-INSPIRE.

I met many wonderful people after coming to IISER and I feel happy to call them my friends. I was fortunate to learn from people with varied interests like music, painting, cinema, food, and many more. I can't thank them enough for their immense impact on my life and thoughts.

Finally, I cannot convey my gratitude to my late parents in words. I learned a great deal from them, and I miss them dearly. My Ph.D. would not be a reality without the support of my amazing elder brother, Abhisek, who helped me to believe in myself. I am grateful to Dr. Somdeb Mitra, Dr. Pradip Gupta, Dipanwita, Anusree di, Pablo and Mr. Amyt Datta who helped me to love myself. This "acknowledgment" is in no way conclusive and there are many people I am grateful to whom I failed to mention here. I wish them well.

Arijeet Dutta

Table of contents

	Thesis Abstract	**1-3**
Chapter 1	**Introduction**	**4-16**
1.1	Multidecadal variability of the Indian summer monsoon (ISM)	5-7
1.2	The Atlantic multi-decadal oscillation (AMO)	8-10
1.3	Observed relationship between AMO and ISM	11-13
1.3.1	Mechanistic understanding	13-15
1.4	Aim and Scope of the Thesis	15-16
Chapter 2	**Investigating the AMO-ISM teleconnection pathways in global climate model simulations**	**17-45**
	Abstract	18
2.1	Introduction	18-21
2.2	Data and methodology	21-23
2.3	Results	24-43
2.3.1	ISM in models	24-28
2.3.2	AMO in models	28-31
2.3.3	AMO-ISM teleconnection	31-43
2.4	Conclusion	43-45
Chapter 3	**Role of upper-tropospheric circulation anomalies in the observed AMO-ISM relationship**	**46-69**
	Abstract	47
3.1	Introduction	47-50
3.2	Data and methodology	50-52
3.2.1	Model	52
3.3	Results	53-65
3.3.1	Midlatitude-ISM link	53-56
3.3.2	Circulation response to ISM heating	56-57
3.3.3	ISM feedback on WCA anomalies	58-60
3.3.4	Impact of AMO on circulation anomalies over WCA	60-65
3.4	Summary	65-66
	Supplementary figures	67-69

Chapter 4	**AMO induced Pacific variability and its impact on ISM**	**70-85**
	Abstract	71
4.1	Introduction	71-73
4.2	Data and methodology	73-75
4.2.1	Model experiments	73-75
4.2.2	Mass streamfunction	75
4.3	Results	76-84
4.3.1	ISM response in pacemaker experiments	76-77
4.3.2	Equatorial Pacific atmospheric bridge	77-79
4.3.3	North Pacific atmospheric bridge	79-81
4.3.4	Delayed Pacific response and AMO-ISM lagged relationship	81-84
4.4	Summary	85
Chapter 5	**Thesis summary**	**86-87**
	Bibliography	88-101
	List of publications	102
	Rights and permission	103

Abstract

The Indian summer monsoon (ISM) exhibits considerable variance in the multi-decadal timescales in observational and paleoclimate proxy records. The summer-mean all-India rainfall exhibits multidecadal fluctuations remaining periodically above the long-term mean for several decades followed by periods when it is below the long-term mean. The multidecadal variance of monsoon is generally attributed to the multidecadal variability over the Atlantic - the Atlantic multi-decadal Oscillation (AMO). Though a robust relationship between the two is observed in the instrumental records, with the limited span of observational records we can capture only two cycles of AMO and the AMO-ISM relationship is inconsistent among the paleoclimate proxy records. While several hypotheses have been put forth to explain the observed relationship, several questions remain with respect to the robustness of the AMO-ISM relationship and the teleconnection pathways. In this thesis, I revisit the AMO-ISM relationship and try to understand the underlying large-scale atmospheric teleconnection processes which connect these climate modes. A combination of observational and hierarchical modelling approaches using intermediate complexity models and long simulations from state-of-the-art global climate models (GCM) were used to infer the observed AMO-ISM relationship.

The first question addressed is understanding how well the proposed modes of AMO-ISM teleconnection are represented in current generation GCM simulations. Last millennium simulations from the Climate Model Intercomparison Project/Paleoclimate Model Intercomparison Project (CMIP5/PMIP3) were analyzed to examine two broad atmospheric teleconnection mechanisms which connect the Atlantic and the ISM. AMO-induced Pacific Ocean variability and associated changes in Walker circulation are found to be robust in different model simulations. However, the models are found to exhibit considerable disagreement in the upper-tropospheric planetary wave response to AMO and the associated impact it can have on the ISM. The study highlights the strength and deficiencies of current climate models in simulating the teleconnection processes which control the decadal and longer-term variability of monsoon and is of great value as these models are also used for future climate projections.

The second question addressed is how the planetary wave responses to AMO modulates the ISM. SST anomalies over the extratropical North Atlantic can drive vortices with equivalent barotropic vertical structures. Idealized model experiments indeed show that equivalent barotropic Rossby wave response across the Euro-Atlantic sector can reach west central Asia (WCA). Upper-level circulation anomalies associated with the Rossby waves over WCA impact ISM through anomalous tropospheric temperature and easterly shear. The study demonstrates significant modulation of WCA anomalies by the AMO in the multi-decadal time scale. It is also found that the observed out-of-phase relationship between AMO and ISM in the recent decades, may be attributed to the anomalous equivalent barotropic responses to the relatively stronger high latitude warming over the North Atlantic during the recent AMO warm phase which altered the entire downstream teleconnection pattern producing cyclonic anomalies over WCA and in turn weaken the ISM.

The third central question addressed is the relative roles of the equatorial and extratropical North Pacific in the observed AMO-ISM relationship. Simple model experiments with an intermediate complexity GCM highlight the vital role played by the Pacific Ocean in the AMO-ISM relationship, in agreement with the more comprehensive GCM simulations. In response to the warm North Atlantic, the equatorial Pacific is found to constrain the Walker circulation resulting in enhanced low-level convergence over India. The North Pacific contribution is found to be weak during summer. Analysis of observational records shows a strong lagged AMO-ISM relationship consistent with the development of a strong meridional gradient in SST over the Pacific Ocean. Further sensitivity experiments are carried out with prescribed forcing confined over tropical and extratropical North Atlantic. Results suggest tropical North Atlantic is the critical driver of the lagged response.

Chapter 1

Introduction

1.1 Multidecadal variability of the Indian summer monsoon

The ISM is one of the leading modes of tropical climate variability; about a third of the global population depends on its hydroclimate variability (Gadgil and Gadgil 2006). ISM contributes to about 70-80% of the annual rainfall over India (Parthasarathy et al. 1993, 1994) and exhibits variability in timescales ranging from intra-seasonal to centennial and longer. Figure 1.1 brings out the interannual and multidecadal availability of ISM during the last century. The all-India rainfall data was obtained from IITM (https://tropmet.res.in/static_pages.php?page_id=53). The multidecadal variability of monsoon is robust and is also evident in paleoclimate reconstructions from different parts of the monsoon domain (Burns et al. 2002; Sinha et al. 2007, 2011; Berkelhammer et al. 2010; Goswami et al. 2016). It is expected that the low-frequency variability of ISM modulates the interannual variability (thin curve) of ISM (Goswami 2006). Hence, understanding the multi-decadal variability of ISM has substantial implications for the seasonal prediction of ISM and hence has great social relevance. Understanding the multi-decadal variability of ISM also has powerful implications in climate change studies and decadal climate predictions of monsoon. The decadal and longer-term variability of monsoon can arise from external forcings as well as internal climate dynamics. External climate forcings like changes in solar irradiance and volcanic activity are known to modulate the monsoon variability in multidecadal timescales (Agnihotri et al. 2002; Bhattacharyya and Narasimha 2005; Bollasina et al. 2011; Fadnavis et al. 2021). The unprecedented rise in atmospheric CO2 concentration coming from human activity and the resulting warming has a significant impact on the monsoon (Wang et al. 2005; Seth et al. 2019; Katzenberger et al. 2021) and the anthropogenic forcing is another factor that should be considered when studying the long-term variability of ISM. A considerable amount of ISM variability in the decadal and longer timescale also arises from

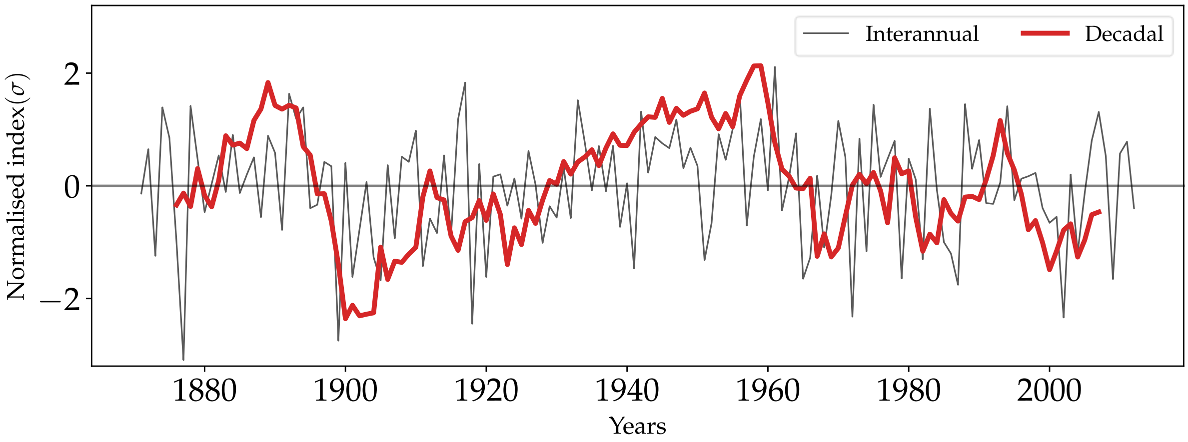

Figure 1.1 Normalised timeseries of the unfiltered (black) and 11-year running mean (red) seasonal (June to September) mean all India rainfall anomaly; rainfall dataset was obtained from Indian Institute of Tropical Meteorology

the ocean-atmosphere-land interactions that are inherent to the climate system. While the ISM is mainly triggered by the interhemispheric pressure gradient between the Indian subcontinent and the southern Indian Ocean, the climate variability over the other ocean basins also influences its variability and predictability. Figure 1.2 shows that during the instrumental period, the multi-decadal variability of ISM is strongly correlated with the multidecadal variability of sea surface temperature (SST) anomalies over different ocean basins. The SST anomalies resemble the well-studied climate modes over these ocean basins. The internal variability associated with the low-frequency climate modes over the Atlantic and Pacific Oceans is known to play a major role in modulating the ISM multidecadal variability (e.g., Krishnan and Sugi 2003; Zhang and Delworth 2006). Remote impacts from the climate modes over the Pacific and Atlantic oceans are observed to have a strong linkage with the ISM variability in the interannual and longer timescales. The canonical El Nino Southern Oscillation (ENSO) – ISM relationship, perhaps one of the most well-studied tropical teleconnections, is a classic example.

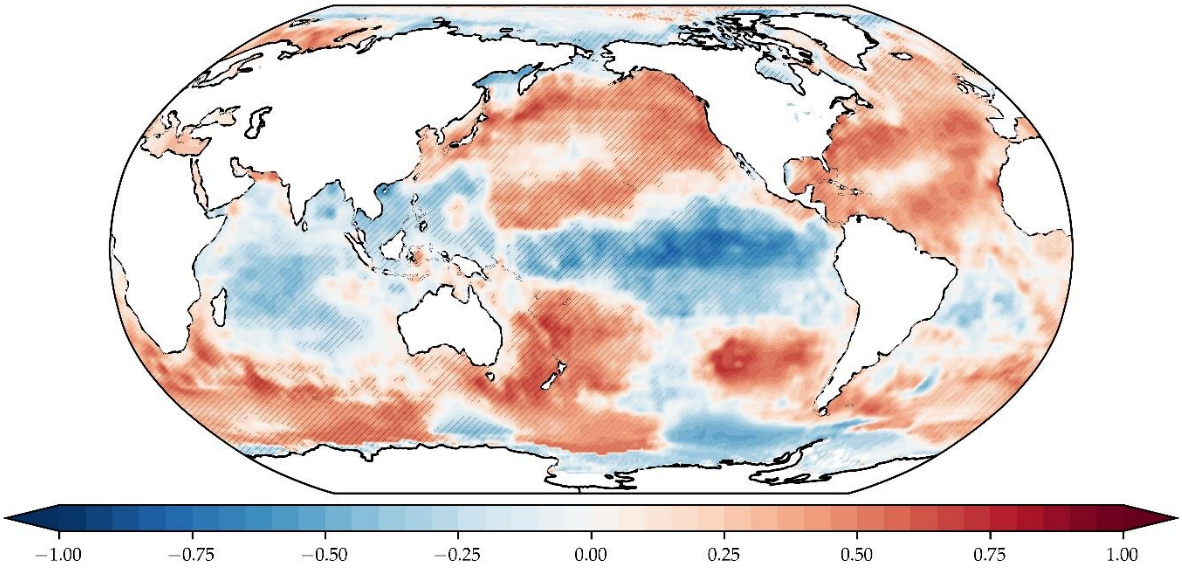

Figure 1.2 Global anomalies of SST associated with ISM: 11-year running mean June-Sept seasonal anomalies of SST correlated with an 11-year running mean ISM rainfall (ISMR); regions with statistically significant correlation are hatched

The major multidecadal mode observed over the Pacific Ocean, namely the Pacific Decadal Oscillation (PDO) (Mantua et al. 1997) has a periodicity of around 30-50 years (Deser et al. 2010) and it exhibits an inverse relationship with the ISM variability (Krishnan and Sugi 2003; Krishnamurthy and Krishnamurthy 2014; Joshi and Kucharski 2017; Huang et al. 2020). In timescales spanning several decades, variability over the North Atlantic Ocean has a significant impact on ISM. The coherent ocean-atmosphere coupled variability over the North Atlantic basin, the Atlantic Multidecadal oscillation (AMO) (Bjerknes 1964; Delworth and Mann 2000; Enfield et al. 2001; Knight et al. 2005), exhibits an in-phase relationship with the ISM multidecadal variability. It exhibits a periodicity of about 60-80 years in the instrumental records and paleoclimate reconstructions (Schlesinger and Ramankutty 1994; Gray et al. 2004a; Parker et al. 2007; Tung and Zhou 2013; Naidu et al. 2020).

1.2 Atlantic multi-decadal oscillation (AMO)

AMO is considered to be the leading mode of SST variability over the North Atlantic Ocean (Dijkstra et al. 2006; Álvarez-García et al. 2008; Zhang et al. 2019) and is thought to be the driver of global scale multi-decadal variability with a significant imprint on other ocean basins (Yang et al. 2020; Joshi et al. 2022). Observational records show a 60-80 years periodicity associated with the AMO (Schlesinger and Ramankutty 1994). The spatial pattern of AMO is characterized by warming/cooling anomalies over the North Atlantic and opposite sign anomalies over the South Atlantic. The anomalies over North Atlantic are much stronger than those over the South Atlantic (Folland et al. 1986). The AMO index is usually defined as the detrended (or global mean removed) SST anomalies area averaged over the North Atlantic domain (75°W -5°E, 0-60°N) (Enfield et al. 2001; Trenberth and Shea 2006). Figure 1.3 shows the AMO index in the instrumental record. It clearly shows strong multi-decadal variability in North Atlantic SST during the past 150 years.

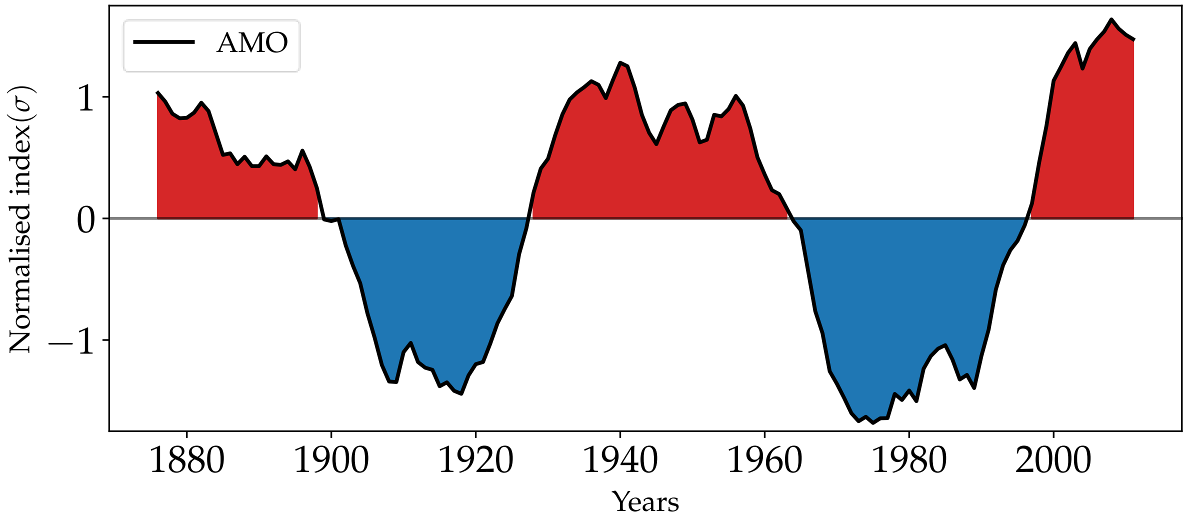

Figure 1.3 11-year running mean AMO index from HadISST data (Rayner et al. 2003)

Figure 1.4 shows the spatial pattern associated with the AMO. Concentrated warming can be seen in the high latitudes whereas the warming is somewhat modest over the lower latitudes over the North Atlantic.

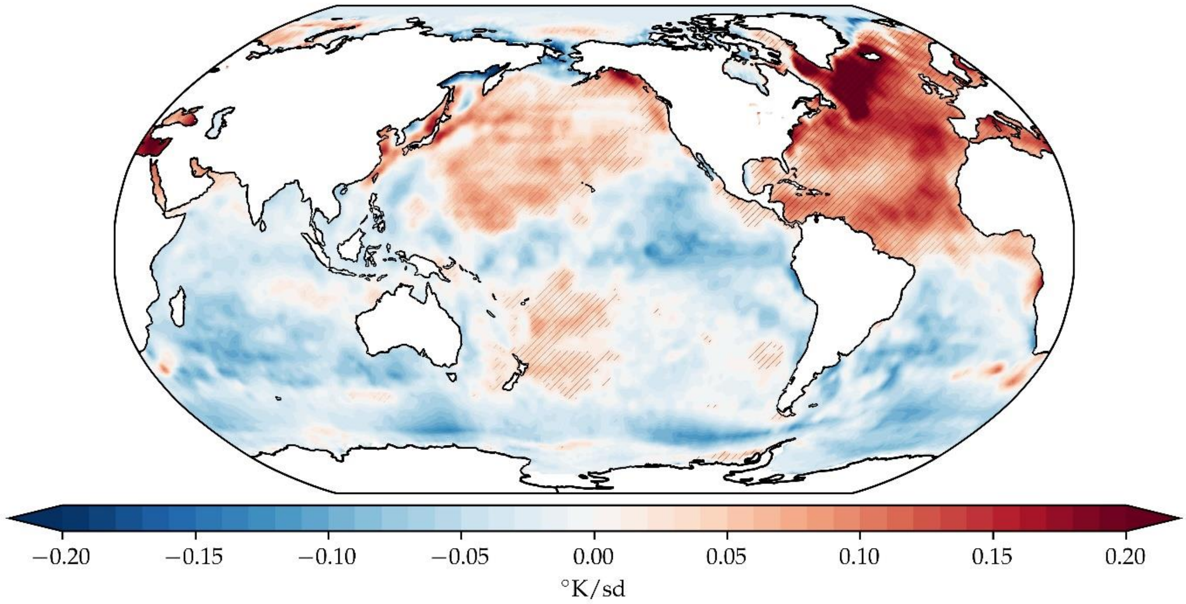

Figure 1.4 SST anomalies associated with AMO: 11-year running mean SST anomalies regressed on the normalized AMO index; regions with statistically significant regression coefficients (based on Student t-test) are hatched

The general consensus in the literature is that AMO might be the surface manifestation of the Atlantic Meridional Overturning Circulation (AMOC). Anomalous meridional heat transport by AMOC is assumed to be the leading contributor to AMO (Zhang et al. 2019 and references therein). Model simulations indicate that the AMO-related anomalies of SST and upper-ocean heat content over the subpolar North Atlantic are primarily driven by the multi-decadal variability of AMOC (Knight et al. 2005; Danabasoglu et al. 2012; Wills et al. 2019). Stochastic atmospheric forcing arising from the extratropical atmosphere over the North Atlantic (Feldstein 2000) can also induce the low-frequency variability associated with AMO (Clement et al. 2015; Cane et al. 2017). Atmospheric general circulation models (AGCM) coupled with slab ocean models (no ocean currents) tend to capture the AMO. The simulated North Atlantic warming was essentially found to be driven by the midaltitude atmospheric forcing which resembles the North Atlantic Oscillation (NAO). External natural and anthropogenic forcing can also contribute to such low-frequency climate variability (Otterå et al. 2010; Booth et al. 2012; Bellucci et al. 2017; Bellomo et al. 2018; Mann et al. 2020, 2022). Hence, during the instrumental period, the multi-decadal variability over North Atlantic can be understood as a combination of both internal climate dynamics and external forcing and it is a challenge to quantify the relative contributions (Vecchi et al. 2017). Nevertheless, there's ample evidence from paleoclimate proxy records that indicate that the AMO is an internal mode of climate variability (Gray et al. 2004a; Shanahan et al. 2009; Mann et al. 2009; Wang et al. 2011, 2017a; Knudsen et al. 2014).

AMO has a significant impact across the global oceans (Figure 1.4). A positive association between the AMO and the SST anomalies over the North Pacific basin is observed. However, the SST anomalies over the equatorial eastern Pacific and Indian Ocean show a strong negative association with the AMO. This widespread teleconnection between the AMO and the global SST anomalies have been reported in numerous studies (Zhang and Delworth 2007; Sun et al. 2017, 2019; Gong et al. 2020; Johnson et al. 2020a; Ahmad et al. 2022). The AMO is also known to impact many other important regional climate features across the globe, viz., shift in Intertropical Convergence Zone (ITCZ), rainfall anomalies over India and Sahel, summer climate over Europe and North America, Atlantic hurricane activity, etc. (Folland et al. 1986; Zhang and Delworth 2006; Sutton and Hodson 2007). Numerous studies have suggested that the AMO and the associated climate anomalies are potentially predictable (e.g., Hermanson et al. 2014; Msadek et al. 2014; Yeager and Robson 2017; Zhang 2017). This has important implications for decadal to multi-decadal climate prediction and socio-economic planning.

1.3 Observed relationship between AMO and ISM

AMO has a significant bearing on the variability of the Indian summer monsoon (Goswami et al. 2006; Zhang and Delworth 2006; Svendsen 2021). Observational datasets covering the last 150 years show a positive association between the AMO and ISM (Figure 1.5) until recently when there seems to be an out-of-phase relationship (Sandeep et al. 2022). In fact, in decades when AMO is in a positive (negative) or warm (cold) phase, more frequent years of above (below) normal ISMR is observed. Positive phase AMO is known to cause a northward shift in the ITCZ resulting in large rainfall anomalies over the Sahel and Indian

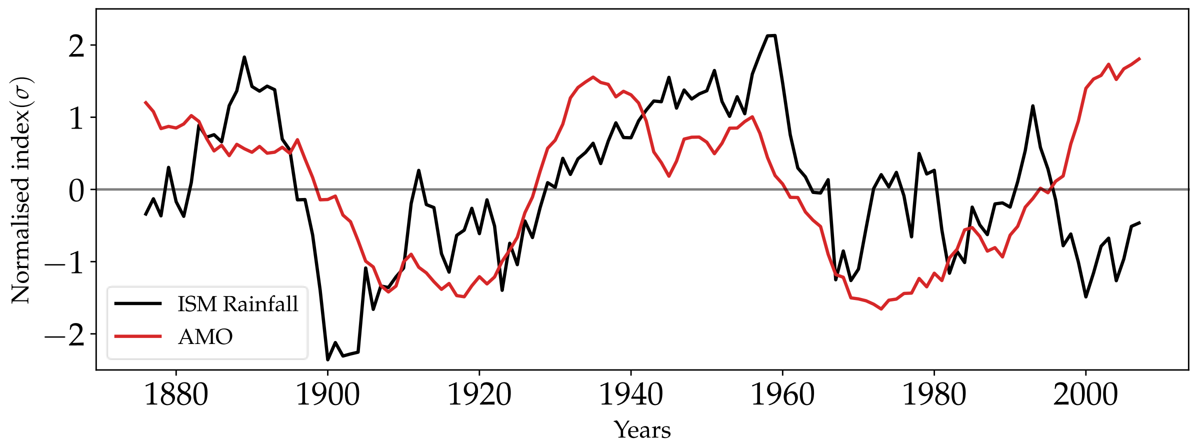

Figure 1.5 11-year running mean normalized timeseries of AMO index and ISMR.

monsoon regions (Zhang and Delworth 2006; Knight et al. 2006; Sutton and Hodson 2007; Monerie et al. 2019). Figure 1.6 shows this positive association with rainfall anomalies over the African and Indian monsoon domains.

The robustness of the observed AMO-ISM relationship has been explored using paleoclimate proxy records. Such studies are crucial to understanding the nature of the AMO-ISM relationship. Given its large periodicity, observational datasets can hardly capture a couple

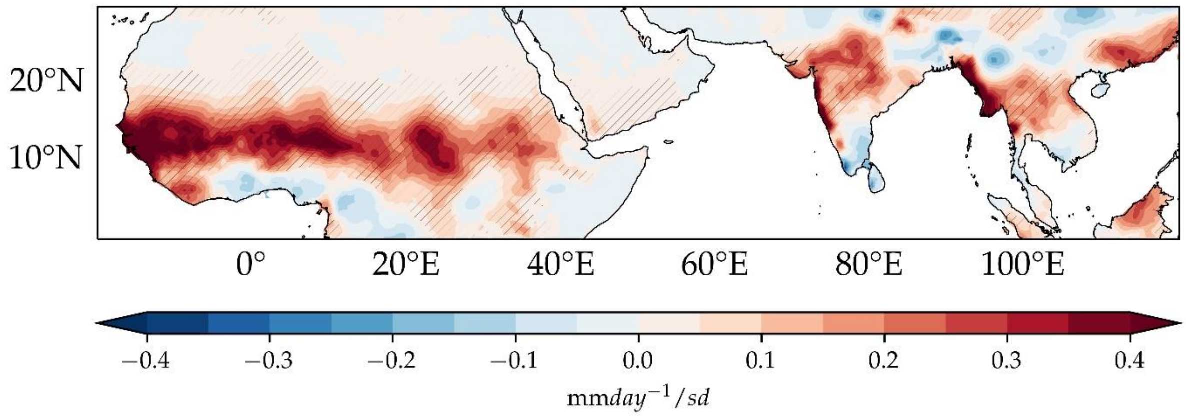

Figure 1.6 11-year running mean June-Sept rainfall anomalies regressed on normalized AMO index.

of cycles of AMO. Paleoclimate records have been used to infer if the observed relationship is an externally forced feature or a natural mode of climate variability. In a recent study by Naidu et al. (2020), reconstructions of SST and sea surface salinity were used to show that the AMO-ISM relationship has been robust during the last two millennia. Statistical analysis of Goswami et al. (2016), shows the presence of coherent multi-decadal variability in proxy records of ISM and North Atlantic SST during the last 500 years. Paleoclimate studies however bring out diverse interpretations of the AMO-ISM relationship. Independent monsoon reconstructions for the past two millennia based on Dandak cave speleothem (Berkelhammer et al. 2010) and Bay of Bengal sediment cores (Naidu et al. 2020) largely attribute the ISM multidecadal variability to AMO. Feng and Hu (2008) analyzed the proxies of ISM, Atlantic SST, and Tibetan heating for the last two millennia and showed that weak monsoon periods correspond to cooler SST conditions over the North Atlantic, but strong monsoon periods do not always accompany warmer conditions over the Atlantic. In another study based on multiple proxy records for the last 500 years, Sankar et al. (2016) showed that the positive relationship between AMO and ISM was not prominent before 1800. In fact, Sankar et al. (2016) found little coherence among proxy reconstruction of ISM prior to 1750 even though all of them show strong multi-decadal variability. Hence the inference regarding the AMO-ISM link from the ISM proxies is inconclusive and more widespread proxy evidence is required to understand the AMO-ISM association in the past. Nevertheless, these studies inherently lack a causal link in the AMO-ISM relationship. Climate models are more helpful for exploring the underlying mechanisms. While some modeling studies (Li et al. 2008; Wang et al. 2009; Malik et al. 2017) corroborate the observed relationship between the AMO and ISM, analysis of a suite of climate model simulations, part of the Coupled Model Intercomparison Project (CMIP) indicate that the AMO-ISM relationship is highly variable among different models (Ting et al. 2011; Luo et al. 2018a). In the CMIP5 historical simulations, only ~16% of the models could reproduce a statistically significant relationship between AMO and ISM (Luo et al. 2018a). Nevertheless, the current generation of climate models is an indispensable tool for making long-term climate forecasts. Studies that used climate model simulations to address the AMO-ISM relationship have discussed multiple possible teleconnection mechanisms (Luo et al. 2011, 2018a; Monerie et al. 2019; Svendsen 2021; Ahmad et al. 2022). However, the complex interplay among these processes makes it challenging to address their relative role and evolution with time. The reliability of decadal climate predictions/projections of monsoon will largely depend on how successful the models are in simulating the different teleconnection mechanisms which modulate the ISM multidecadal variability.

1.3.1 Mechanistic understanding

As mentioned in the previous section, warm (cold) phase AMO induces northward (southward) migration of the ITCZ resulting in large rainfall anomalies over the Sahel and Indian region. The northward (southward) movement of ITCZ is linked with enhanced (weakened) meridional heat transport by AMO. Cooling over the extratropical northern hemisphere alters the meridional thermal contrast and results in a southward migration of ITCZ (Broccoli et al. 2006; Kang et al. 2008; Frierson and Hwang 2012). This also results in weaker monsoons in the South Asian region (Broccoli et al. 2006; Mohtadi et al. 2016). An opposite situation emerges for an anomalously warm North Atlantic which results in northward movement of ITCZ and enhanced ISM rainfall (Zhang and Delworth 2006; Knight et al. 2006; Han et al. 2016; Monerie et al. 2019).

Since the Pacific Ocean is known to constrain the ISM variability in the interannual to decadal timescales AMO impacting the ISM via the Pacific Ocean variability is also a possibility. In fact, AMO impacting the low-level convergence over the South Asian region through changes in the Pacific Ocean has been discussed in many studies (Kucharski et al. 2016a; Sun et al. 2017, 2019; Monerie et al. 2019). Numerous studies have shown evidence of the strong impact of AMO on the decadal-multi-decadal variability of North Pacific and equatorial Pacific climate. AMO can induce variabilities over the Pacific Ocean in two ways. Tropical Atlantic warming (cooling) can trigger anomalous Walker circulation resulting in cooler (warmer) equatorial eastern Pacific (Kucharski et al. 2016a). The extra-tropical North Atlantic warming can also warm the North Pacific through AMO-induced subsiding motion (Sun et al. 2017) and through the weakening of the mean westerly winds (Zhang and Delworth 2007). The resulting Pacific SST anomalies can impact the ISM through changes in Hadley and Walker circulation (Feudale and Kucharski 2013; Joshi and Kucharski 2017; Luo et al. 2018a, b).

Modulation of the interannual atmospheric variability over the midlatitude North Atlantic was found to play a significant role in the AMO-ISM teleconnection. AMO modulates the leading mode of atmospheric variability over the North Atlantic, known as the North Atlantic Oscillation (NAO) (Goswami et al. 2006; Peings and Magnusdottir 2014). Positive (negative) phase AMO tends to induce more frequent negative (positive) NAO years. A negative (positive) phase NAO during boreal summer tends to induce a warmer (cooler) troposphere over the South Asian region. The resulting meridional gradient in tropospheric temperature between the Indian subcontinent and the Indian Ocean controls the strength of ISM. However, the subseasonal evolution of summertime NAO and how the downstream teleconnection involved (Watanabe 2004) alters the tropospheric temperature is not fully understood (Saeed et al. 2014). (Krishnamurthy and Krishnamurthy 2016), used observation and model experiments to show that summer NAO (SNAO) plays a crucial role in driving the observed AMO-induced low-level winds over the ISM domain. However, the role of NAO is not fully understood and there are studies that did not find any significant NAO impact (Li et al. 2008; Wang et al. 2009; Luo et al. 2011a; Monerie et al. 2019).

Recent studies (Rajesh and Goswami 2020; Borah et al. 2020; Goswami et al. 2022) have highlighted the strong role played by quasi-stationary waves in the observed multi-decadal association between the North Atlantic SSTs and ISM. Extratropical SST anomalies over the North Atlantic Ocean can trigger barotropic circulation anomalies in the intraseasonal timescale (Goswami et al. 2022). These barotropic structures can trigger downstream Rossby waves that interact with the monsoon circulation anomalies (e.g., Ding and Wang 2007; Syed et al. 2012). The resulting ISM anomalies are phase-locked with the barotropic vorticity observed over the North Atlantic (Rajesh and Goswami 2020). Borah et al. (2020), showed that this mechanism plays a pivotal role in the observed ISM anomalies during non-ENSO drought years. While these observational evidences are shading new light to the AMO-ISM teleconnection it is imperative to study them in a hierarchy of climate models to better infer the physical mechanisms.

1.4 Aim and Scope of the Thesis

While several hypotheses have been put forward to explain the observed relationship between the AMO and ISM, the exact mechanism remains elusive. Given the fact that the

AMO-ISM relationship can be unstable, its evolution in a warming climate remains uncertain (Luo et al. 2018b, a, c; Ahmad et al. 2022; Sandeep et al. 2022). Hence it is imperative to understand the fidelity of the current state-of-art climate models in representing AMO-ISM teleconnections. This is the theme of *Chapter 2*. It discusses the AMO-ISM relationship as simulated by the state-of-art global climate models (GCM). These 1000-year simulations part of the Climate Model Intercomparison Project/Paleoclimate Model Intercomparison Project (CMIP5/PMIP3) *last millennium (past1000)* experiments were explored to look for the robustness of the currently understood teleconnection pathways. Models exhibit robustness in the Pacific Ocean response to AMO as the critical pathway of AMO-ISM teleconnection. However, the stationary wave response to AMO is poorly represented in the models. *Chapter 3* is dedicated to the discussion of the stationary wave response to AMO and its impact on the multi-decadal variability of ISM. Reanalysis products showed significant wave activity associated with AMO. Such wave activity was shown to modulate the interannual variability of ISM through changes in meridional gradient in tropospheric temperature and easterly shear. The source of these wave activity was investigated using simple model experiments. Equivalent barotropic vortices over extratropical North Atlantic were shown to be the key mechanism. Finally, *Chapter 4* discusses the role of AMO-induced Pacific Ocean variability in the observed AMO-ISM relationship. The strongest correlation between AMO and ISM was shown to be associated with a lagged Pacific response to AMO. Such lagged response in SST is consistent with simple model experiments. *Chapter 5* summarises the thesis work and discusses the future direction of work.

Chapter 2

Investigating the AMO-ISM teleconnection pathways in global climate model simulations

Abstract

Understanding the natural variability of the Indian summer monsoon (ISM) is a crucial aspect relevant for decadal climate predictions and climate change studies. The multidecadal variability of ISM is known to have a close association with the Atlantic multidecadal oscillations (AMO). Several teleconnection pathways have been suggested to explain the co-variability of the AMO and ISM in multidecadal timescales. One hypothesis is that the AMO modulates the interannual North Atlantic Oscillation (NAO) mode and there by influences the monsoon via the Eurasian temperature modulations. Another possibility is the AMO modulating the monsoon via the Pacific pathway through the atmospheric bridge mechanism and associated modulations of the Hadley-Walker circulations. The last millennium (LM) (851AD-1848AD) climate simulations part of the CMIP5/PMIP3 give an opportunity to better understand the fidelity of climate models in capturing the AMO-ISM teleconnection mechanisms. In this study, we explore how well the proposed mechanisms are represented in eight global climate models (GCM) LM simulations. Such a study, assessing the validity of different AMO-monsoon teleconnection mechanisms in different model climates provides crucial information about how reliable the GCMs may be in making decadal climate predictions.

2.1 Introduction

The boreal summer monsoon serves as the main source of precipitation over the South Asian region and forecasting its variability in the intraseasonal and inter-annual timescales is of great relevance for socio-economic planning and policy making in the South Asian countries. The interannual variability of monsoon is strongly modulated by the low frequency modes of monsoon variability in the decadal and longer timescales. Observational records indicate that the seasonal mean Indian Summer monsoon (ISM) exhibits multidecadal variability with a periodicity of ~60 years (Mooley and Parthasarathy 1984; Krishnamurthy and Goswami 2000; Goswami 2006; Zhou et al. 2010) and seasonal mean ISM rainfall was found to be above the long term mean during the decades 1871–1900 and 1931–1960 and was below the long-term mean during 1901–1930 and 1961–1990 (Mooley and Parthasarathy 1984). The multidecadal variability of monsoon is also evident in paleoclimate reconstructions from different parts of the monsoon domain (Burns et al. 2002; Sinha et al. 2007, 2011; Berkelhammer et al. 2010; Goswami et al. 2016). While climate forcing like changes in solar irradiance and volcanic activity are known to modulate the monsoon variability in multidecadal timescales (Agnihotri et al. 2002; Bhattacharyya and Narasimha 2005; Bollasina et al. 2011), internal variability associated with low-frequency climate modes over the Atlantic and Pacific Oceans also plays a major role in modulating ISM multidecadal variability (Krishnan and Sugi 2003; Zhang and Delworth 2006). Coherent ocean-atmosphere coupled variability over the North Atlantic basin, the Atlantic Multidecadal oscillation (AMO) (Bjerknes 1964; Delworth and Mann 2000; Enfield et al. 2001; Knight et al. 2005), exhibits an in-phase relationship with the ISM multidecadal variability. It exhibits a periodicity of about 60-80 years in the instrumental records and paleoclimate reconstructions (Schlesinger and Ramankutty 1994; Gray et al. 2004b; Parker et al. 2007; Tung and Zhou 2013; Naidu et al. 2020).

The AMO has been established as one of the major drivers of the multidecadal variability of ISM during the instrumental period (Goswami et al. 2006; Lu et al. 2006; Zhang and Delworth 2006; Feng and Hu 2008; Joshi and Rai 2015; Krishnamurthy and Krishnamurthy 2016), and the decades of warmer (cooler) than normal SST anomalies over the Atlantic are associated with higher (lower) than normal precipitation over the ISM domain. However, some recent modeling studies suggest that the AMO-ISM relationship might be non-stationary and the recently observed out-of-phase relationship between AMO and ISM might be indicative of the non-stationarity (Luo et al. 2018c; Ahmad et al. 2022; Sandeep et al. 2022)

Studies investigating the multidecadal linkages between the Atlantic and the ISM identify three main pathways of teleconnection. In the interannual timescale, the North Atlantic Oscillation (NAO) exerts a downstream impact on the ISM by modulating the surface temperature over Eurasia and the moisture flux by the southwesterly winds over the ISM domain (Chang et al. 2001; Srivastava et al. 2002; Roy and Kripalani 2019). Using data from the instrumental period, (Folland et al. 2009; Peings and Magnusdottir 2014; Krishnamurthy and Krishnamurthy 2016) showed that a positive AMO phase is conducive to the frequent occurrence of negative NAO phase over the Atlantic in summer, which in turn leads to strong monsoon conditions over the ISM domain. Atmospheric heating anomalies associated with warm SST anomalies over the north Atlantic can also induce planetary wave responses across Eurasia, which can lead to upper-level circulation anomalies over central Asia that can alter the ISM strength through easterly shear modulation (Luo et al. 2011a). Several observation/modelling studies also indicate that the AMO influence on the ISM might be mediated by the Pacific (Zhang and Delworth 2007; Kucharski et al. 2016b; Sun et al. 2017, 2019). Warming over the Atlantic Ocean can induce secondary warming over the Western Pacific through an atmospheric bridge mechanism and in turn lead to strong ISM. The extratropical-tropical SST gradient over the North Pacific was found to be a crucial factor in the AMO-ISM teleconnection in the CMIP5 model simulations (Luo et al. 2018a), as a stronger gradient over the North Pacific signifies an enhanced Walker circulation and a stronger ISM. In this chapter, we explore the AMO-ISM relationship in the Last millennium (LM) simulations by climate models participating in the Paleo climate Modeling Intercomparison Project phase 3 (PMIP3), in light of the above-discussed teleconnection mechanisms. LM simulations have provided useful record of ISM variability and opportunity to look into the impact of internal climate variability on ISM (Tejavath et al. 2019; Ashok et al. 2022). By examining the AMO-ISM teleconnections during the LM in different model climates, we hope to gain insight on the robustness of the relationship over longer periods. Understanding how the relationship emerges in different model climates would provide crucial information on the natural variability of the climate modes, which holds immense value for decadal climate prediction. The study also aims to identify the dominant teleconnection pathways through which the Atlantic influences the ISM.

2.2 Data and methodology

The AMO-ISM teleconnection in the Last Millennial (LM) simulations (850-1850) by eight climate models from the Paleoclimate Model Intercomparison Project phase 3 (PIMP3) (Braconnot et al. 2012) archive is analyzed in the study. The LM simulations were included as a part of the PMIP3 to gain a long-term perspective for detection and attribution studies and to evaluate the models' ability in simulating the multidecadal and longer time scale climate variability. The LM simulations were forced with historical reconstructions of total solar irradiance, volcanic aerosols and greenhouse gas concentrations (Schmidt et al. 2012). Topography, vegetation and ice sheets were maintained as same as the pre-Industrial control conditions. Atmospheric and oceanic fields of monthly resolution from eight PMIP3 coupled global climate model (GCM) simulations were downloaded from the Earth System Grid Federation (ESGF) data servers and https://www.wdc-climate.de/ui/ (see Table 2.1 for the list of models). As an observational counterpart, only for the purpose of comparing with the known climate features during the instrumental period, mean sea level pressure, air temperature, and wind data from 20th Century reanalysis (1901-2012), Hadley Centre Sea Ice and Sea Surface Temperature data (1901-2012) (Rayner et al. 2003) and monthly precipitation data from

Global Precipitation Climatology Project (GPCP, Adler et al. 2003) (1979-2012) and Climate Research Unit (Harris et al. 2020) (1901-2012) were used. Long record of monthly all-India rainfall data (1871-2012) from Indian Institute of Tropical Meteorology (IITM) was used to bring out the dominant multi-decadal mode of ISM. All observation and model fields were re-gridded to a 2°×2° uniform grid.

Model abbreviation	Model/Institute	Resolution
BCC-CSM-1	Beijing Climate Center, Climate system model version 1.1	T42, 26 levels
CCSM4	Community Climate System Model version 4, NCAR	1.25° × 0.942°, 26 levels
CSIRO-Mk3L-1-2	Commonwealth Scientific and Industrial Research organization Mark version 3.6.0	T21, 18 levels
GISS-E2-R	NASA Goddard Institute for Space Studies	2.5° × 2.0°, 40 levels
HadCM3	Hadley Centre Coupled Model version 3	3.75° × 2.5°, 19 levels
MIROC-ESM	University of Tokyo National Institute for Environmental Studies & JAMSTEC	T42, 80 levels
MPI-ESM-P	Max Plank Institute of Meteorology	T63, 47 levels
MRI-CGCM3	Meteorological Research Institute Japan	T102 , 48 levels

Table 2.1: List of PMIP3 models

Anomalies of different fields were computed as departures from monthly climatology computed over the last 100 years of LM simulation, i.e., from 1750-1850. The overall trend in the LM simulations was removed using least square fit method. To identify robust multidecadal spectral signature from the long time series, power spectra was computed using the Welch method (Welch 1967). The power spectra were estimated by applying fast Fourier transform (FFT) to 200-year segments with 40% overlap, and then the average spectra were computed. The theoretical red-noise spectrum is estimated from the lag-1 autocorrelation value of the original time series and the 90% significance limit was estimated using the Chi-square test.

To compute the Atlantic Multidecadal variability (AMV) index, the annual mean sea surface temperature (SST) was averaged over the North Atlantic (75°W -5°E, 0-60°N). The global average SST time series was then subtracted from this time series, to remove the influence of other globally uniform climate signals (Trenberth and Shea 2006). This method of removing the global mean SST signal from the North Atlantic SST variability was found to be useful in bringing out the AMV-related signals in climate model simulations (Lyu and Yu 2017). Since our focus is to understand climate variability in the multidecadal timescales, a 30–100-year Lanczos filter (Duchon 1979) was applied to the model AMV time series, while a 30-year low-pass filter was applied to the HadISST based AMV time series. These filtered time series represent the respective AMO indices which is used for further analysis. To calculate the probability distribution of parameters during different AMO phases, we used the gaussian kernel density estimate (Rosenblatt 1956; Parzen 1962). The PDF is given as

$$p_n(x) = \frac{1}{nh}\sum_{i=1}^{n} K(x)\left(\frac{X_i - x}{h}\right)$$

Where n is number of data points, h is smoothing bandwidth and $K(x)$ is the gaussian kernel function given as $\frac{1}{\sqrt{2\pi}}\, e^{\frac{-x^2}{2}}$. Kernel density estimate basically smoothens each data point X_i into small density bumps and then sum all these small bumps together to obtain the final density estimate.

2.3 Results

2.3.1 ISM in models

The climatological mean state over the ISM domain was first examined in the LM simulations by the eight GCMs. The June to September (JJAS) mean precipitation averaged over the Last Millennia is shown in Figure 2.1. While it is not meaningful to estimate the model biases relative to present-day observations, the climatological mean (1979-2012) ISM precipitation in the GPCP v2 dataset (Adler et al. 2003) is shown alongside for easy comparison with present-day monsoon features. Earlier studies (e.g., Menon et al. 2013; Sengupta and Rajeevan 2013) have documented the skill of these models in simulating the ISM features in the CMIP5 historical simulations. The main features of the ISM in the LM simulations do not differ much from the monsoon features in the historical simulations (cf: Figure 3, Menon et al., 2013). While models like CCSM4, MPI and MIROC simulate the mean monsoon precipitation pattern with relatively good fidelity, GISS, MRI-CGCM3, HADCM3, BCC and CSIRO underestimate the precipitation over Indian landmass, and this has been recognized as a fundamental bias in climate models (Dai 2006; Sabeerali et al. 2015). Power spectral analysis of ISM rainfall (averaged over 60°-100°E, 5°-27°N) in the 20th century reanalysis brings out a 50–100-year multidecadal signal along with a higher frequency multidecadal mode around 30 year (Figure 2.2). A similar distribution of spectral power is observed in the LM simulations by BCC, CCSM4 and MRI-CGCM3, while in most other models a broad spectral power in the 10–60-year range is observed.

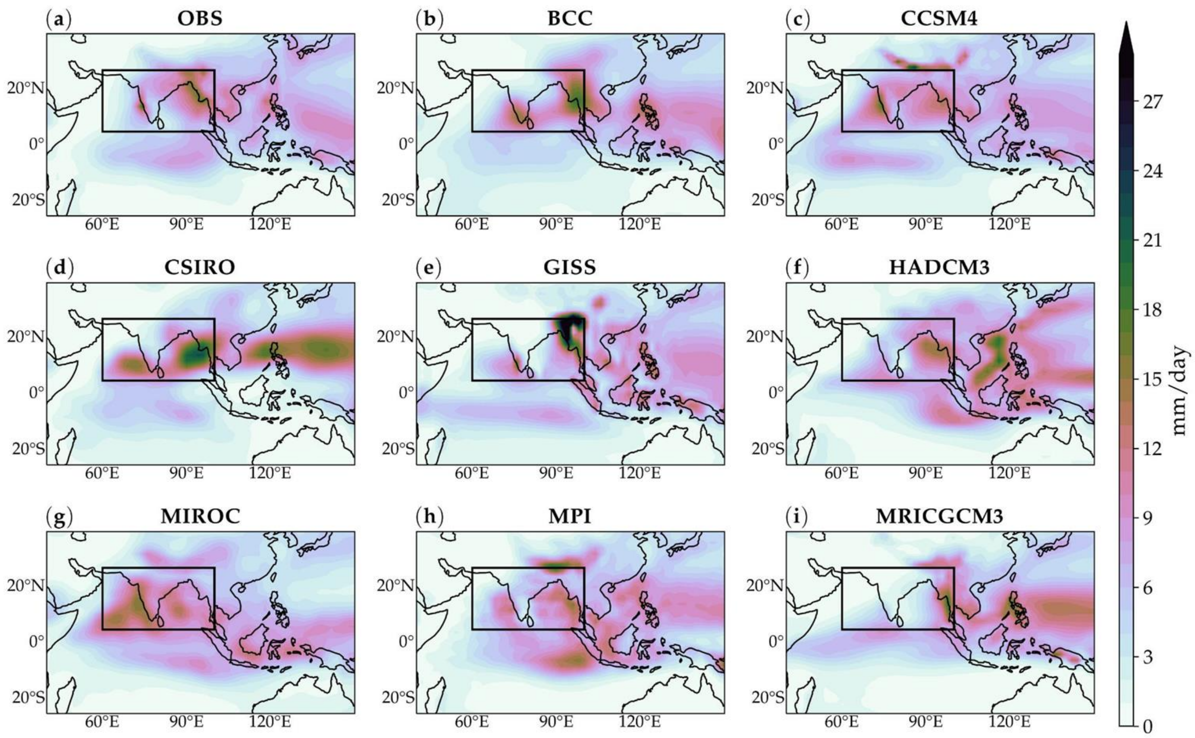

Figure 2.1 June to September (JJAS) mean monsoon rainfall in the (a) GPCP data (1979-2012) and (b)-(i) PMIP3 models LM simulations from 850-1850 AD

The climatological representations of seasonal mean monsoon winds at 850hPa pressure level and near surface air temperature (10m) in the LM simulations are shown in Figure 2.3. As an observational counterpart from the instrumental period, JJAS mean fields from the 20th Century reanalysis are shown alongside. The simulation of these dynamic and thermodynamic fields gives valuable information about the models' ability in simulating the large-scale monsoon system. While there are significant biases in the model simulated monsoon precipitation, most models simulate the summertime heating and low-level winds over the ISM landmass with reasonably good skill, as in the case of historical simulations (Sengupta and Rajeevan 2013). The models capture the high surface temperature conditions over the Thar desert region and

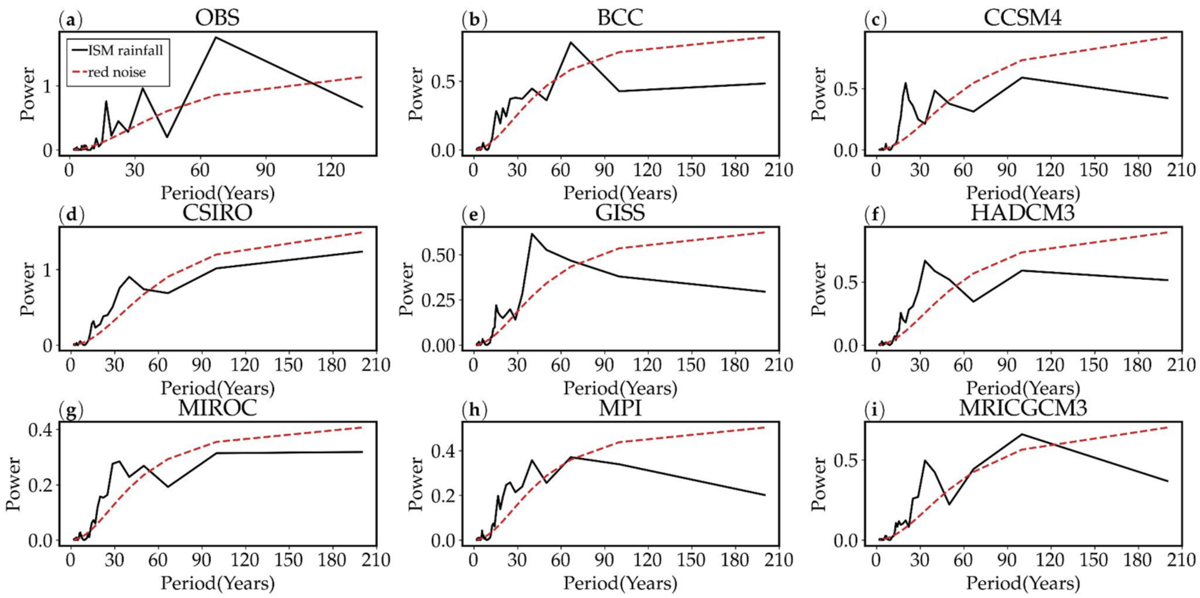

Figure 2.2 Power spectra of (a) IITM all-India mean ISM rainfall data(1871-2012)and (b)-(i) JJAS mean ISM rainfall averaged over 60°-100°E, 5°-27°N in the PMIP3 models LM simulations from 850-1850 AD. Red dashed line represents the red noise spectra.

adjoining areas over northwest India and the warm conditions over the northern Indian Ocean. Most models also simulate the cross equatorial low level flow from the Somalia coast towards the Indian subcontinent, albeit some small differences in the strength and extent of the low-level Jetstream (LLJ). The vertically averaged free tropospheric temperature over the monsoon domain measures the monsoon diabatic heating and hence is a useful index for the strength of ISM (Goswami and Xavier 2005). The climatological mean patterns of upper level (200 hPa) circulation and free tropospheric temperature (averaged from 500-200 hPa) over the ISM domain are shown in Figure 2.4. The co-location of the upper tropospheric anticyclones and the maximum heating zone is evident in the 20th Century reanalysis. The seasonal mean free tropospheric temperature over the ISM domain is underestimated in most models relative to 20th century observations, but the broad features of the upper-level circulation including the upper tropospheric anticyclone and tropical easterly jet are simulated by most of the models.

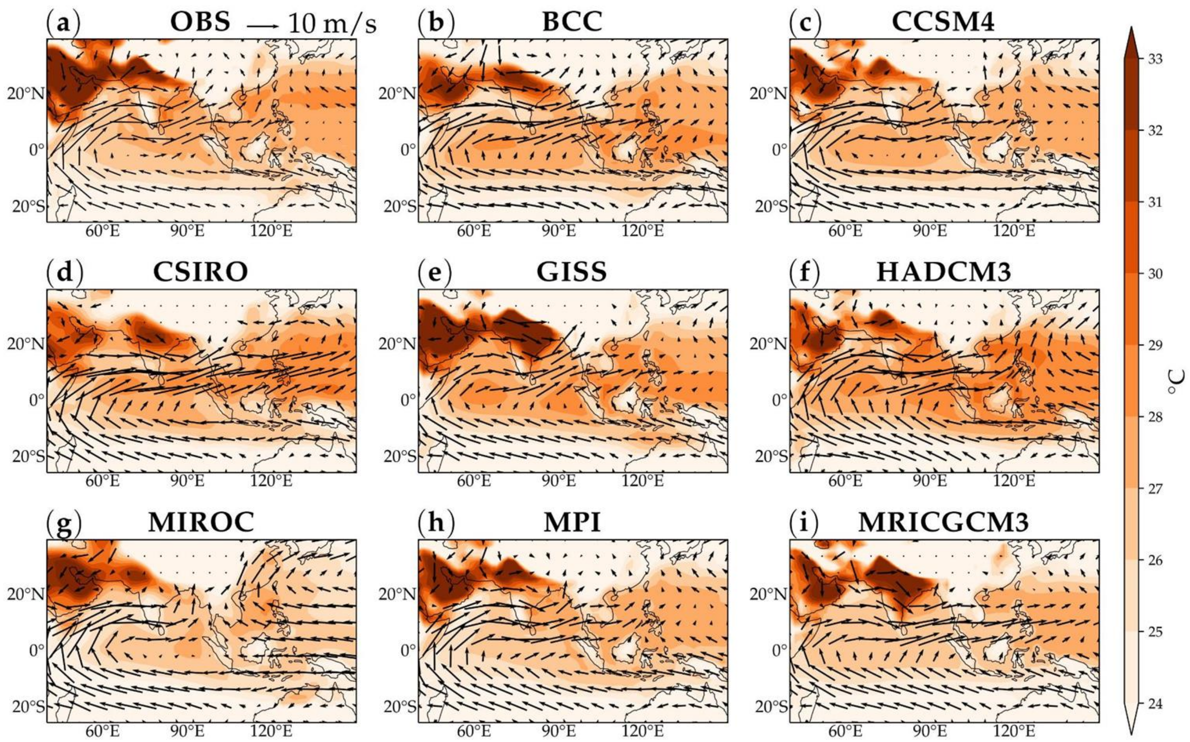

Figure 2.3 JJAS mean 850 hPa winds (vectors) and surface air temperature (shaded) in (a) 20th Century reanalysis V2 (1901-2012) and (b)-(i) PMIP3 models LM simulations from 850-1850 AD.

Most of the models also capture the north south gradient in tropospheric temperature over the ISM domain. BCC, GISS and MPI have a relatively poor representation of the monsoon core zone of heating in terms of both intensity and spatial extent. From the analysis of the mean monsoon features, it can be surmised that even though the models have some weaknesses in the simulation of monsoon precipitation, they mostly capture the heating and mean circulation features associated with the large-scale monsoon system.

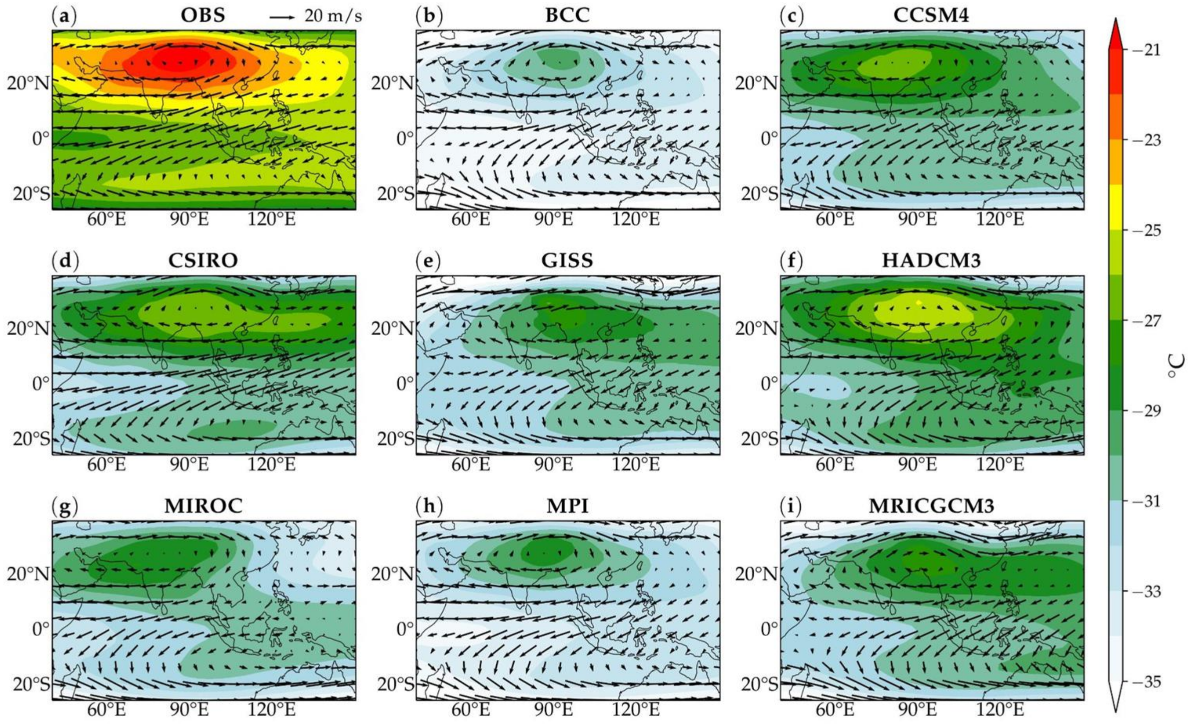

Figure 2.4 JJAS mean 200 hPa winds (vectors) and free tropospheric temperature (500-200 hPa) in (a) 20th Century reanalysis V2 (1901-2012) and (b)-(i) PMIP3 models LM simulations from 850-1850 AD.

2.3.2 AMO in models

To delineate how the multidecadal variability over the Atlantic Ocean is captured in the LM simulations, we examined the power spectra of the basin averaged AMV index (Figure 2.5). The periodicity of AMO derived from observations and paleoclimate reconstructions fall in the 50–80-year timescale (Schlesinger and Ramankutty 1994; Gray et al. 2004a; Parker et al. 2007; Tung and Zhou 2013). A broad range of spectral power is observed in the 30–100-year timescale in most of the models. Significant spectral power in the 10–30-year timescale is also present in some models such as, CCSM4, MPI, BCC and GISS. Earlier studies which examined the AMV in the historical and pre industrial simulations by CMIP models (Ting et al. 2011; Peings et al. 2016; Ratna et al. 2019) have also reported a wide range of spectral power in the multidecadal timescale over the Atlantic. Both observations and models indicate that apart from the basin wide mode of multidecadal warming/cooling which is known as the Atlantic Multidecadal Oscillations (AMO), a tri-pole pattern of variability with cold SST anomalies over western Atlantic between 10°N-40°N sandwiched between warm SST anomalies to the east of Newfoundland, and over the tropical eastern Atlantic, is also dominant over the Atlantic (Wu and Liu 2005; Fan and Schneider 2012; Lin et al. 2019).

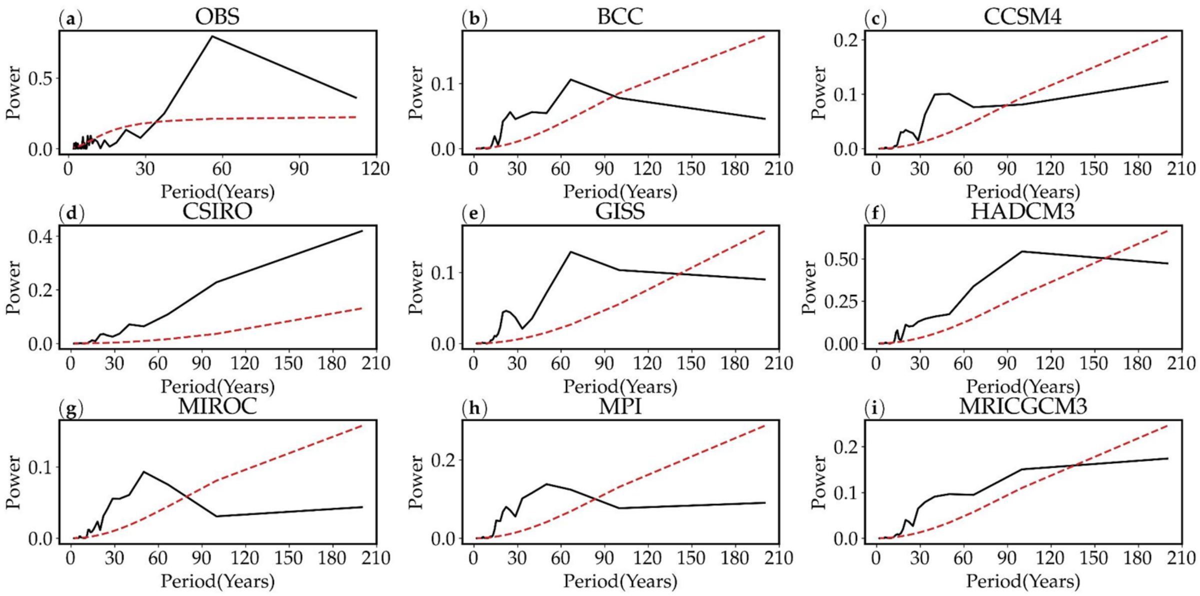

Figure 2.5 Power spectra of north Atlantic SST area averaged over (75°W -5°E, 0-60°N) in (a) HADISST (from 1901-2012) and (b)-(i) PMIP3 models LM simulations from 850-1850 AD. Red dashed line represents the red noise spectra.

Since the focus of the present study is to understand the multidecadal scale influence of the Atlantic on the ISM, a common 30–100-year band is chosen as representative of AMO in the models and the 30-100 year filtered AMV timeseries is used as the AMO index in the remaining analysis. The spatial structure of the model simulated AMO was examined by compositing 30–100-year filtered SST anomalies for positive and negative AMO phases (Figure 2.6). The positive (negative) phases of AMO were identified as when the normalized AMO index is greater than 1.0 (less than -1.0) standard deviation. In most models the basin

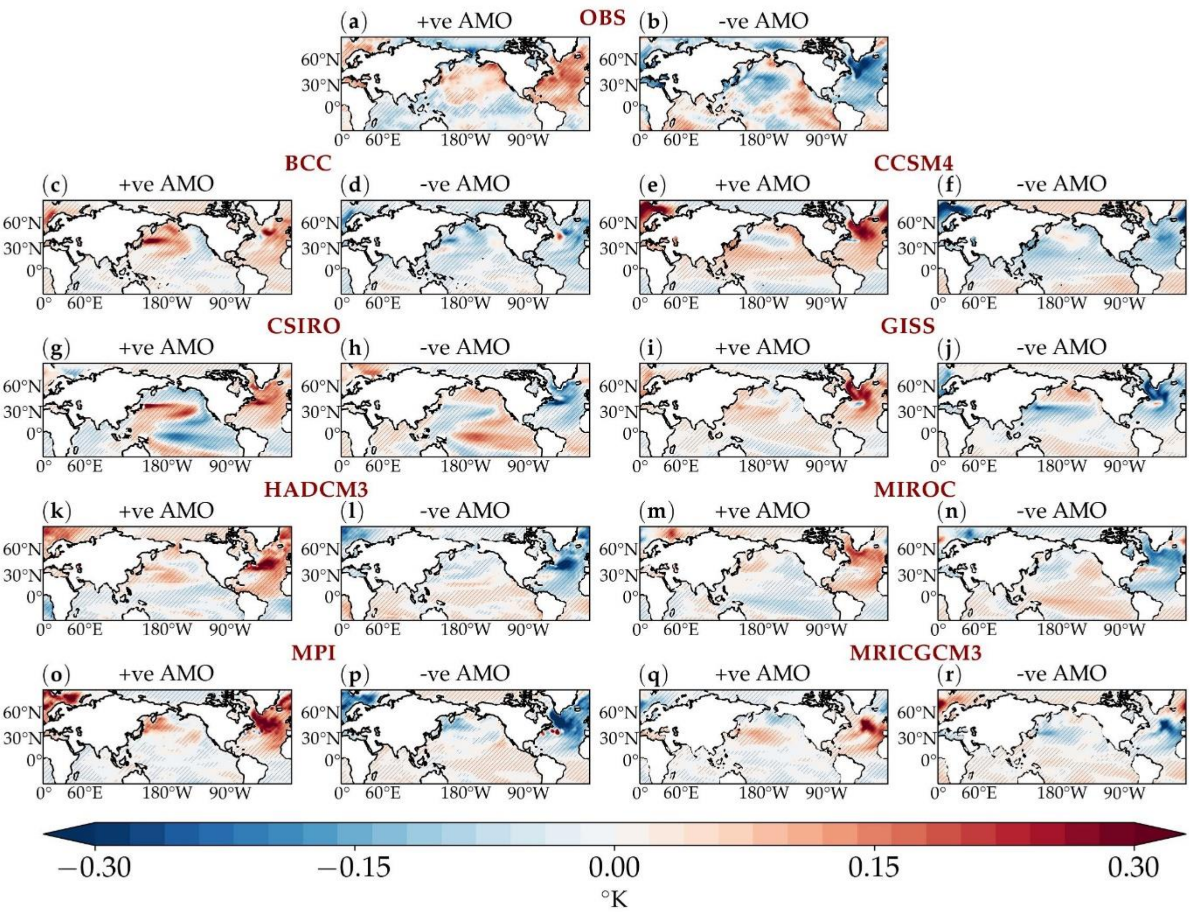

Figure 2.6 30-100 year filtered, SST anomalies composited for positive and negative phases of AMO in (a) HADISST and (b)-(i) PMIP3 models LM simulations

wide warming/cooling signature is evident over the North Atlantic, while in some models like BCC, CSIRO, and MRICGCM3 the warm/cold SST anomalies are concentrated over the eastern part of the Atlantic basin. Warm SST anomalies over the north Pacific is evident in the positive AMO phase composites of many models, but the response is diverse among the different models. While positive SST anomalies are observed over most part of the north Pacific in CCSM4, GISS and MPI, it is relatively weak in MIROC and HADCM3. Very strong SST anomalies restricted to the western Pacific domain are observed in the BCC, MRICGCM3 and CSIRO simulations. The negative SST anomalies over tropical Pacific are simulated in most models except CCSM4, MPI and GISS. In these three models, the Pacific exhibits basin wide warming during positive AMO phase and basin wide cooling during negative AMO phase. It is interesting to note that the SST anomalies over the Indian ocean are in tandem with the SST anomalies over tropical central pacific, during positive/negative AMO phases.

2.3.3 AMO-ISM teleconnection

Next, we explore the AMO-ISM relationship in the LM simulations and examine the different teleconnection pathways through which the AMO influences the ISM variability. The correlation between the AMO index and 30-100 year filtered rainfall averaged over the ISM domain (60E-100E, 5N-27N) during the LM are shown in Table 2.2. A significant (90% confidence level) positive correlation is observed for the models CCSM4, MRI CGCM3, CSIRO, HADCM3 and BCC, while for MIROC, GISS and MPI, the correlation is negative or insignificant. On the other hand, Luo et al. (2018a) reported a positive correlation between AMO and ISM rainfall in all models except MIROC and HADCM3 in the CMIP5 historical simulations. Considering the biases in the simulation of mean monsoon precipitation, the AMO-ISM relationship in the LM simulations were also explored using a TT gradient based index (Goswami and Xavier 2005) and a zonal wind shear-based index (Webster and Yang 1992) for the ISM. The meridional gradient of TT anomalies between the equatorial Indian ocean and the northern land mass plays a major role in maintaining the monsoon circulation and can be considered as an indicator of ISM strength (Goswami and Xavier 2005; Xavier et al. 2007). The TT gradient over the ISM domain was calculated as the difference in vertically averaged TT between a north box (50E-100E, 15N-35N) over Indian land region and a south box (50E-100E, 15S-5N) over the Indian Ocean. A significant positive correlation is observed between 30-100 year filtered TT gradient over the ISM domain and the AMO index in the models CCSM4, CSIRO, MRICGCM3, MPI and GISS. The correlation is not significant

	AMO-ISM (easterly shear)	AMO-ISM (TT gradient)	AMO-ISM (rainfall)
Observation	-0.49	0.80	0.60
BCC	-0.09*	0.02*	0.17
CCSM4	-0.34	0.34	0.51
CSIRO	-0.27	0.31	0.31
GISS	-0.33	0.18	0.04*
HADCM3	-0.06*	-0.06*	0.14
MIROC	0.04*	-0.15	-0.24
MPI	-0.31	0.22	0.003*
MRICGCM3	-0.34	0.31	0.35

Table 2.2 Correlation between the AMO index and rainfall based, TT gradient based and easterly wind shear-based ISM indices in observations and PMIP3 models LM simulations

for BCC and HADCM3 and negative in the case of MIROC. The LLJ and the upper-level tropical easterly jet together generate a strong wind shear over the monsoon domain which gives a measure of the strength of the monsoon circulation. The zonal wind shear index is defined as the vertical shear of zonal wind averaged over the region 0-20N, 40-110E. The wind shear-based index also exhibits a significant correlation with the AMO in all the models except MIROC, BCC and HADCM3. It implies that the multidecadal variability of the circulation and

TT over the ISM domain in five of the eight models are largely related with the Atlantic multidecadal variability. In the remaining part of the chapter, we analyse how each of the proposed teleconnection processes are represented in these five models and explore how it impacts the AMO-ISM relationship.

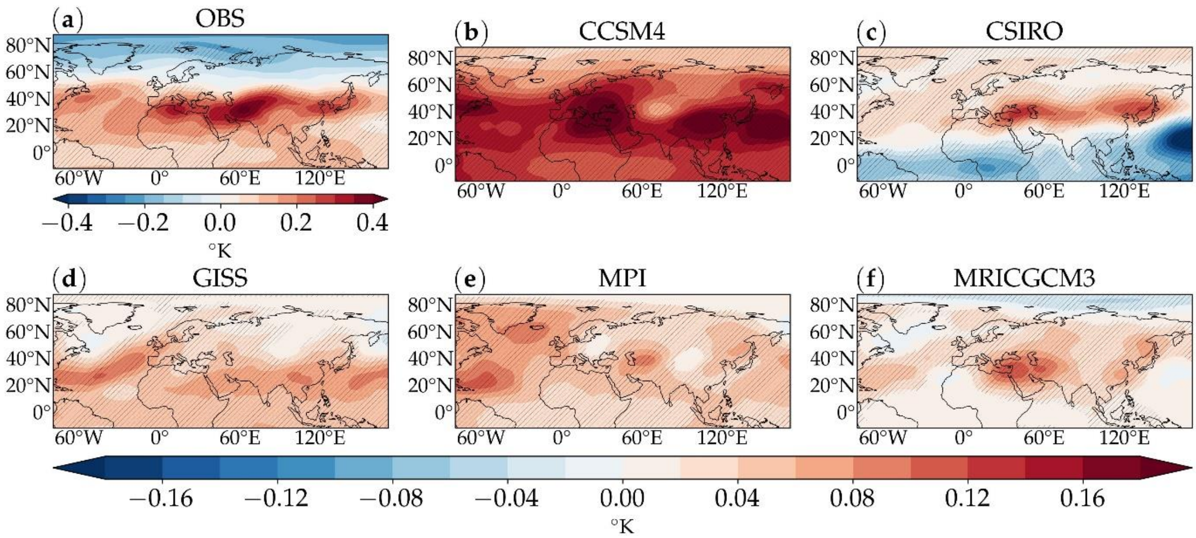

Figure 2.7 30-100 year filtered free tropospheric temperature anomalies composited for the positive phase of AMO in (a) 20th Century reanalysis and (b)-(f) PMIP3 models LM simulations. Hatched regions represent statistical significance at 90% level.

Modulation of surface temperature and TT over Eurasia is an important factor in the AMO-ISM teleconnection, and a positive (negative) AMO phase is known to be associated with warm tropospheric temperature anomalies over Eurasia and Tibet (Goswami et al. 2006). 30-100 year filtered tropospheric temperature (TT) anomalies (averaged from 500hPa to 200hPa) composited for positive AMO years are shown in Figure 2.7. In the 20th Century reanalysis, during AMO positive phase, maximum positive TT anomalies are observed over the South Asian region, extending from the Mediterranean to the East Asian monsoon domain. All the models simulate an extended band of warm TT anomalies over the South Asian region during positive AMO phase. The TT modulation may happen due to different teleconnection effects. The AMO can induce strong upper tropospheric circulation responses across Eurasia and such teleconnection patterns are associated with significant tropospheric temperature anomalies (Lin et al. 2016; Wu et al. 2016). Barotropic instability over the jet exit region over the North Atlantic gives rise to a quasi-stationary Rossby wave trains

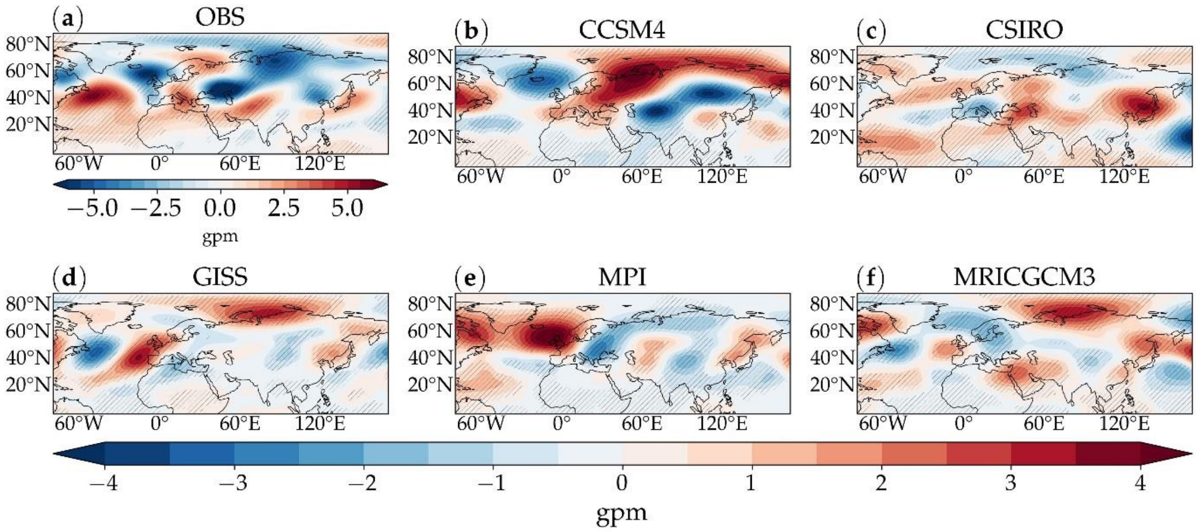

Figure 2.8 30-100 year filtered 200 hPa eddy geopotential height anomalies composited for the positive phase of AMO in (a) 20th Century reanalysis and (b)-(f) PMIP3 models LM simulations. Hatched regions represent statistical significance at 90% level.

which can induce positive geopotential height anomalies over the South Asian region. An enhanced South Asian high would lead to increased low-level convergence and an amplified meridional TT gradient over the ISM domain (Zhang and Delworth 2006; Luo et al. 2011; Li et al. 2008; Wang et al. 2009). 30-100 year filtered upper level (200hPa) geopotential height anomalies were composited for the positive AMO phase to bring out the upper-level teleconnection pattern associated with the AMO (Figure 2.8). While an arching teleconnection pattern extending from the Atlantic to central Asian region with alternating positive and negative geopotential height anomalies is evident in the 20th century reanalysis, the model simulated teleconnection patterns are widely different from the observations. Although

CCSM4 and MPI LM simulations capture the arching wave train pattern, there are differences in the spatial scale of the geopotential height anomalies and the anomalies are negative over the South Asian domain. Thus, the upper-level wave responses associated with the AMO are not well represented in the models and they may not be responsible for inducing positive TT anomalies over the ISM domain.

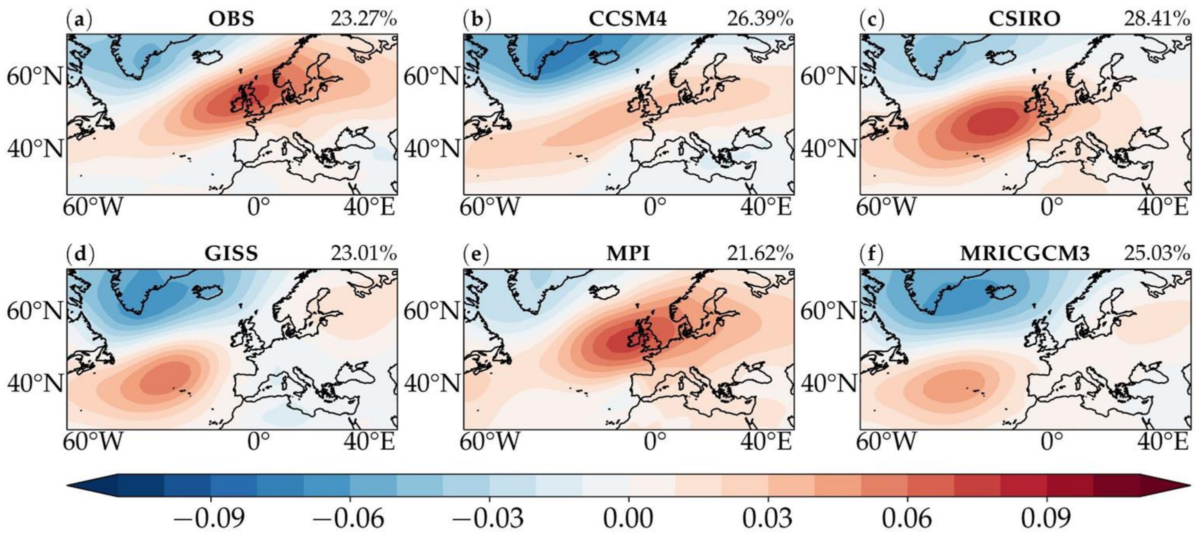

Figure 2.9 Summer NAO pattern in (a) 20th Century reanalysis and (b)-(f) PMIP3 models LM simulations. SNAO pattern is identified as the leading EOF of Jul-Aug Sea Level Pressure over the North Atlantic domain (70°W-50°E, 25°N-70°N). Variance explained by the mode is indicated as percentages.

The AMO can also impact the ISM by modulating the interannual mode over the Atlantic - the summer NAO (SNAO). It is characterized by an oscillation of the meridional pressure gradient between the Arctic and the subtropical Atlantic and is known to impact the global climate and the ISM. Studies (Baines and Folland 2007; Peings and Magnusdottir 2014a; Roy and Kripalani 2019) indicate that a positive (negative) AMO phase would favour a greater number of SNAO negative (positive) events, which in turn would give rise to positive (negative) TT anomalies over Eurasia and in turn affect the meridional TT gradient over the ISM domain. The wind anomalies associated with negative SNAO extending from the Sahel to the western Arabian sea would enhance the south westerly monsoon flow and increase the moisture flux towards the Indian subcontinent, favouring a strong monsoon (Krishnamurthy and Krishnamurthy 2015). Empirical orthogonal function (EOF) analysis of summer time (July-August) mean sea level pressure (SLP) anomalies over the north Atlantic (70°W-50°E, 25°N-70°N) (Folland et al. 2009) is used to extract the summer SNAO dipole structure in the 20th Century reanalysis and the LM simulations (Figure 2.9).

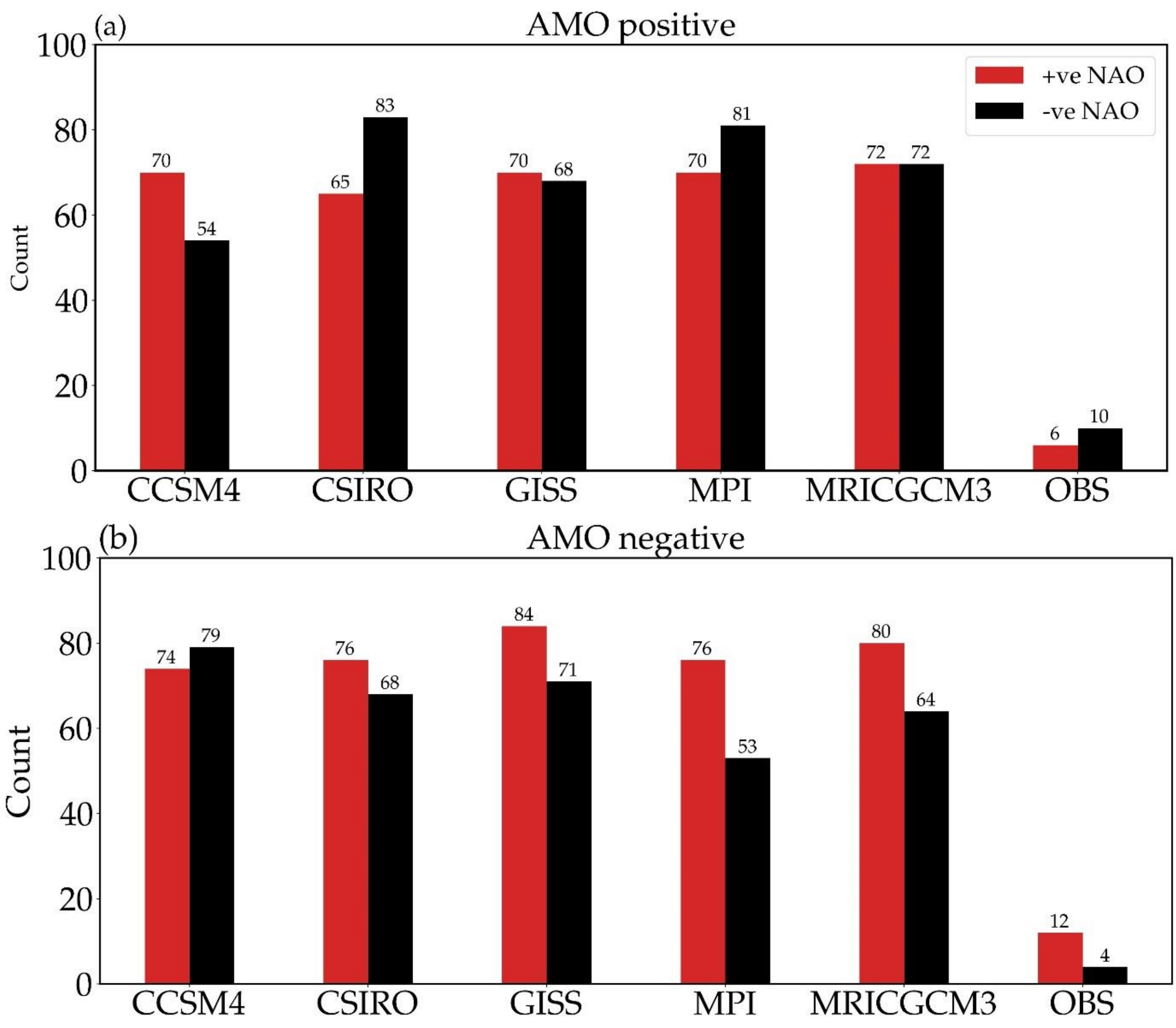

Figure 2.10 Frequency of occurrence of summer NAO in the positive and negative phases during a) AMO positive phase b) AMO negative phase in observations and PMIP3 models LM simulations

In all the models, the first EOF mode of SLP captures the north-south dipole structure associated with SNAO, and the corresponding principal component time series is considered the representative SNAO index for further analysis. The SNAO pattern is northeastward shifted compared to its winter counterpart, with the southern node observed over northwest Europe (Hurrell et al. 2003; Folland et al. 2009). However, in the LM simulations, the shifted SNAO pattern is captured only by CCSM4 and MPI. (Wang et al. 2017b) examined the NAO patterns in the CMIP5 historical simulations and reported a wide discrepancy in the locations of NAO high and low pressure centers in the model simulations. They also reported that most of the CMIP5 models

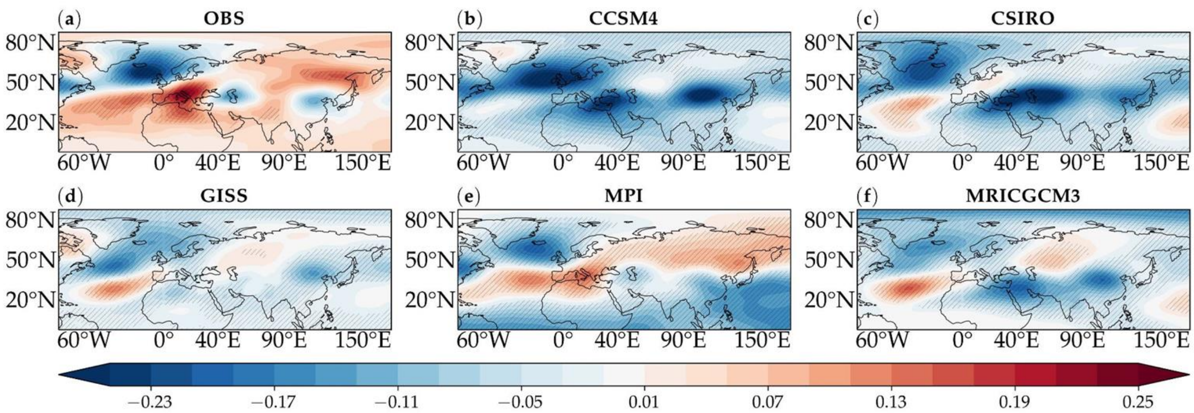

Fig 2.11 Regression coefficients obtained when unfiltered JJAS tropospheric temperature (500-200mb) anomalies are regressed onto the SNAO index in (a) 20th Century reanalysis and (b)-(f) PMIP3 models LM simulations. The regression coefficients are multiplied by -1 to represent the state corresponding to negative SNAO. Hatched regions represent statistical significance at 90% level.

tend to underestimate the multidecadal variability of NAO. We find that the multidecadal variability of NAO is underestimated in most models. However, as in observations, the multidecadal (30-100 year) variability of SNAO is found to be negatively correlated with the AMO in all the model simulations except CCSM4 (Table 2.3). We further examined the frequency of occurrence of positive and negative phases of SNAO during positive and negative AMO phases (Figure 2.10). SNAO positive and negative phases were identified as when the SNAO index is greater than/less than ±1 standard deviation. In CCSM4 AMO positive phase favors more NAO positive states and vice versa, while in the other four models - CSIRO, MPI, MRICGCM3, and GISS, relatively a greater number of NAO positive states are observed during AMO negative phase, consistent with the observations. On the other hand, the TT anomalies regressed on to the negative SNAO index (Figure 2.11) brings out a downstream response quite different from observations. While a negative SNAO phase in observations is associated with positive TT responses over Eurasia, in all the models, except MPI, the TT response is negative over Eurasia. Moderate positive TT responses are observed over northern and central Europe in GISS and MRICGCM3 simulations but largely the TT responses over the ISM domain is negative in all the models.

	AMO-NAO	AMO-Pacific SST gradient
Observation	-0.38	0.27
CCSM4	0.31	0.15
CSIRO	-0.23	0.49
GISS	-0.19	0.29
MPI	-0.38	0.21
MRICGCM3	-0.15	0.46

Table 2.3 Correlation of the AMO index with the 30-100 years filtered SNAO index and 30-100 years filtered extratropical-tropical SST gradient over the Pacific, in observations and PMIP3 models LM simulations. Principal components corresponding to the EOF modes shown in Figure 2.9 represent the SNAO indices. SST gradient is defined as the difference between area averaged SST anomalies over the north Pacific (25°-45°N, 150°E–140°W) and equatorial east Pacific (15°S-15°N, 180°E–95°W)

Similar TT responses are observed in the multidecadal timescale as well (Figure not shown). As the AMO modulation of the SNAO variability in CCSM4 is opposite of that in observations, a positive AMO phase may be conducive for positive SNAO in the model and it can induce positive downstream TT responses over Eurasia and the ISM domain. On the other hand, in the case of the other four models, the multidecadal modulation of interannual SNAO variability is consistent with observations, but the discrepancies in the downstream responses associated with the SNAO makes this mode of teleconnection to be misrepresented in the models.

The AMO can also modulate the TT gradient over the ISM domain by influencing the SST over the Indian and Pacific Ocean domains (Dong et al. 2006; Zhou et al. 2015; Sun et al. 2017). The Southern Indian Ocean SST response of relatively cooler SST anomalies during positive AMO and warmer SST anomalies during negative AMO is simulated by four out of five models - CSIRO, CCSM4, MPI and MRICGCM3 (Figure 2.6). This favors a positive TT gradient over the ISM domain and hence a stronger monsoon. Several studies have shown that the AMO exerts a significant impact on the Pacific variability (Zhang and Delworth 2007; Sun et al. 2017; Gong et al. 2020; Johnson et al. 2020b) which affects the ISM. The key features of the observed AMO induced Pacific SST response include warm anomalies over most part of north Pacific (Sun et al, 2017; Gong et al. 2019) and cold anomalies over equatorial eastern Pacific (Kucharski et al. 2016b; Johnson et al. 2020b) . The SST response is very similar to the PDO and in fact studies have shown that part of the PDO variability may be forced by the AMO (Zhang and Delworth 2007; Johnson et al. 2020b; Yang et al. 2020) . The SST response over the Pacific can have a strong impact on the ISM (Feudale and Kucharski 2013; Krishnamurthy and Krishnamurthy 2014; Joshi and Kucharski 2017; Luo et al. 2018a) through modulation of the Walker circulation (Krishnamurthy and Goswami, 2000). While the positive AMO phase is found to be associated with positive SST anomalies over most part of the north Pacific in CCSM4, GISS and MPI, the positive SST anomalies are restricted only to the western Pacific domain in MRICGCM3 and CSIRO simulations (Figure 2.6). CCSM4, GISS and MPI also fail to simulate the negative SST response observed over tropical eastern Pacific. In these three models, the Pacific exhibits basin wide warming during positive AMO phase and basin wide cooling during negative AMO phase.

Warm SST anomalies over subtropical and extratropical north Pacific are considered to be a response to the Atlantic-Pacific atmospheric bridge mechanism. Upper-level divergence over the Atlantic and convergence and descending motion over northern Pacific, combined with ocean-atmosphere coupled feedbacks can result in warm SST anomalies over subtropical north Pacific (Sun et al. 2017; Gong et al. 2019). Cool SST anomalies over the equatorial eastern Pacific during the warm AMO phase are thought to be a result of anomalous zonal circulation triggered by warm tropical Atlantic. Low level convergence and ascending motion over tropical Atlantic causes large scale subsidence over equatorial eastern Pacific. Resulting high sea level pressure anomalies drive more easterly winds and upwelling and hence cooling over the region (Kucharski et al. 2016b). Warming over subtropical north Pacific and cooling over eastern equatorial Pacific leads to a strong extratropical-tropical SST gradient. Positive (negative) phase of AMO induces a positive (negative) extratropical-tropical SST gradient between the north Pacific and central Pacific. Such SST gradient impacts the ISM through modulation of

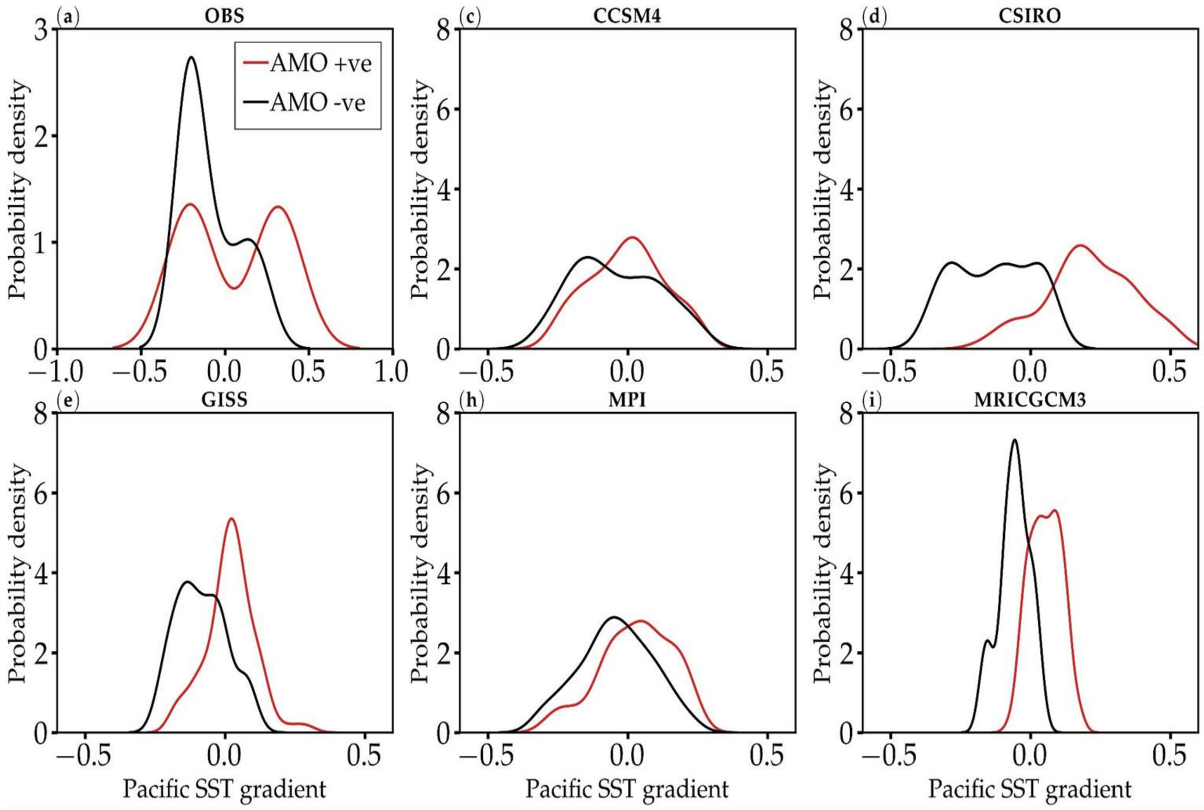

Figure 2.12 Probability distribution of 30-100 year filtered extratropical-tropical gradient values over the Pacific during positive and negative AMO phases in (a) HADISST and (b)-(i) PMIP3 models LM simulations. SST gradient is defined as the difference between area averaged SST anomalies over the north Pacific (25°-45°N, 150°E–140°W) and equatorial east Pacific (15°S-15°N, 180°-95°W)

Hadley-Walker circulation anomalies. Analysing the historical simulations by 22 coupled models that were part of the CMIP5, Luo et al. (2018a), showed that models which captured the positive AMO-ISM relationship also successfully simulated the strong extratropical-tropical SST gradient over the Pacific domain. The gradient was calculated between an extratropical Pacific box (25°N–45°N, 150°E–140°W) and tropical eastern Pacific box (15°S–15°N, 180°E–95°W) (following Luo et al. 2018a) using 30-100 year filtered SST anomalies. A strong positive correlation is observed between the Pacific SST gradient and the AMO in all the models (Table 3), with the strongest correlation exhibited by CSIRO, MRICGCM3 and

GISS models. The probability distribution of the extratropical-tropical SST gradient over the Pacific during positive and negative AMO phases was further examined (Figure 2.12).

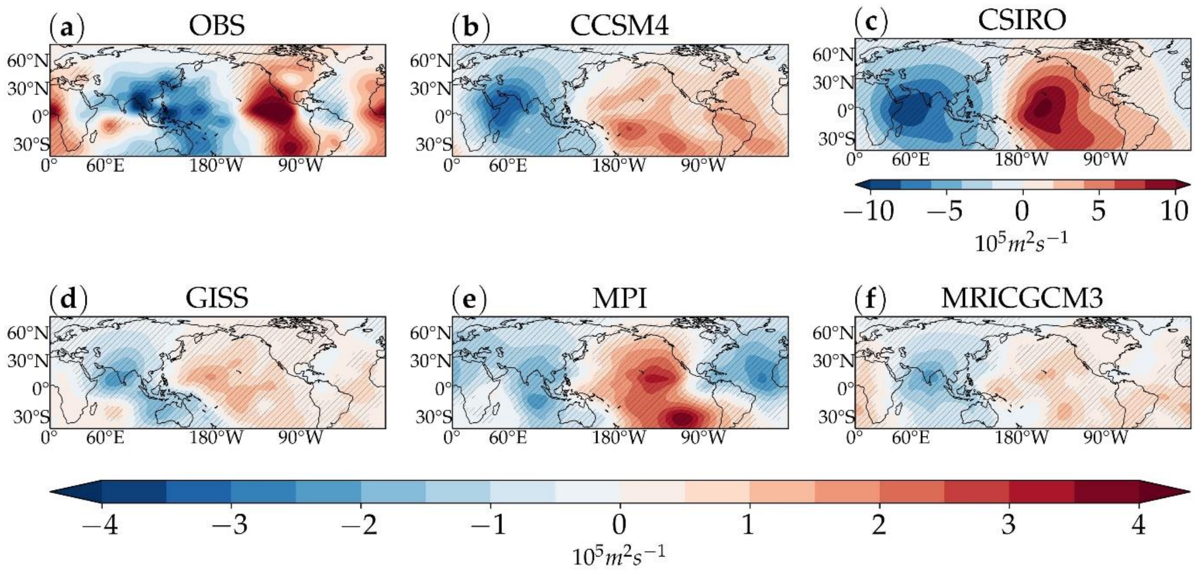

Figure 2.13 30-100 year filtered 200 hPa velocity potential anomalies composited for the periods when the 30-100 year filtered extratropical-tropical gradient index values were positive over the Pacific, in (a) 20th Century reanalysis and (b)-(f) PMIP3 models LM simulations

In CSIRO, MRI CGCM3 and GISS, it is evident that a positive AMO phase favours a stronger positive SST gradient over the Pacific, while the separation is not very distinct in the other models. The Pacific SST distribution can impact the ISM, mainly through the modulation of Walker circulation which was robust during the last millennium (Tejavath et al. 2019). 200 hPa velocity potential anomalies composited for periods of strong positive SST gradient over the Pacific (Figure 2.13) brings out this aspect of the teleconnection. The enhanced Walker circulation with upper-level convergence over central Pacific and upper-level divergence over the Indian and Atlantic Ocean domains is evident in all the models. Although the strength and location vary among the models all the models show more westward center of upper-level divergence compared to observation.

It can be summarized that while CCSM4 and GISS exhibit basin wide warming over the Pacific during positive AMO phase, CSIRO and MRICGCM3 captures the Pacific SST response more realistically. The latter models simulate the extra-tropical - tropical SST gradient over the Pacific with fidelity and capture the responses in the Walker circulation. Even though the GISS and CCSM4 model fails to simulate the negative SST responses over equatorial East Pacific, it captures the Pacific SST gradient modulation by the AMO.

2.4 Conclusion

In this chapter, the observed AMO-ISM relationship is investigated in the Paleoclimate Model Intercomparison Project phase 3 (PMIP3) last millennium (LM) simulations by eight climate models. The LM simulations are useful for gaining a better understanding of the models' ability in simulating the multidecadal and longer time scale climate variability. The model simulated ISM precipitation, circulation and temperature fields were examined, and it was observed that the LM mean monsoon features are very similar to the monsoon features in the historical simulations. While there are some fundamental biases in the simulation of monsoon precipitation by many models, the mean monsoon circulation and heating associated with the large-scale monsoon system are well simulated by most of the models. Similar to the historical and preindustrial simulations by CMIP models, the LM simulations also bring out a broad range of spectral power in the multidecadal timescale over the Atlantic. The AMO in the LM simulations has a periodicity of 30-100 years and capture the basin wide warming signal over the North Atlantic in most models, while in some models like BCC, CSIRO, and MRICGCM3 the warm SST anomalies are concentrated over the eastern part of the Atlantic basin. While a consistent positive correlation is not observed between AMO and ISM rainfall in many models, a significant positive correlation is observed between tropospheric temperature based and wind shear-based monsoon indices and the AMO in five out of the eight models - CCSM4, CSIRO, MRICGCM3, MPI and GISS. The AMO-ISM relationship in these five models is further explored based on proposed pathways of teleconnection.

Broadly two pathways of AMO-ISM teleconnection are examined, 1) the Eurasian pathway: AMO modulating the monsoon via modulation of tropospheric temperature anomalies over Eurasia and 2) the Pacific pathway: AMO modulating the monsoon via the Atlantic - Pacific atmospheric bridge and associated SST and circulation responses over the Pacific domain. Barotropic instability over the north Atlantic can give rise to upper tropospheric quasi-stationary Rossby wave trains which induce geopotential height anomalies over the South Asian high region and in turn affect the low-level convergence and TT gradient over the monsoon domain. While an arching teleconnection pattern extending from the Atlantic to central Asian is evident in the 20th century reanalysis, through which the AMO induces positive TT anomalies over the ISM domain, none of the models are able to capture such a mode of teleconnection in the LM simulations. In the case of oceanic forcing driving atmospheric teleconnections, proper simulation of the upper atmospheric and downstream responses largely depends on the simulated SST pattern. Inter-model differences in the AMO induced upper-level teleconnection hence may be related to the differences in models' simulated spatial pattern of AMO. The TT modulation over Eurasia via the interannual SNAO mode was also explored. A positive AMO phase is known to be conducive for frequent occurrence of negative SNAO phase over the Atlantic, which can have downstream impact on the TT anomalies over Eurasia which is conducive for the ISM. Except CCSM4, in all the other four model simulations, a positive phase AMO is found to favor more SNAO negative states, and the multidecadal SNAO variability is negatively correlated with the AMO consistent with the observations. However, the downstream TT response is quite the opposite of what is expected from observations. While a negative SNAO phase induces positive TT anomalies over the ISM domain in the 20th century reanalysis, in all the models a negative SNAO induces negative TT anomalies over the ISM domain. The discrepancies in the model simulated downstream responses associated with SNAO makes this mode of AMO-ISM teleconnection invalid in four of the five models. In CCSM4 however, this mode of teleconnection seems feasible mainly because the AMO bears a positive correlation with the SNAO multidecadal variability.

An important aspect of the Pacific pathway of AMO-ISM teleconnection are the Pacific SST responses induced by the AMO. Positive anomalies in the North pacific and negative SST anomalies in the equatorial eastern Pacific are the signature responses observed over the Pacific in the 20th century reanalysis. While a similar response is observed in MRICGCM3 and CSIRO simulations, a positive AMO phase is found to be associated with basin wide positive SST anomalies in CCSM4 and GISS. A strong positive correlation is observed between the Pacific SST gradient and the AMO in all the models, with the strongest correlation exhibited by CSIRO, MRICGCM3 and GISS models. Consistent with earlier studies, such gradient is also accompanied by anomalous Walker circulation with strong upper-level convergence over central Pacific and divergence over Indian monsoon domain. Therefore, the Pacific pathway might be a robust teleconnection process in the simulated AMO-ISM relationship in the PMIP3 models.

Chapter 3

Role of upper-tropospheric circulation anomalies in the observed AMO-ISM relationship

- Abstract

The leading model of upper-tropospheric circulation anomaly over the Northern hemispheric is known as the circum-global teleconnection (CGT) pattern. The CGT and ISM impact one another through the circulation responses over West Central Asia (WCA). In this chapter, we investigate the role of AMO in the CGT-ISM interaction. Analysis indicates that the Atlantic forced CGT responses play a lead role in modulating the ISM in the interannual timescale, by modulating the upper-level anticyclones over WCA and in turn affecting the ISM easterly vertical wind shear. Our analysis indicates significant modulation of WCA anomalies by the AMO in the multi-decadal time scale, implying that the Atlantic-CGT-WCA-ISM pathway of teleconnection has a low-frequency counterpart. We further demonstrate that the observed out-of-phase relationship between AMO and ISM in the recent decades, may be attributed to the relatively stronger high latitude warming over the North Atlantic during the recent AMO warm phase. The equivalent barotropic responses to the extra-tropical north Atlantic Sea surface temperature (SST) anomalies alter the entire downstream teleconnection pattern producing cyclonic anomalies over WCA and in turn weakening the ISM.

3.1 Introduction

The Northern hemispheric subtropical jet stream and its seasonal variability play an important role in atmospheric teleconnections (Beverley et al. 2019). The subtropical jet stream exhibits strong interannual variability over a number of geographic locations, and these locations gain significant prominence in the zonal teleconnection pattern observed in the midlatitude upper atmosphere (CGT) (Branstator 2002; Ding and Wang 2005). The pattern consists of prominent vortex centres extending from the north Atlantic to north America across Asia (He et al. 2018, 2020). Barotropic instability of the summer mean flow over the North Atlantic jet exit region is considered to be one of the main triggering mechanisms for the quasi-stationary Rossby waves and it gives rise to upper-level anticyclones over west central Asia (WCA hereafter), east of the Caspian Sea (Ding and Wang 2005; Yasui and Watanabe 2010; Borah et al. 2020). Studies (Sato and Takahashi 2006; Kosaka et al. 2009) show that the quasi-stationary wave trains which originate over the north Atlantic get anchored over WCA through barotropic energy conversions from the Asian Jet. Upper-level anticyclonic (cyclonic) anomalies over WCA are of particular relevance to the Indian summer monsoon (ISM) as it is known to enhance (weaken) the easterly shear over the ISM domain and lead to stronger (weaker) monsoon instability (Ding and Wang 2005, 2007). The midlatitude-ISM interaction via the WCA has been reported by several earlier studies (Kripalani et al. 1997; Krishnan et al. 2009).

Downstream from the North Atlantic domain, the diabatic heating associated with the ISM is considered as another important forcing mechanism which helps in maintaining the CGT (Ding and Wang 2005; Beverley et al. 2021). ISM diabatic heating triggers westward propagating Rossby waves which cause upper-level divergence anomalies over the Mediterranean and WCA. These anomalies contribute to the downstream CGT pattern (Gill, 1980; Rodwell and Hoskins, 1996; Stephan et al., 2019; Beverley et al., 2021; Son et al., 2021). The downstream component of the CGT pattern, extending from WCA, across the Pacific is also known as the Silk Road Pattern (Lu et al. 2002; Enomoto et al. 2003; Kosaka et al. 2009). Thus, the upper-level circulation anomalies over WCA feature both in the CGT impact on ISM and the ISM impact on CGT. While an equivalent barotropic structure is observed over the major centres of action of CGT over the Atlantic, western Europe, east Asia, north Pacific, and north America, the structure is baroclinic over WCA, implying that the diabatic heating effect of ISM also influences the region.

In one of the main studies examining CGT-ISM interactions, (Ding and Wang 2005), proposed two mechanisms. One in which the barotropic instabilities over the North Atlantic jet exit region triggering the CGT and the ISM play a secondary role in reinforcing the downstream cells through Rossby wave energy dispersion. Alternately, the ISM might play the lead role in maintaining the CGT and the Atlantic instabilities might be helping in reinforcing and maintaining the downstream anomalies. Using lagged singular value decomposition analysis between outgoing longwave radiation (OLR) fields over India and 200 hPa geopotential height fields over Eurasia, (Ding and Wang 2007), showed that the teleconnection pattern originating over the North Atlantic leads the ISM variability by 10-15 days. Ding and Wang, (2005), suggest that during early summer, the ISM might have an upper hand in maintaining the CGT, while mutually reinforced feedback between the CGT and ISM might be at play during late summer. The first question we explore in this chapter is whether the ISM plays a primary/secondary role in the Atlantic-ISM interactions in the seasonal timescale, focusing on the WCA region which forms the middle ground for the ISM-CGT interactions.

It is well known that the dominant internal mode of Atlantic variability - the Atlantic multi-decadal oscillation (AMO), is a major driver of ISM variability in the multidecadal timescale (Goswami et al. 2006; Zhang and Delworth 2006; Joshi and Pandey 2011; Krishnamurthy and Krishnamurthy 2016; Luo et al. 2018a; Svendsen 2021; Joshi et al. 2022). The AMO can impact the ISM by changing the meridional temperature gradient between the Indian landmass and the Indian Ocean (Goswami et al. 2006; Msadek et al. 2011; Joshi and Rai 2015). AMO warm (cold) phase can lead to the northward (southward) shift of the inter-tropical convergence zone (ITCZ) over the ISM domain, which in turn strengthen (weaken) the ISM (Zhang and Delworth, 2006; Ratna et al., 2020). Studies have also shown that the SST anomalies associated with AMO can trigger upper-level teleconnection responses which eventually impact the ISM (Wang et al. 2009; Luo et al. 2011b; Joshi and Ha 2019; Ratna et al. 2020). Studies using both observation and modeling experiments, suggest that the interdecadal variability of northern hemispheric CGT has a strong association with the AMO

(Lin et al. 2016; Wu et al. 2019). The 200 hPa geopotential height anomalies associated with AMO show significant variability over WCA (Wang et al. 2009; Luo et al. 2011b; Gao et al. 2019; Sandeep et al. 2022). As the Atlantic modulation of CGT – circulation responses over WCA – modulation of ISM, is considered as a major pathway for Atlantic-ISM interactions in the intraseasonal and interannual timescale (Ding and Wang, 2007; Saeed et al., 2011), in this chapter, we also explore the Atlantic, ISM and WCA multidecadal variability and examine whether the Atlantic impact on the ISM via WCA may be an effective mode of teleconnection in the multidecadal timescale as well.

3.2 Data and methodology

The main datasets used in the study are monthly mean fields of air temperature, geopotential height and zonal and meridional wind data from 20th century reanalysis (Compo et al. 2011), available from National Oceanic and Atmospheric Administration (NOAA), for the period 1871-2012. These datasets are available at 20 vertical levels and have a horizontal resolution of 2° x 2°. The Japanese 55-year Reanalysis (Kobayashi et al. 2015) products for the period 1958-2012 are also used in the study. The JRA-55 dataset is available at 37 vertical levels and have a horizontal resolution of 1.25° x 1.25°. Monthly timeseries of all-India rainfall for the period 1871-2012 is obtained from the Indian Institute of Tropical Meteorology (https://tropmet.res.in/static_pages.php?page_id=53). The June-September mean all India rainfall time series is used as the ISM index. Monthly gridded precipitation data of 1° x 1° horizontal resolution for the period 1901-2012 from Climate Research Unit (CRU) (Harris et al. 2020) is also used in the study. Monthly climatology is computed for the entire span of the datasets and the monthly anomalies are computed by removing the climatology from the monthly mean fields. The seasonal (June to September) anomalies are computed from the monthly anomalies and to bring out the interannual signal, a 8 years high-pass Lanczos filter

(Duchon 1979) is applied to the seasonal anomalies. The multi-decadal signal is isolated by applying a 11-year running mean.

The upper-level analysis of different fields is performed at the 200 hPa pressure level. To measure the strength of the upper-tropospheric anti-cyclone over WCA, a WCA index is defined by area averaging the 200 hPa geopotential height seasonal anomalies over WCA (60°-70°E, 30°-40°N) and normalizing the timeseries with its standard deviation. The zonal mean is removed from the geopotential anomalies before area averaging, so that the index captures the eddy component of the geopotential field over WCA. While the domain is slightly different from the choice of WCA domain followed by Ding and Wang, (2005) and (Watanabe and Yamazaki 2014), the region is chosen as it shows the strongest association with rainfall over India. The results of the study are found not to be too sensitive to the choice of the domain. Easterly shear of zonal winds is estimated as the difference between seasonal mean winds at 200 hPa and 700 hPa pressure levels. The mean tropospheric temperature (TT) anomalies are calculated by vertically averaging the air temperature (TT) anomalies between 200 hPa and 500 hPa pressure levels. In order to bring out the planetary scale wave pattern, the zonal mean is removed from the stream function and TT fields, and the resultant anomalies are hereafter referred to as the eddy fields.

The AMO index is calculated using the Hadley centre SST monthly data (Rayner et al. 2003), of 1° x 1° horizontal resolution, for the period 1871-2017, following the methodology discussed in (Trenberth and Shea 2006). The SST anomalies are area averaged over the north Atlantic (75°W-5°E,0°-60°N) and the global mean (60°S-60°N) SST anomaly is removed from the time series to remove the global warming signal. An 11-year running mean is applied to the timeseries and it is normalized by dividing by the standard deviation of the time series, to produce the AMO index. Other SST datasets used are the NOAA Extended Reconstructed Sea Surface Temperature, V4 (Huang et al. 2015) and COBE SST2 from the Japanese Meteorological Center (Hirahara et al. 2014).

3.2.1 Model

A dry linear baroclinic model (LBM) (Watanabe and Kimoto 2000) was used to look for planetary wave response to monsoon diabatic heating and north Atlantic vorticity anomalies. It has been extensively used to study the linear response of the atmosphere to steady forcing (Kosaka et al. 2009; Yasui and Watanabe 2010; Cen et al. 2020; Son et al. 2021). It is a spectral model with sigma vertical coordinates. LBM was set up with T42 horizontal resolution and 20 vertical levels. The model incorporates biharmonic horizontal diffusion, Newtonian damping and Rayleigh friction. The model was linearised against the summer mean basic state derived from the NCEP/NCAR (Kalnay et al. 1996) reanalysis. Patterns in 200 hPa eddy streamfunction were studied in response to idealised steady heating and vorticity forcings as discussed in the next section.

3.3 Results

3.3.1 Midlatitude-ISM link

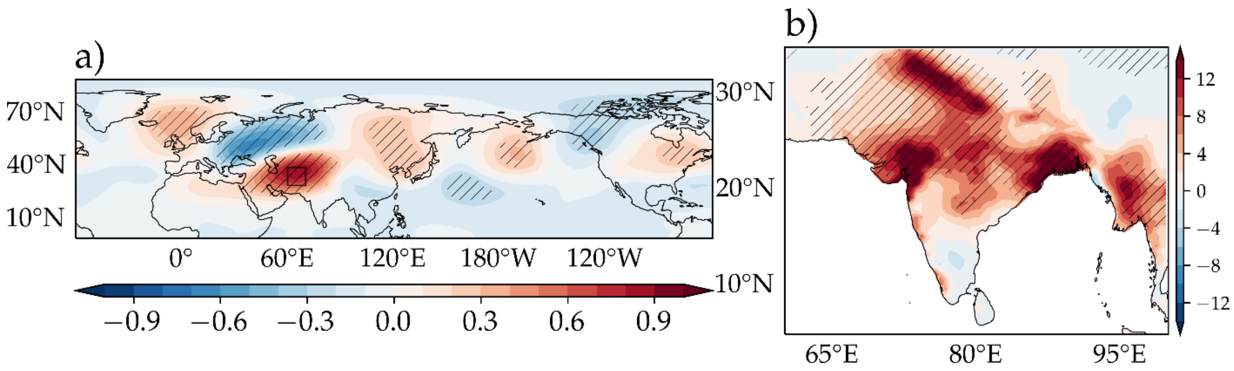

Figure 3.1 (a) One point correlation map between the WCA index and 200 hPa geopotential height anomalies at all grid points during the boreal summer season; black rectangular box indicates the WCA region (30-40N;60-70E); (b) June to September precipitation anomalies (mm/month) over the ISM domain regressed on to the WCA index; hatched regions indicate statistical significance. Geopotential height is from 20CRv2 and rainfall is from CRU datasets.

The upper-level circulation anomalies over WCA represent a significant component of the circum-global teleconnection (CGT) pattern (Ding and Wang, 2005; Branstator, 2002) and it exhibits large variability in the interannual time scale (e.g., Ding and Wang, 2005). Figure 3.1a shows the one-point correlation map of the WCA index with the 200 hPa geopotential height anomalies at all the grid points over the northern hemisphere during the boreal summer season. It clearly brings out the co-variability of WCA anomalies with circulation anomalies over north Atlantic, east Asia, north Pacific and North America, consistent with the CGT pattern reported by several earlier studies. WCA represents the region of interaction between midlatitude westerlies and the monsoon circulation (e.g., Ding and Wang, 2005; 2007; Krishnan et al., 2009), and hence upper-level circulation anomalies over WCA holds significant relevance for the ISM. The WCA index from 1871-2012 shows a significant correlation of 0.33 (at 99%

confidence level) with the ISM precipitation index, indicating a strong association between the two. Seasonal (JJAS) precipitation anomalies over the ISM domain regressed onto the normalised WCA index (Figure 3.1b) further brings out the significant association of WCA circulation anomalies with the precipitation anomalies over central India, north-west India, and the Himalayan foothills.

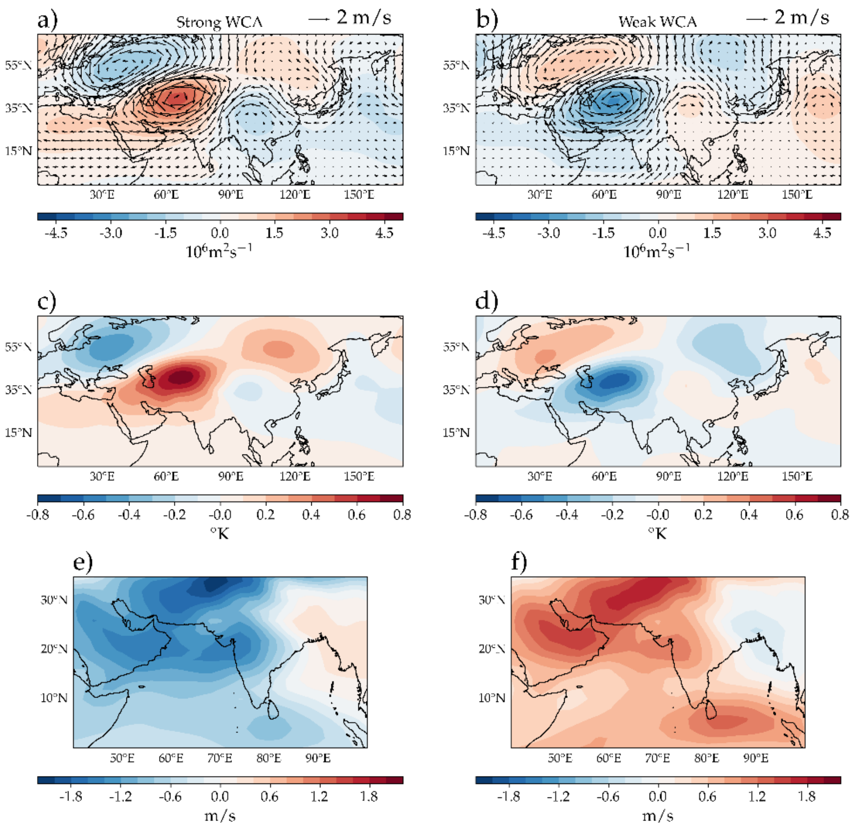

Figure 3.2 Composites of 200 hPa eddy stream function (shaded) and wind vectors (a, b), tropospheric temperature (c, d) and easterly shear (e, f) for strong (left panel) and weak (right panel) WCA years.

To bring out the circulation and heating responses over the ISM domain associated with extreme circulation anomalies over WCA in interannual timescale, strong and weak WCA years were identified using the WCA index. Strong (weak) WCA years were identified as years when the normalised WCA index was greater (less) than 1.0 (-1.0) standard deviation. From the 142 years of data, 25 strong WCA years and 23 weak WCA years were identified. Seasonal eddy fields of 200 hPa stream function, TT, and easterly shear of zonal winds are composited for the strong and weak WCA years (Figure 3.2). Figure 3.2a and b shows the 200 hPa eddy stream function composites for strong and weak WCA years. Composite mean wind fields vectors are overlaid to further bring out the circulation patterns. Cyclonic (anticyclonic) anomalies are observed over northwest Europe and over the Great plains of China, while anticyclonic (cyclonic) anomalies are observed over WCA and East Asia during strong (weak) WCA years. The anticyclonic (cyclonic) anomalies over WCA are associated with positive (negative) tropospheric temperature anomalies over the ISM domain (Figure 3.2c and d). Tropospheric temperature anomalies during strong/weak WCA years can affect the convection over northwest India and Pakistan (Saeed et al. 2011). Associated with the anticyclonic (cyclonic) anomalies during strong (weak) WCA years, upper-level easterly (westerly) wind anomalies are observed over central and northwest India (Figure 3.2a and b). Ding and Wang, (2007), hypothesised that the strengthening of easterly wind shear associated with the strong upper-level anticyclones over WCA can strengthen the monsoon instability and lead to higher precipitation. Figure 3.2e and 3.2f show the composite mean of easterly vertical shear over the ISM domain for strong and weak WCA years. Strong (weak) easterly vertical shear is observed over the ISM domain during strong (weak) WCA years. The analysis was repeated using JRA 55 dataset (Figure S1) and the results are consistent. The analysis affirms that upper-level circulation anomalies over WCA is an integral part of the CGT-ISM teleconnection, and it has a significant impact on the ISM rainfall in the interannual time scale.

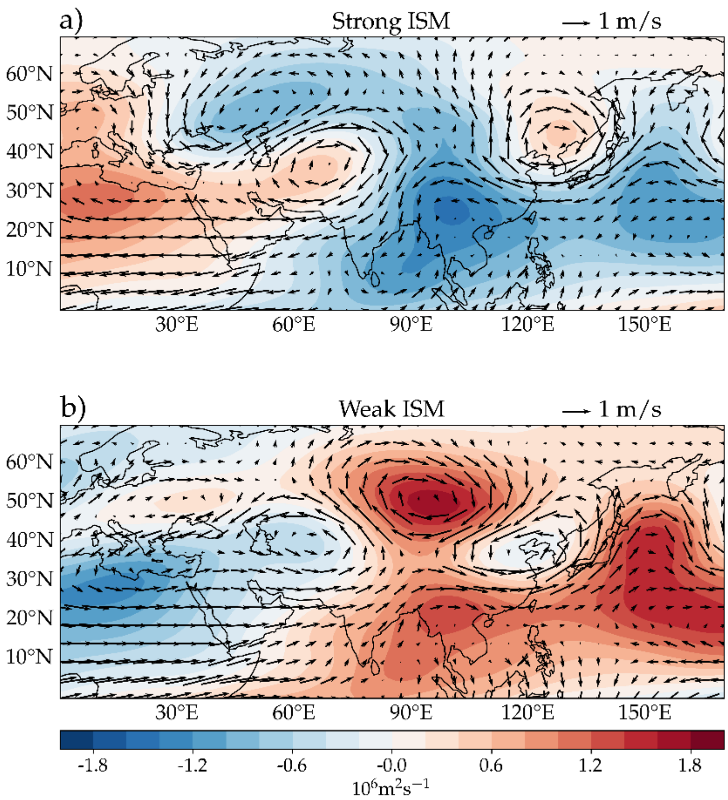

Figure 3.3 Composites of 200 hPa eddy stream function (shaded) and wind vectors for strong (a) and weak (b) ISM years.

3.3.2 Circulation response to ISM heating

ISM (being a strong source of diabatic heating) can generate upper-level circulation anomalies over WCA and the Mediterranean region by the monsoon-desert mechanism (Rodwell and Hoskins, 1996; Stephan et al., 2019; Beverley et al., 2021). To explore the role of ISM in generating circulation anomalies over WCA, composites of 200 hPa eddy stream function field are examined for strong and weak ISM years (Figure 3.3). Years when the normalized ISM index amplitude is greater than 0.7 (less than -0.7) are identified as strong (weak) ISM years. We have chosen a threshold of 0.7 so that strong and moderately strong ISM years are included in the analysis. The results remain the same for higher thresholds. 36 strong ISM years and 30 weak ISM years are identified. The composites clearly bring out the circulation anomalies over the Mediterranean and WCA. The upper-level circulation anomalies observed in Figure 3.3 are a product of the interactions between the subtropical jet stream with the westward propagating Rossby waves forced by monsoon diabatic heating and its downstream responses (Rodwell and Hoskins, 1996).

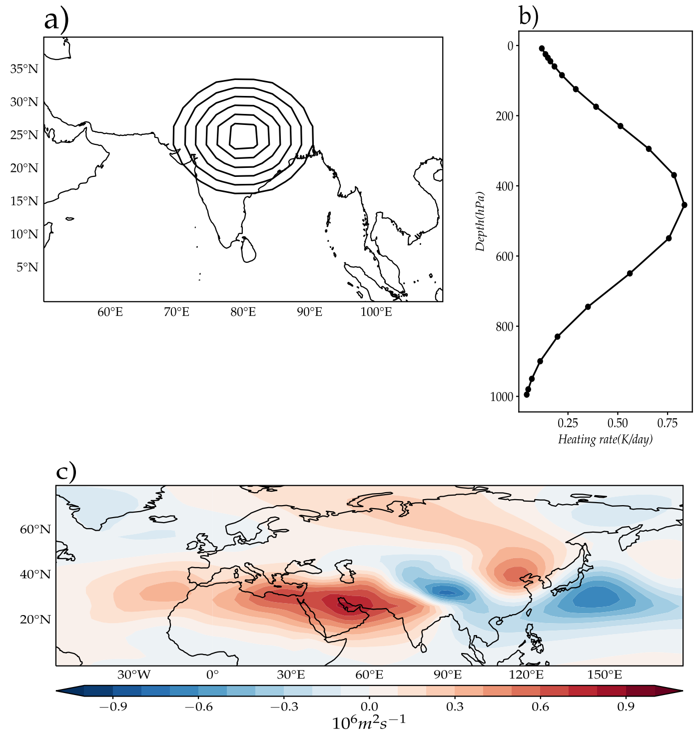

Figure 3.4 (a) Spatial and (b) vertical structure of idealised diabatic heating forcing over India; (c) 200 hPa eddy streamfunction response to the prescribed forcing on 20th day of integration

Upper-level circulation response to ISM diabatic heating was explored using the LBM simulation. LBM was forced with an idealised heating structure (Figure 3.4) resembling the ISM heating. This highly idealised forcing has an elliptic horizontal structure with maximum heating in the mid-levels. LBM was integrated for 30 days and a quasi-steady response was seen in 18 days. Figure 3.4c shows the 20th day response in 200 hPa circulation anomalies to the idealised heating. It is evident that ISM is a significant driver of the downstream CGT, consistent with earlier reports (Beverley et al. 2021; Son et al. 2021).

3.3.3 ISM feedback on WCA anomalies

To isolate the Atlantic impact on WCA circulation anomalies via the CGT, it is important to remove the ISM feedback on WCA circulation anomalies. A positive correlation (0.33) exists between the WCA and ISM indices in the interannual timescale. The correlation and our mechanistic understanding indicate that strong (weak) WCA years will invariably be associated with strong (weak) ISM years respectively. Of the 25 (23) strong (weak) WCA years, 14 (8) are also strong (weak) ISM years. Composites of eddy stream function at 200 hPa, TT and easterly shear of zonal winds are constructed for the strong (weak) WCA years, excluding the years when the ISM is concurrently strong (weak). Since we have chosen a +/- 0.7 threshold for identifying strong/weak ISM years, we believe that removing these years will remove the influence of even moderately strong/weak ISM. However, it is possible that some feedback associated with ISM may persist. The strong WCA and weak WCA difference composites are shown in Figure 3.5 along with the difference composites, when the ISM influence is excluded.

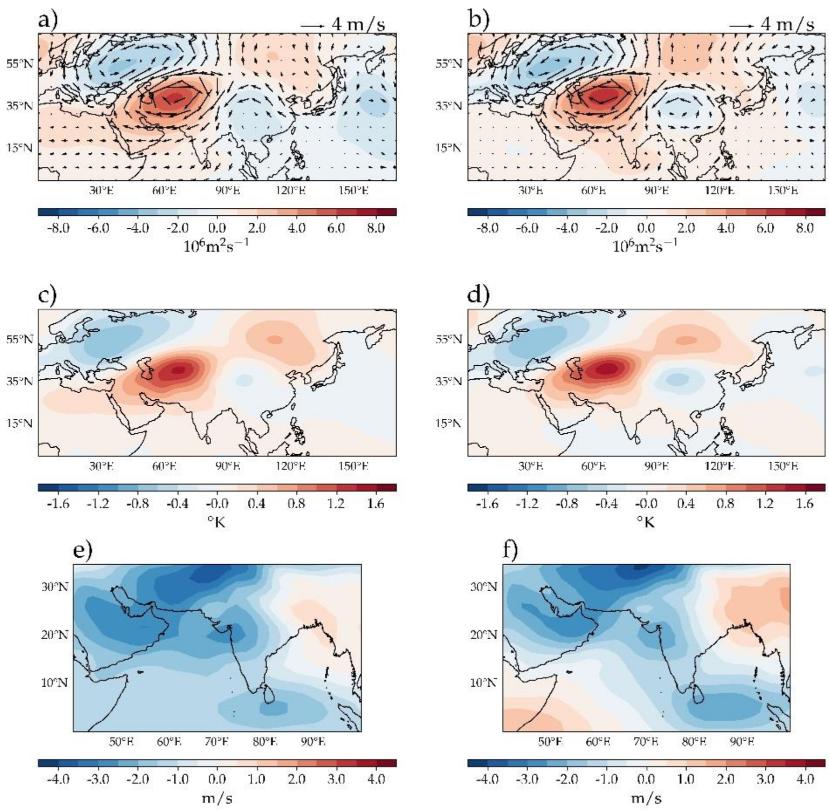

Figure 3.5 Left panel shows the difference between strong and weak WCA composites of 200 hPa eddy stream function (shaded) and wind vectors (a), tropospheric temperature (c) and easterly shear (e). Right panel shows the same difference in composites for 200 hPa eddy streamfunction and wind vectors (b), tropospheric temperature (d) and easterly shear (f), but the strong (weak) WCA composites were constructed by excluding the cases when the ISM was concurrently strong (weak).

The difference composites bring out the positive stream function and TT anomalies over WCA and the associated negative wind shear response over the ISM domain. Comparing the difference composites of wind and TT anomalies with (Figure 3.5 a, c, e) and without (Figure 3.5 b, d, f) ISM feedback, it can be inferred that even without the ISM feedback, the upper-level circulation anomalies are prominent over WCA (Figure 3.5 b, d, f). These findings indicate that, while the WCA region might be under the influence of circulation responses associated with ISM diabatic heating, the circulation anomalies over the region have an existence more or less independent of the ISM. It also means that the north Atlantic may be considered as the major source for the zonal teleconnection pattern and the WCA anomalies. It can be inferred that the Atlantic primarily drives the summertime CGT and it impacts the ISM through the WCA circulation anomalies. The circulation responses to the ISM diabatic heating further act as positive feedback reinforcing the upper-level anticyclones over WCA and forcing the downstream CGT.

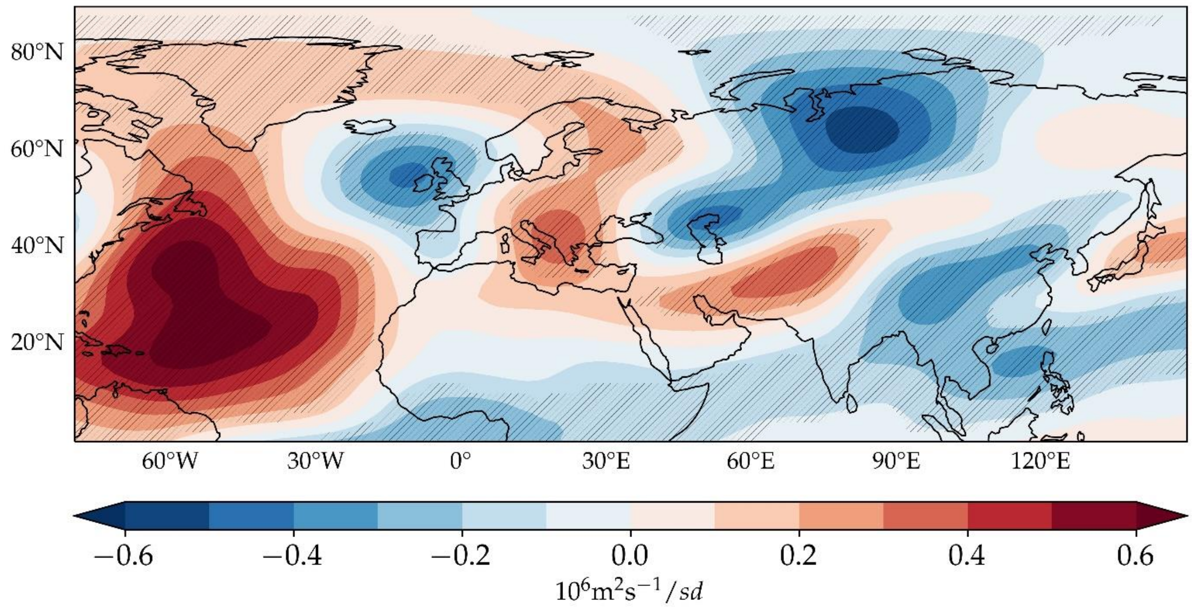

Figure 3.6 11-year running mean JJAS anomalies of 200 hPa eddy stream function regressed onto the AMO index. The regression coefficients are significant at 95% confidence level in the hatched regions.

3.3.4 Impact of AMO on circulation anomalies over WCA

The AMO and the ISM exhibit similar variability in the multidecadal timescale, and the Atlantic is considered as a major forcing for the ISM multidecadal variability. Since the WCA emerges as a major juncture in the Atlantic-ISM interactions in the interannual timescale, the feasibility of this mode of teleconnection is next explored in the multidecadal timescale. Multidecadal filtered 200 hPa eddy stream function fields are regressed on to the AMO index to bring out the upper-level teleconnection pattern associated with the AMO (Figure 3.6). Luo et al. (2011), showed the presence of a similar teleconnection pattern associated with the AMO in climate model simulations, which was interpreted as a manifestation of atmospheric Rossby waves, forced by extra-tropical north Atlantic SST anomalies. The arching wave pattern from the Atlantic forcing region across Eurasia is evident in Figure 3.6. Similar Rossby wave-train was also reported by Joshi and Ha (2019) characterized by alternate positive and negative polarity centres, extending from the North Atlantic to South Asia through Europe, acting as

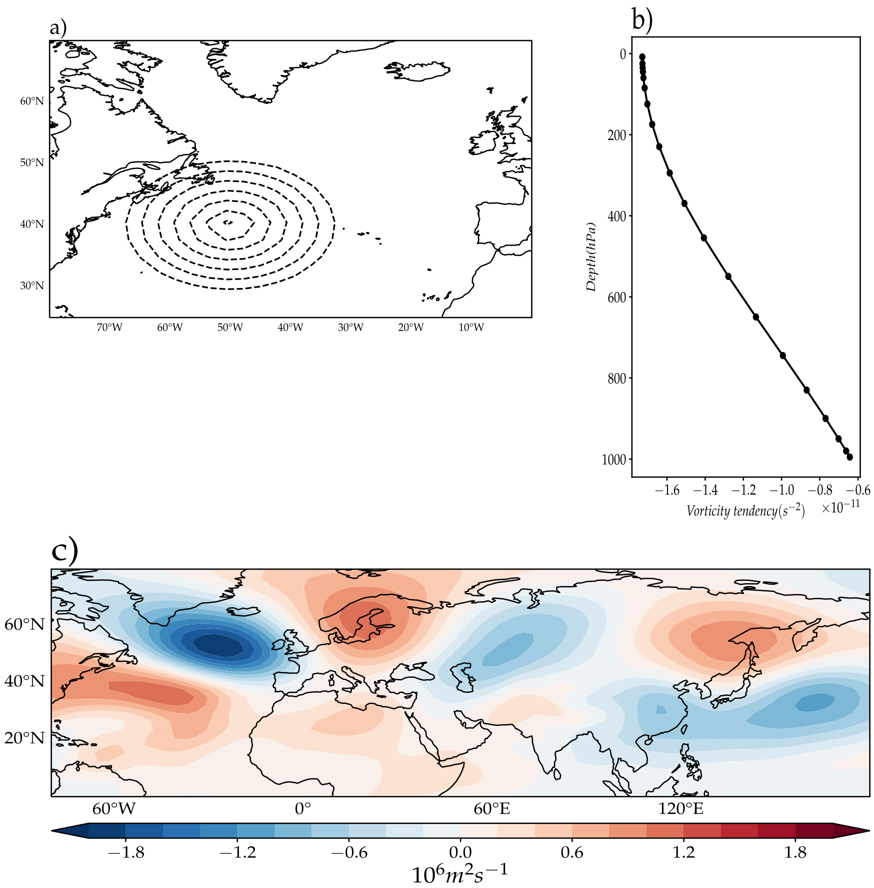

Figure 3.7 (a) Spatial and (b) vertical structure of idealised vorticity forcing over extratropical north Atlantic; (c) 200 hPa eddy streamfunction response to the prescribed forcing, on 20th day of integration

Another path for the extra-tropical signals to extend its influence up to the Indian monsoon region. In order to investigate the source of this teleconnection pattern LBM was forced with idealised vorticity anomalies over extratropical north Atlantic (Figure 3.7). Choice of such idealised equivalent barotropic structure of vorticity over the region is consistent with observational evidence reported in recent times (Borah et al. 2020b; Rajesh and Goswami 2020; Goswami et al. 2022). These studies suggest that in intraseasonal timescale extratropical SST anomalies over north Atlantic can trigger such vorticity structures which trigger downstream Rossby waves. In our LBM simulation, quasi-steady response was achieved in 18 days of integration. Figure 3.7c shows the 20th day response to idealised forcing which remarkably resembles the observed teleconnection.

Positive regression anomalies (Figure 3.6) observed over WCA implies that the region bears significance in the Atlantic-ISM teleconnection in the multidecadal time scale as well. Climate model simulations by Sandeep et al, 2022, also showed that a positive AMO phase can induce upper-level anticyclonic anomalies over WCA. The AMO, WCA and ISM indices exhibit coherent multi-decadal variability (Figure 3.8), and significant positive correlations are observed between the three indices (AMO and WCA - 0.34; AMO and ISM - 0.41; WCA and ISM - 0.47; all are statistically significant at 99% confidence level).

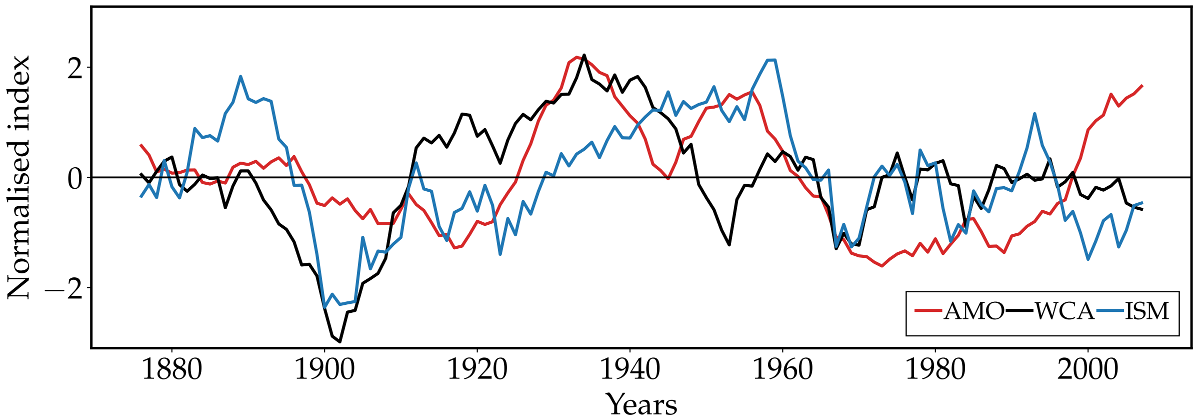

Figure 3.8 Multidecadal AMO, WCA and ISM indices from 1871-2012.

Figure 3.8 shows that during the recent AMO warm phase, the AMO is out-of-phase with both the WCA and the ISM. The AMO-ISM out-of-phase relationship in recent decades has been reported by several earlier studies (Sankar et al. 2016; Luo et al. 2018c; Naidu et al. 2020; Ahmad et al. 2022; Sandeep et al. 2022). While the exact mechanism still remains an open research problem, Indian Ocean warming and associated weakening of meridional thermal contrast over the monsoon domain is considered a plausible explanation for the observed weakening of monsoon in the recent AMO warm phase (Luo et al., 2018a; Sandeep et al., 2022). (Sabeerali et al. 2019) reported that the inverse relationship between the Atlantic Zonal mode and the ISM has strengthened in the recent decades, while based on climate model simulations, Ahmad et al., (2022) suggest that the natural SST variability over subtropical western North Pacific might be at play in changing the AMO-ISM relationship. On the other hand, Naidu et al, 2020, attribute the weakening of monsoon in the recent decades to the impact of aerosols and land use changes. (Wang et al. 2021) Sandeep et al., (2022) showed that the weakening of ISM during the recent AMO warm phase is associated with cyclonic anomalies over WCA. We further explore the AMO induced upper-level teleconnection and recent out-of-phase association between the AMO and ISM. To understand this further, we examine the upper-level teleconnection pattern during two positive AMO epochs, P1 (1926-1961) and P2 (1999-2012) (Figure 3.9 a, b). It is evident that the geopotential height anomalies over WCA

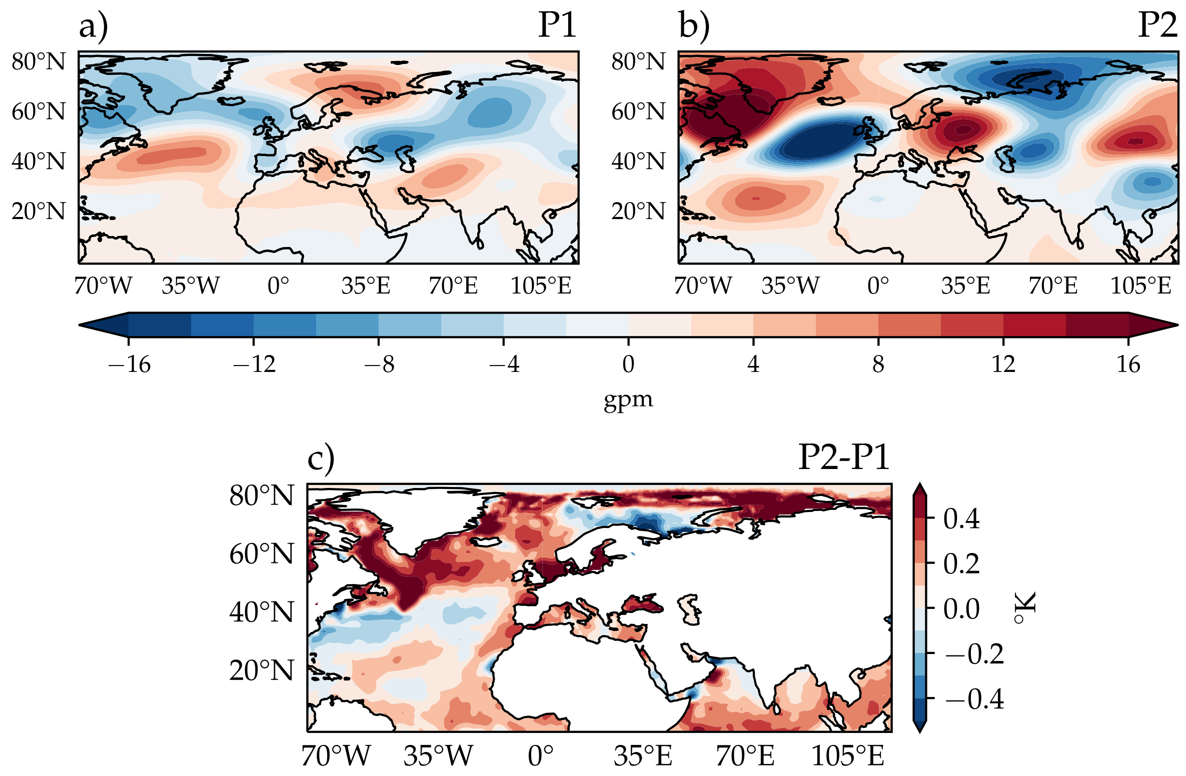

Figure 3.9 Composites of 200 hPa eddy geopotential height field during the two AMO warm epochs (a), P1 (1926–1961) and (b) P2 (1999–2012); (c) Difference between SST composites for the two epochs (P2-P1).

are anti-cyclonic during the first epoch P1 and cyclonic in the recent epoch P2. It is not just over WCA, the entire teleconnection pattern from the Atlantic sector to Asia is very different during the two epochs. Apart from WCA, the circulation anomalies over subtropical north Atlantic, the Mediterranean and East Asia, all show opposite anomalies during the recent epoch. The teleconnection pattern is very similar in the 200 hPa eddy geopotential height field composite during the P2 epoch in the JRA-55 dataset (Figure S2)

As the Atlantic is the main forcing domain for the teleconnection pattern, we further examined the SST anomalies over the north Atlantic during the two epochs in three different SST datasets (Figure S3). The SST difference composite for the two phases (P2-P1) (Figure 3.9c, HadISST) brings out the relatively warmer subpolar north Atlantic and the relatively cooler subtropical north Atlantic in the recent epoch. Using intermediate complexity model experiments, Ratna et al., (2021), demonstrated the sensitivity of atmospheric responses to the pattern and extent of SST anomalies over the north Atlantic and the Arctic regions. From the composite maps of 850 hPa and 500 hPa eddy geopotential height fields during the two epochs (Figure S4), it is evident that the high latitude warming alters the equivalent barotropic response over north Atlantic region. Equivalent barotropic responses to extra-tropical north Atlantic SST results from the interaction between local baroclinic response to heating and transient eddy vorticity fluxes (Kushnir et al. 2002). Such structures can alter the downstream teleconnection and the circulation anomalies over WCA (Borah et al. 2020). Therefore, the changes in the north Atlantic SST anomalies might explain the observed differences in the downstream responses and the overall teleconnection pattern changes. While earlier studies (Sandeep et al, 2022; Luo et al., 2018a) attribute the recent out-of-phase relationship between AMO and ISM to Indian ocean warming, we show that changes in the upper-level teleconnection associated with the AMO may also play a key role in modulating the circulation anomalies over WCA, and the cyclonic anomalies over WCA might in turn weaken the ISM by modulating the easterly vertical shear and tropospheric temperature over the region.

3.4 Summary

In this chapter, AMO-ISM teleconnection was explored through the possible modulation of midlatitude-ISM interaction. Northern hemispheric summer time CGT, which is the leading mode of midlatitude upper-level circulation variability, has a strong bearing on interannual variability of ISM. Circulation anomalies over north Atlantic and the Indian summer monsoon diabatic heating are the two main forcings which maintain the Northern hemispheric summertime CGT. Circulation anomalies over WCA forms a critical juncture in the CGT-ISM interaction. The CGT influences the ISM through the strong upper-level anticyclonic circulation anomalies over WCA and the ISM diabatic heating can also produce similar circulation responses over WCA and thus affect the CGT. A dry linear baroclinic model simulates the response to ISM heating reasonably well. Analysis of the WCA composites, including and excluding the ISM feedbacks, indicate that the circulation anomalies over WCA can have an existence more or less independent of the strength of the ISM. While the Rossby wave response associated with the monsoon may act as positive feedback in strengthening the WCA anomalies, the upstream forcing from the north Atlantic may have an upper hand in generating the WCA anomalies. In fact, equivalent barotropic vorticity forcing over extra tropical north Atlantic was shown to induce upper-level teleconnection with strong circulation anomalies over WCA. Such teleconnection pattern is remarkably similar to that related to AMO. As the influence of the Atlantic on the ISM via the WCA is evident in the interannual timescale, the feasibility of this mode of teleconnection is also explored in the multidecadal time scale. The significant co-variability of the AMO, WCA and ISM indices in the multidecadal timescale clearly supports this notion. Analysis of the upper-level teleconnection pattern associated with the AMO indicate that the multidecadal changes in circulation over WCA might play an important role in the Atlantic-ISM interactions in the multidecadal timescale as well.

Many studies have reported that the AMO-ISM association has weakened and become out-of-phase in recent decades. Earlier studies have reported that during the recent positive AMO phase, the upper-level anomalies are cyclonic over WCA and this has been attributed to the weakened meridional thermal contrast over the ISM domain, induced by Indian Ocean warming. Our analysis of the upper-level teleconnection patterns during the recent and previous AMO positive epochs reveals that it is not just the WCA anomalies that are different in the recent AMO positive epoch. The entire teleconnection pattern extending from the north Atlantic forcing domain has undergone major changes in the recent decade, which is found to be associated with the high latitude warming over the north Atlantic. We propose that the equivalent barotropic responses to the extra-tropical north Atlantic SST anomalies, in turn alter the downstream teleconnection and the circulation anomalies over WCA. The cyclonic anomalies over WCA might in turn weaken the ISM by modulating the easterly vertical shear and tropospheric temperature over the region.

Supplementary Figures

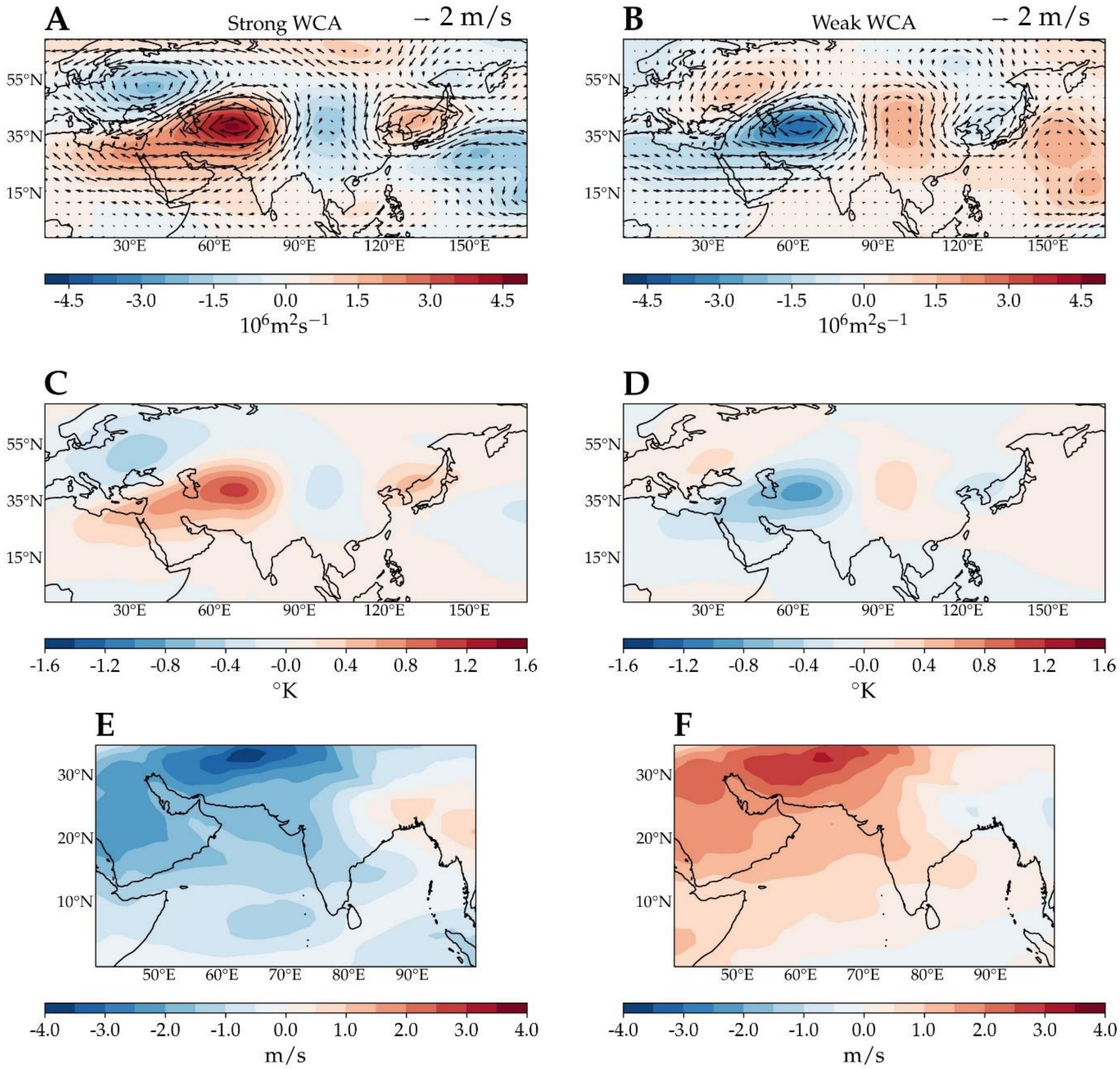

Figure S1 Same as Figure 3.1, but using JRA-55 dataset

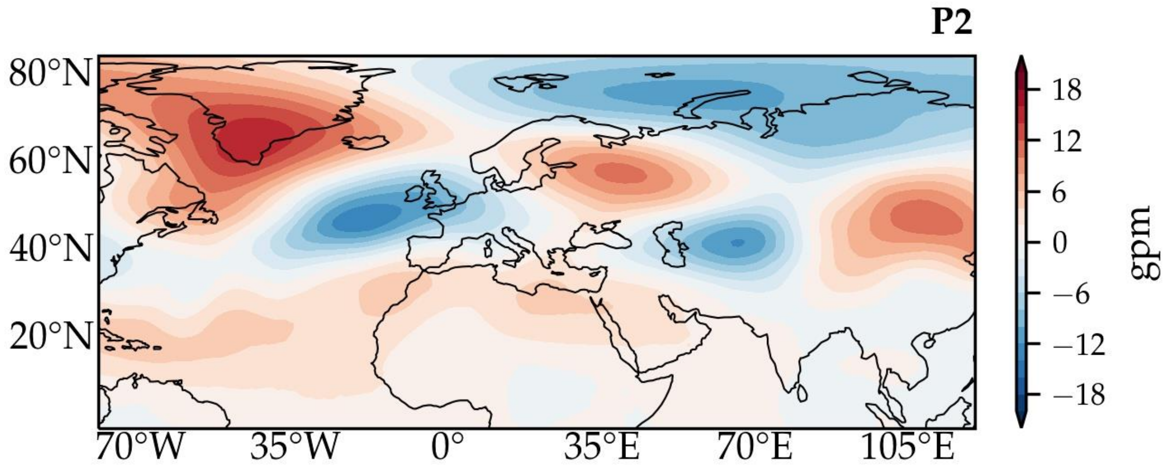

Figure S2 Composite of 200 hPa eddy geopotential height field during the P2 epoch in the JRA-55 dataset

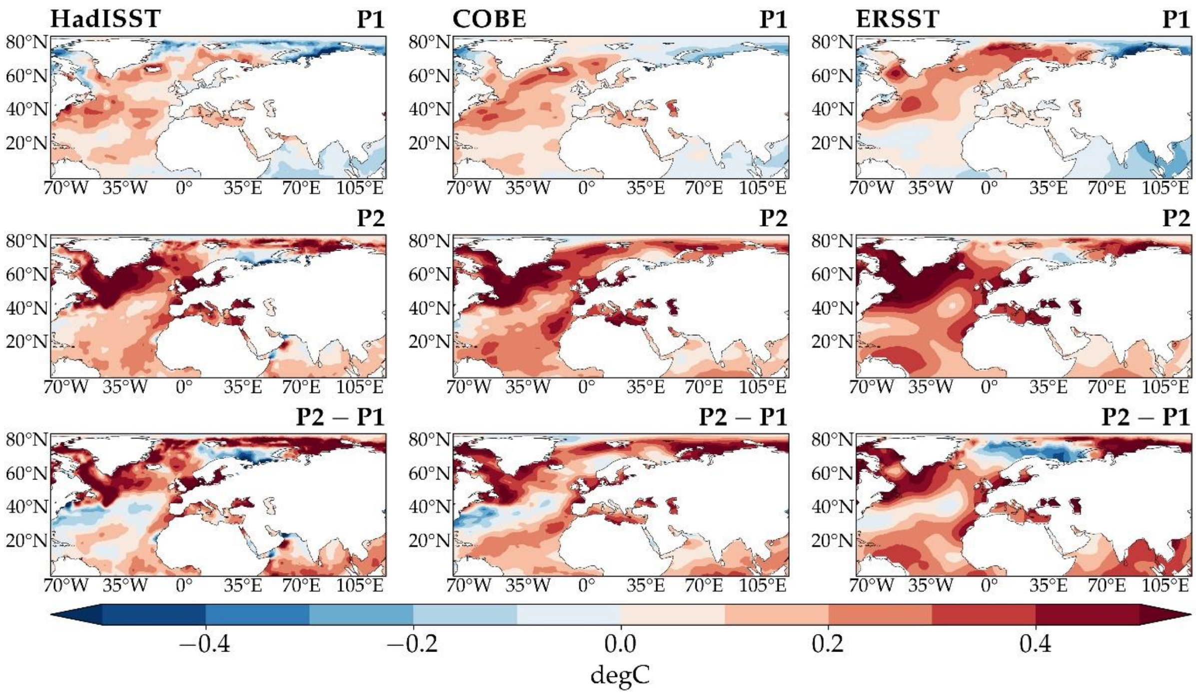

Figure S3 Composites of JJAS SST anomalies for the AMO warm epochs (P1:1926-1961 and P2:1999-2012) and difference in composites between P2 and P1, calculated for three different SST datasets

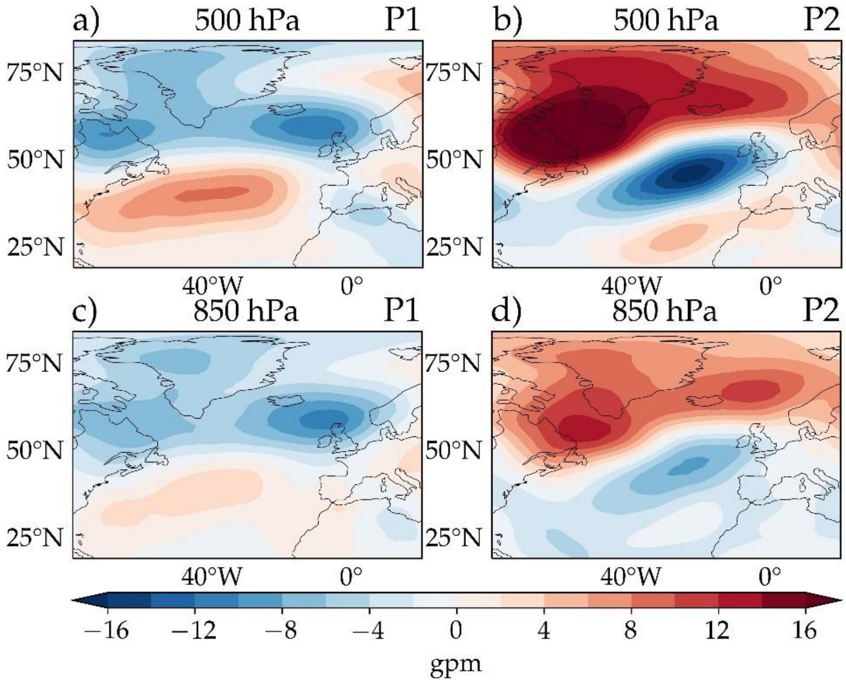

Figure S4 Composite mean of eddy geopotential height fields for the AMO warm epochs P1 (A and C) and P2 (B and D) at 500 hPa (A and B) and 850 hPa (C and D)

Chapter 4

AMO induced Pacific variability and its impact on ISM

• Abstract

The role of AMO induced Pacific Ocean variability and its impact on ISM in the multi-decadal timescales are explored, in a suit of Atlantic pacemaker experiments, using a simplified coupled general circulation model (GCM). Changes in the Walker circulation induced by the air-sea interaction over the equatorial Pacific Ocean is found to be the key bridge between the AMO and ISM, which is consistent with earlier studies. North Pacific SST responses associated with the atmospheric bridge mechanism on the other hand is also known to induce low-level convergence over the Western Pacific and hence thought to be crucial in the ISM multi-decadal variability. However, both observations and model simulations show a weak North Pacific bridge during the summer monsoon season. The extratropical-tropical SST gradient between the north Pacific and equatorial Pacific is shown to be a crucial aspect of the observed AMO-ISM relationship. The strongest AMO-ISM correlation exists when the AMO leads the ISM by 8 years which is likely to be related to the delayed north Pacific response to AMO forcing. The strongest extratropical-tropical SST gradient is also observed when the AMO leads the ISM by 8 years. However, this delayed Pacific response is not markedly different from the concurrent response in model simulations. Additional sensitivity experiments indicate a larger impact of tropical north Atlantic in the observed teleconnection, compared to its extratropical counterpart. Our analysis also shows a better representation of observed AMO-ISM relationship when the GCM incorporates a full dynamical ocean model instead of a thermodynamic (slab) ocean model. And the difference primarily arises from the realistic simulation of Walker circulation anomalies associated with the AMO.

4.1 Introduction

The AMO has a significant bearing on the variability of ISM (Goswami et al. 2006; Wang et al. 2009; Monerie et al. 2019). The warm phase of AMO is known to cause a northward shift in the Intertropical Convergence Zone (ITCZ) resulting in large rainfall anomalies over Sahel and the Indian monsoon regions (Sutton and Hodson 2005; Zhang and Delworth 2006; Knight et al. 2006). The AMO can also impact the ISM through extratropical wave trains (Li et al. 2008; Dutta and Neena 2022), modulation of interhemispheric thermal contrast and modulation of El Nino Southern Oscillation (ENSO) variability (Wang et al. 2009; Luo et al. 2018a). Since the Pacific Ocean is known to constrain the ISM variability in the interannual to decadal timescales (e.g., Krishnamurthy and Goswami 2000), the Pacific Ocean acting as a mediating link in the Atlantic - ISM interactions in the multi-decadal timescale are a distinct possibility. In fact, the AMO impacting the low-level convergence over the South Asian region through changes in the Pacific Ocean has been discussed in many studies (Kucharski et al., 2016a, b; Sun et al., 2017, 2019; Monerie et al., 2019). Numerous studies have shown evidence for the strong impact of AMO on the decadal to multi-decadal climate variability in the north Pacific and equatorial Pacific (Liu and Alexander 2007; Zhang and Delworth 2007; Okumura et al. 2009; Yeh et al. 2015; Johnson et al. 2020a). The AMO can induce variabilities over the Pacific Ocean in two ways. Tropical Atlantic warming (cooling) can trigger an anomalous Walker circulation resulting in cooler (warmer) equatorial eastern Pacific (Dong et al. 2006; Kucharski et al. 2016). The extra-tropical north Atlantic warming can also warm the north Pacific through AMO induced subsidence (Sun et al. 2017; Gong et al. 2020) and through weakening of the mean westerly winds and poleward eddy transport (Zhang and Delworth 2007). Sun et al. (2017), showed that such north Pacific warming can induce a secondary circulation through wind-evaporation-SST feedback which lowers the mean sea level pressure over equatorial western Pacific. The resulting low-level convergence can impact the climate over the Indian subcontinent (Sun et al. 2019). The overall Pacific response to AMO forcing is indeed reflected in the SST gradient that develops between the extratropical north Pacific and equatorial eastern Pacific. Such SST gradient has been shown to be a crucial aspect of the model simulated AMO-ISM relationship (Luo et al. 2018a, b). In this chapter the potential impacts of the north Pacific and equatorial Pacific atmospheric bridge mechanisms are explored in the context of observed AMO-ISM relationship.

4.2 Data and methodology

The primary datasets used are monthly mean fields of sea level pressure and winds from 20th century reanalysis (20CR, Compo et al. 2011), available from National Oceanic and Atmospheric Administration (NOAA), for the period 1901-2012. We also used monthly mean field of sea surface temperature, HadISST (Rayner et al. 2003). Monthly data of All India rainfall was obtained from the Indian Institute of Tropical Meteorology (https://tropmet.res.in/static_pages.php?page_id=53). The AMO index is defined as the normalised time series of global mean removed, area averaged (75°W -5°E, 0-60°N) north Atlantic SST anomalies (Trenberth and Shea 2006).

4.2.1 Model experiments

The model experiments discussed in this chapter are conducted using the atmospheric general circulation model (AGCM) -Simplified Parameterizations, primitive-Equation DYnamics or "SPEEDY" developed at the Abdus Salam International Centre for Theoretical Physics (ICTP) (Kucharski et al. 2013). It is a spectral model with T30 horizontal resolution. The model has 8 vertical levels. The AGCM is coupled with ocean model NEMO (Nucleus for European Modelling of the Ocean) (Madec 2008) with OASIS coupler (Valcke 2006). NEMO has 31 vertical levels. It has ORCA2 tripolar grids with horizontal resolution of ½° over tropics and 2° elsewhere. This SPEEDY-NEMO coupled model configuration uses a flux correction scheme following Kröger and Kucharski 2011. The coupled model is restarted from a 300-year long control run. Subsequently, a transient run from 1872 to 2012 was performed. Multiple ensemble runs were made by restarting the model and applying small atmospheric perturbations. The analysis was performed from 1900 to 2012 after discarding initial years owing to spin up. Additionally, the model is also coupled with a slab ocean model (SOM). SOM which has a depth of 30m in the tropics and 60m in the extratropics, which is the typical mixed layer depths found in these regions and it is maintained at a constant value. We adopted the same methodology used by Kucharski et al, 2016. Figure 4.1 shows a schematic of the experiment design and Table 4.1 summarises the pacemaker experiments performed. In the control run (***CTRL***), the AGCM is forced with climatological SSTs over Indo-Pacific basin whereas over the Atlantic Ocean, it is forced with observed monthly varying SSTs. In the pacemaker run, the AGCM is either coupled with the SOM (***ATL_SOM***) or NEMO (***ATL_NEMO***) over Indo-Pacific basin and it is forced with observed monthly varying SSTs over the Atlantic Ocean. In order to avoid the instabilities occurring in the boundaries, a sponge layer of width 7.5° is added where the SST anomalies are calculated as the weighted average of prescribed SST anomalies and model SST anomalies.

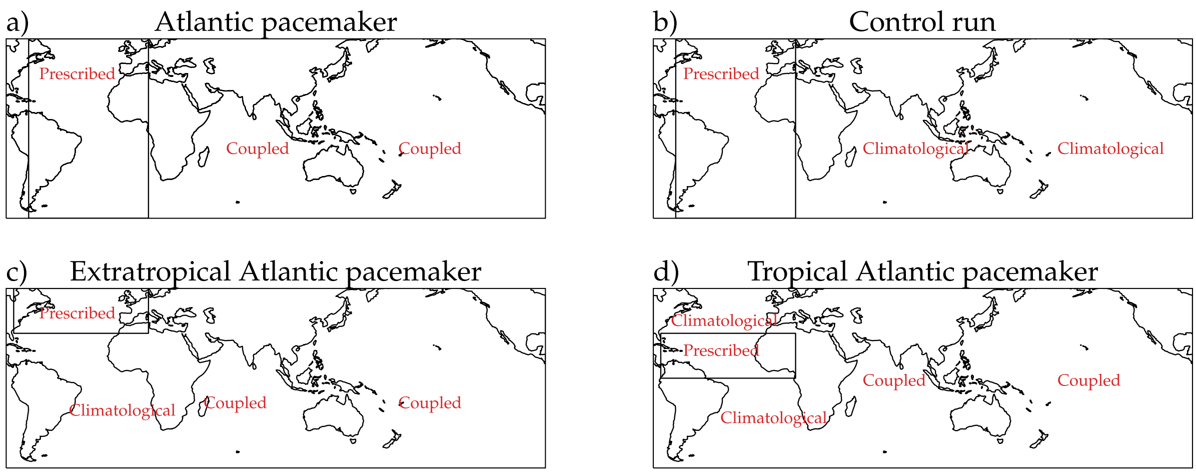

Figure 4.1 Schematic showing pacemaker experiment designs

The weight linearly drops from 1 at the domain to 0 outside the sponge layer. The difference between the pacemaker and control run essentially brings out the role of air-sea interactions over the Indo-Pacific basin. Two other suits of pacemaker experiments were also carried out labelled as ***EXTROP_ATL_NEMO*** and ***TROP_ATL_NEMO***. For the former, over the

Atlantic Ocean, the model was prescribed with observed SST north of 30°N and climatological SST over the rest of the Atlantic. For the later experiment, over the Atlantic Ocean, the model was prescribed with observed SST from 0°N to 30°N and climatological SST over the rest of the Atlantic. In both of these experiments, the Indo-Pacific basin remains fully coupled.

EXPERIMENT	Forcing over Atlantic	Indo-Pacific basin	Ocean model	No of ensembles
CTRL	Observed SST	Climatological SST	None	6
ATL_SOM	Observed SST	Coupled	Slab	6
ATL_NEMO	Observed SST	Coupled	NEMO	9
EXTTROP_ATL_NEMO	Observed SST from 30N to 60N; climatological SST elsewhere	Coupled	NEMO	9
TROP_ATL_NEMO	Observed SST from 0N to 30N; climatological SST elsewhere	Coupled	NEMO	9

Table 4.1 Summary of pacemaker experiments

4.2.2 Mass streamfunction

The zonal mean meridional circulation is represented using the zonal mass stream function,

$$\psi_m(\varphi, p) = \frac{2\pi a \cos\varphi}{g} \int_0^{p_s} v(\varphi, p)\, dp$$

Where v is zonal mean meridional wind, p_s is the surface pressure, φ is the latitude, a is the radius of Earth and g is the acceleration due to gravity. This definition of ψ_m is consistent with the conservation of mass. ψ_m is a useful metric of strength and extent of Hadley circulation (e.g., Nguyen et al. 2013). To calculate the probability distribution of parameters during different AMO phases, we used the gaussian kernel density estimate (Rosenblatt 1956; Parzen 1962). All the analysis was performed on summer (June to September) seasonal anomalies unless otherwise specified. An 11-year running mean was applied to the seasonal anomalies to bring out the multi-decadal signal. Statistical significance was tested using Student-t test.

4.3 Results

4.3.1 ISM response in pacemaker experiments

First, we investigated the AMO-induced changes in the monsoon circulation in observations, control and pacemaker experiments. Mean sea level pressure (SLP) and 850 hPa winds were regressed on the normalised AMO index (Figure 4.2). Observations (Figure 4.2d) show a large area of negative SLP anomalies over the Indian subcontinent as well as strengthened low-level south-westerly wind anomalies. Such a monsoon response is linked with the northward migration of ITCZ as discussed in Zhang and Delworth, 2006. Next, we explored the relative contributions from the direct atmospheric forcing induced by AMO and the Pacific Ocean mediated response induced by the AMO, in the observed AMO-ISM relationship. Consistent with Kucharski et al, (2016b), who looked into annual mean fields, the direct atmospheric response, in the absence of any air-sea interaction, tend to weaken the ISM (Figure 4.2a). An extended region of positive SLP anomalies is observed over the Indian subcontinent. Such positive SLP anomalies are consistent with largescale subsidence as discussed in Sect 4.3.2. However, when the Indo-Pacific coupling was allowed, the ISM response somewhat improved, especially when full dynamical coupling was allowed (Figure 4.2c). Pacemaker experiment with a slab ocean (ATL_SOM) simulates a weaker monsoon albeit a reduction in positive SLP anomalies compared to the control run. However, when a full dynamical ocean model is used (ATL_NEMO), there's a considerable drop in SLP over the subcontinent suggesting low-level convergence over the region. Although the Pacemaker experiments have limitations in simulating the observed low-level winds over the ISM domain, on comparing with the control simulation (Figure 4.2e-f) it is evident that the Indo-Pacific feedback reduces the sea level pressure and contributes to the low-level convergence over the ISM domain.

The AMO induced ISM anomalies were also explored in the changes in the mean meridional circulation. It is quantified by the zonal mean meridional stream function (ψ_m) as discussed in Section 4.2.2. Figure 4.3a and 4.3c shows the climatological mean ψ_m in observations and pacemaker simulation. It is interesting to note that the model climatology is remarkably similar to the observed mean. The observed ψ_m anomalies in response to the AMO, show strong upward motion north of 20°N (Figure 4.3b). This is consistent with the fact that the north Atlantic warming associated with the AMO tend to shift the ITCZ northward (Zhang and Delworth, 2006). The Pacemaker experiments indeed captures the observed strengthening of the meridional circulation and the ISM as is evident in Figure 4.3d.

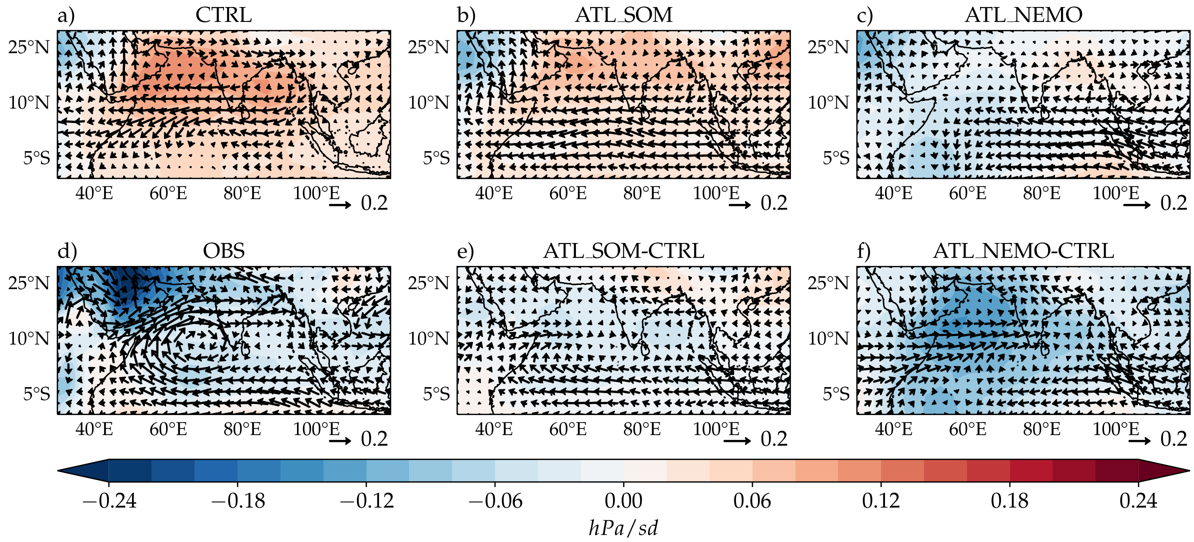

Figure 4.2 Anomalies of sea level pressure (shading) and 850 hPa winds (vectors) are regressed on the AMO index for model experiments (a-c), observation (d); the difference maps between pacemaker experiments and control experiment are plotted (e-f)

4.3.2 Equatorial Pacific atmospheric bridge

To further understand the AMO impact on the ISM, the AMO-induced zonal circulation anomalies are examined. Figure 4.4d shows the 850 hPa velocity potential anomalies regressed on the AMO index and it brings out the regions of low-level convergence and divergence associated with the AMO. Strong low-level convergence associated with warm SSTs is evident over the tropical Atlantic. The resulting zonal circulation anomalies cause a characteristic SST response over the Pacific Ocean which consists of strong cooling over the central and eastern and equatorial and warming over the north Pacific and western equatorial Pacific (Section 4.3.4).

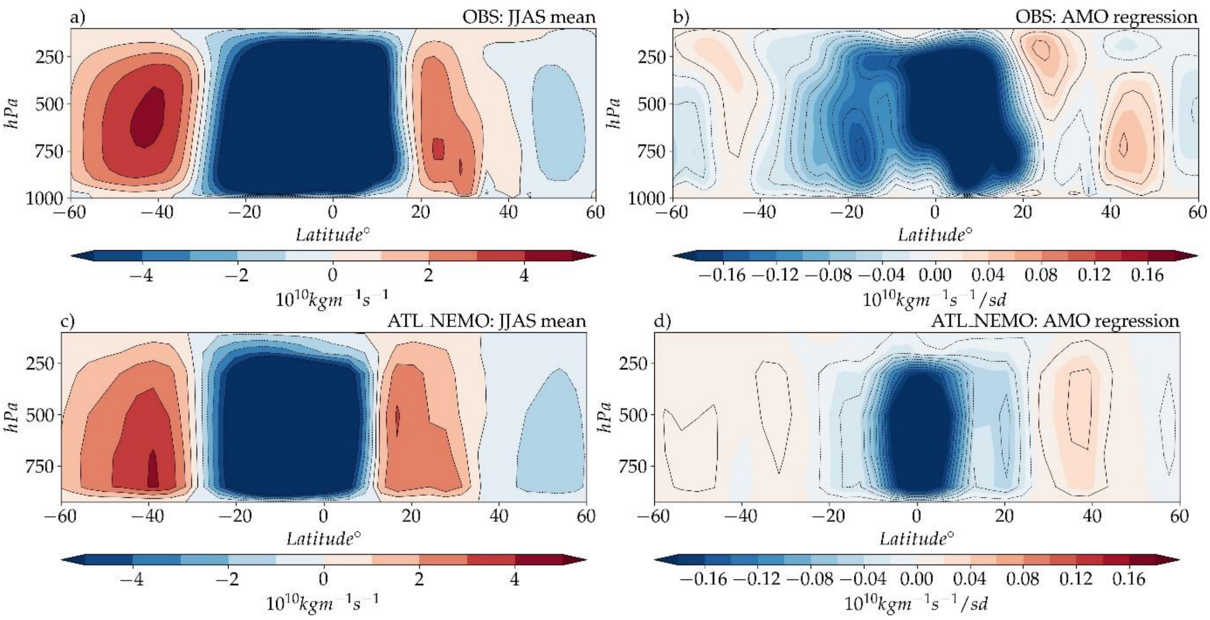

Figure 4.3 (Left) Summer climatology of zonal mean meridional streamfunction in (a) observation and (c) ATL_NEMO simulation; (right) decadally filtered, boreal summer anomalies of zonal mean meridional streamfunction regressed on normalised AMO index for (b) observation and (d) ATL_NEMO

Figure 4.4d shows large scale low-level divergence over eastern equatorial Pacific resulting from large scale subsidence over the region in response to Atlantic warming. The CTRL experiment fail to simulate the anomalous Walker circulation realistically (Figure 4.4a), which resulted in a weaker monsoon as seen in Figure 4.2a. The Walker circulation anomalies became more realistic when the slab ocean model (ATL_SOM) was incorporated to represent the Pacific Ocean feedback (Figure 4.2b). Finally, the ATL_NEMO which incorporates the full ocean dynamical coupling simulates the observed Walker circulation anomalies reasonably well. It is to be noted that the observed anomalous Walker circulation is much more pronounced when the AMO leads by almost a decade compared to the simultaneous association (Yang et al. 2020). But the such lagged response is not much different from the simultaneous response in the pacemaker runs (Section 4.3.4).

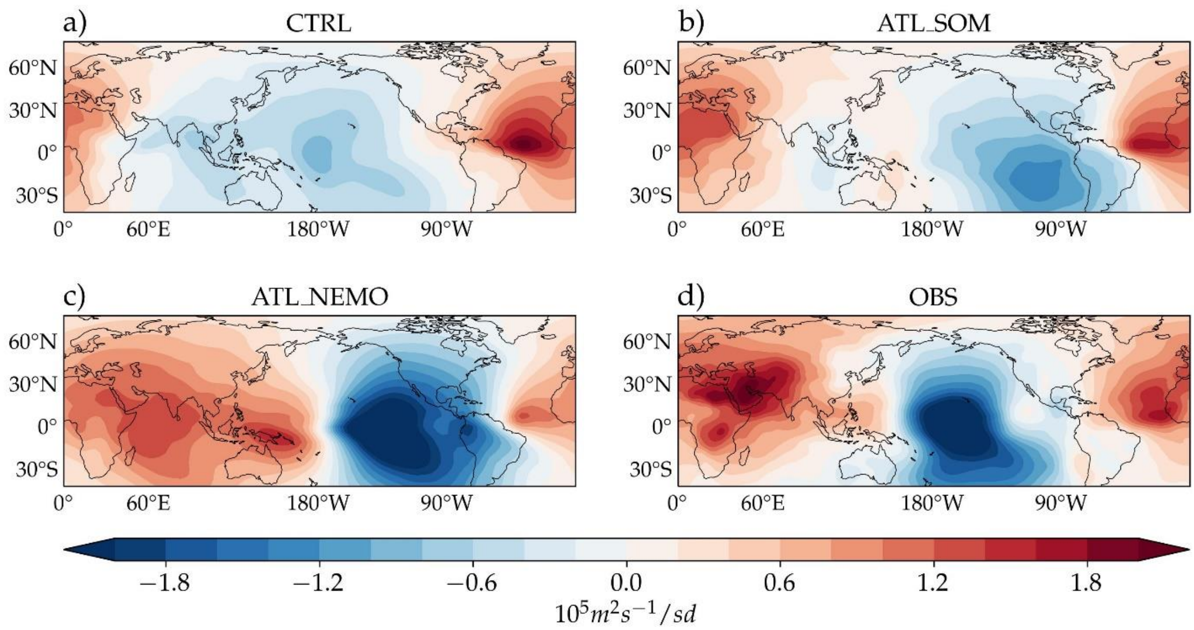

Figure 4.4 11-year running mean JJAS anomalies of 850 hPa velocity potential regressed on normalized AMO index

4.3.3 North Pacific atmospheric bridge

We also looked into the possibility of a north Pacific atmospheric bridge in modulating the ISM. Warming over the north Atlantic tend to induce a subsiding motion over the north Pacific. This weakens the Aleutian low which subsequently weakens the westerly winds. Wind-evaporation-SST feedback warms the SST over the north Pacific. Sun et al, 2017,2019 showed such warming over north Pacific can induce a secondary circulation response which tend to enhance the low-level convergence over the western Pacific. We investigated whether a similar mechanism during the summer might impact ISM through modulation of low-level convergence over the monsoon domain.

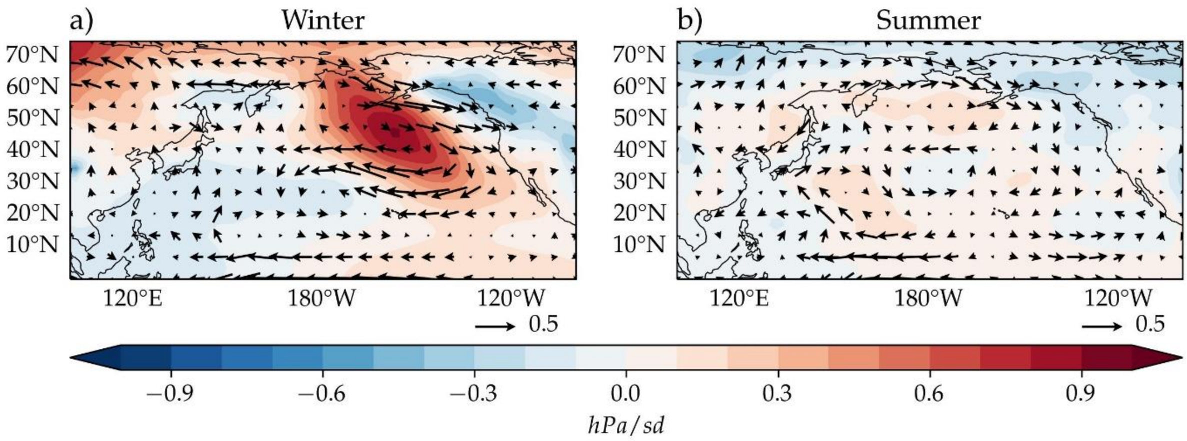

Figure 4.5 Sea level pressure (shading) and 850 hPa winds (vectors) regressed on the normalised AMO index over north Pacific during (a) Dec-Feb and (b) Jun-Sept

Figure 4.5a shows that during winter the north Pacific bridge is prominent, however, during summer the north Pacific bridge is hardly present (Figure 4.5b). Model experiments also captured this strong winter response reasonably well (Figure 4.6a-c). Unlike its winter counterpart, the AMO induced north Pacific SLP anomalies are not organised during summer, suggesting a little impact of the proposed bridge mechanism during summer (Figure 4.5b, 4.6d-f). Control and pacemaker experiments also show little response over the north Pacific through direct atmospheric forcing arising from AMO.

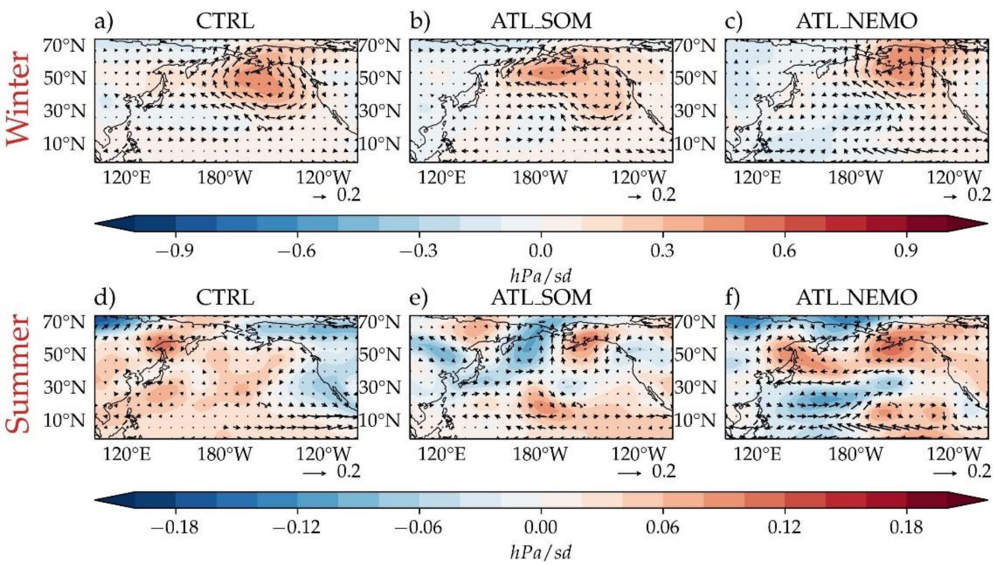

Figure 4.6 Sea level pressure (shading) and 850 hPa winds (vectors) regressed on the AMO index over north Pacific during (a-c) Dec-Feb and (d-f) Jun-Sept

This suggests the atmospheric bridge has a significant seasonality and it might not be crucial for the observed AMO-ISM association.

4.3.4 Delayed Pacific response and AMO-ISM lagged relationship

Figure 4.7 shows the global SST anomalies associated with AMO. The SST gradient between the extratropical north Pacific and equatorial Pacific is an essential measure of Pacific response to AMO. Figure 4.7a-b show that the pacemaker experiments do simulate this strong SST gradient but somewhat overestimate the observed pattern. Studies have shown that a strong positive Pacific SST gradient results in an enhanced Hadley circulation over the ISM domain and are associated with positive ISM anomalies (Luo et al. 2018a, b). In fact, a weak correlation (statistically significant) does exist between the Pacific SST gradient and ISMR in decadal timescale (Figure 4.8c) as well. Luo et al. 2018a, showed that CMIP5 models which capture the AMO-ISM relationship reasonably well, exhibit a strong Pacific SST gradient. The Pacific response is much more pronounced when the AMO leads the Pacific SST anomalies by almost a decade (Yang et al. 2020). Zhang and Delworth, 2007, attributed the delayed response to the timescale of ocean dynamical adjustment and associated air-sea interaction that takes place over the north Pacific.

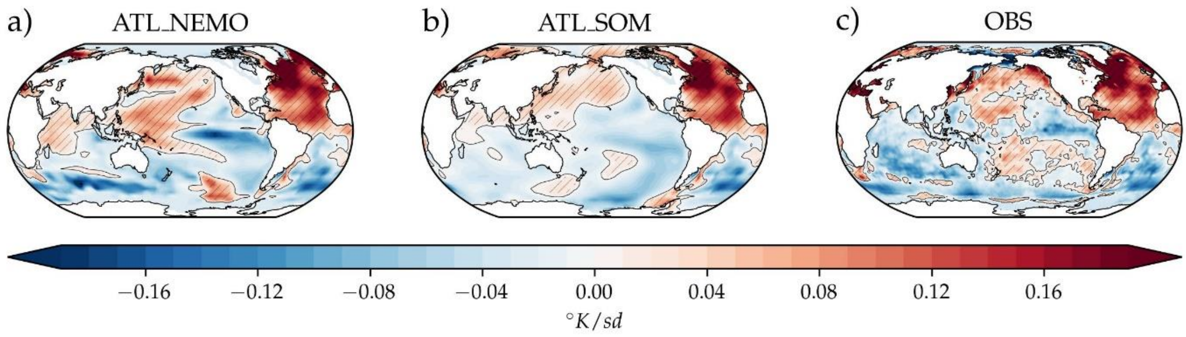

Figure 4.7 Summer time global SST anomalies regressed on AMO index; hatched regions indicate statistically significant regression coefficients

The oceanic Rossby waves takes about 7-9 years to travel from eastern extratropical north Pacific to western extratropical north Pacific which enhances the north Pacific warming through air-sea interaction. Figure 4.8b shows the probability density functions of Pacific SST gradient for AMO phases. It is clear from the figure that the Pacific SST gradient is well organised with respect to AMO phases when AMO leads the SST anomalies by 8 years. In fact, the AMO-ISM correlation is highest when the AMO leads ISM by 8 years (Figure 4.8a). The delayed north Pacific response possibly drives such lagged association. Yang et al, 2020, showed that the AMO induced Walker circulation anomalies are more pronounced when the Pacific SST gradient is well developed at a lag of almost a decade.

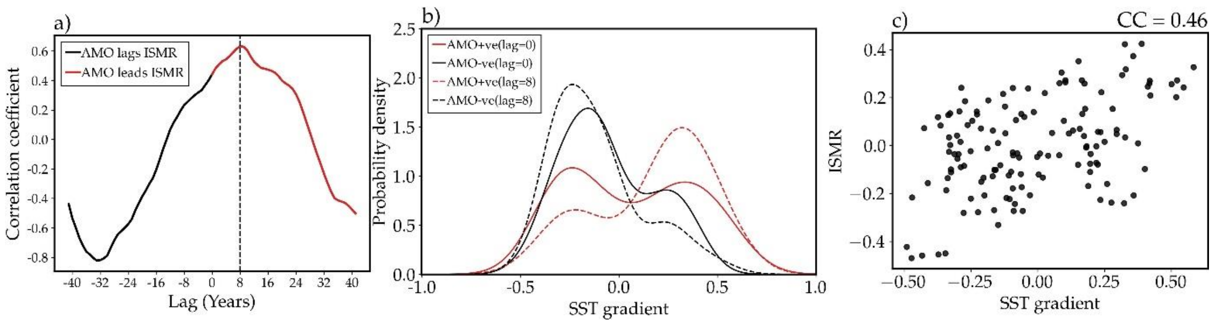

Figure 4.8 a) Lead-lag correlation between decadally filtered AMO index and ISMR; b) probability density functions of Pacific SST gradient for AMO positive and negative phases; solid curves indicate concurrent association and dashed curves are drawn for cases when AMO leads Pacific SST anomalies by 8 years; c) scatter plot showing the relationship between decadally filtered ISMR and Pacific SST gradient; correlation coefficient is shown on top right

The ATL_NEMO experiment shows a well-developed Pacific gradient in response to AMO forcing at zero lag which persists for a decade (Figure 4.9a). Hence, unlike the response in observations, the model does not show a significant difference in delayed response compared to concurrent response. Such a strong concurrent response is also reflected in the fact that at zero lag the AMO induced Walker circulation anomalies in the model simulation are much more vigorous over the monsoon domain compared to observations (Figure 4.4c, d). A strong meridional gradient in SST tends to enhance the Walker circulation anomalies.

While the AMO manifests as a basin scale feature over the north Atlantic, the signal is stronger over the extratropics and higher latitudes (Fang et al. 2022). The descending branch of Atlantic Meridional Overturning Circulation (AMOC) associated with dense water mass formation in the high latitudes significantly impacts the SST over these regions.

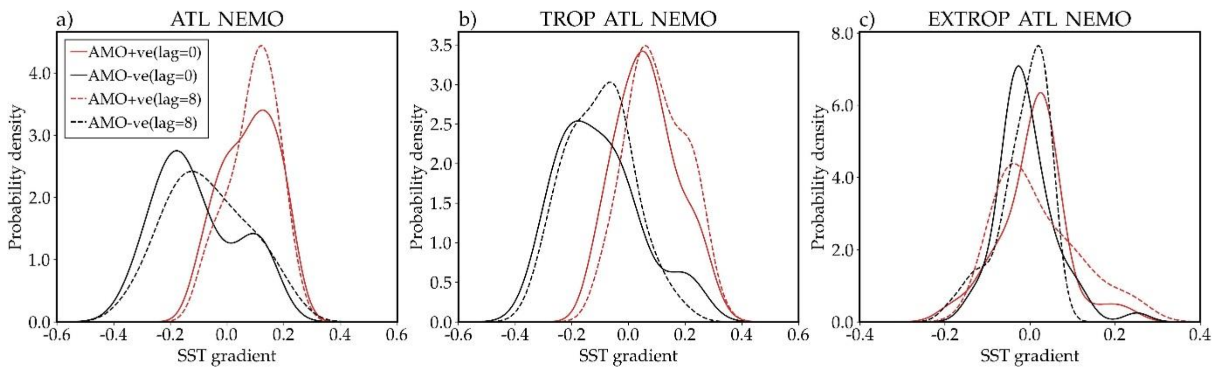

Figure 4.9 Same as Figure 4.8b, but for different pacemaker experiments

Hence it is imperative to examine if the monsoon response simulated in the pacemaker experiment is actually coming from the extratropical forcing or not. It is evident from Figure 9 the tropical Atlantic plays a key role in setting up the extratropical-tropical SST gradient. In fact, Johnson et al. (2020b), showed that the eastern equatorial Pacific response to tropical north Atlantic heating can trigger a meridionally arching wave response towards north Pacific. Such a response can in turn induce SST anomalies over extratropical north Pacific. These results indicate the importance of tropical north Atlantic SST anomalies in driving the Pacific SST gradient and hence modulate the strength of ISM in multi-decadal timescale. Nevertheless, the impact of extratropical north Atlantic forcing needs to be further explored using more comprehensive climate model simulations.

4.4 Summary

In this chapter, the AMO induced Pacific variability and its impact on ISM are explored using simple model experiments with an intermediate complexity coupled GCM. Pacemaker experiments were carried out where the model was forced by observed Atlantic Ocean variability and the results explain the concurrent AMO-ISM relationship through equatorial atmospheric bridge mechanism. An anomalous Walker circulation resembling the La Nina conditions over the Pacific aids in enhancing the low-level convergence over the ISM domain and strengthening the monsoon. Coupling the atmospheric model with a full dynamical ocean model tends to capture the ISM variability much more realistically compared to coupling with a slab ocean model. This comes from the fact that the anomalous Walker circulation is better simulated with a full dynamical ocean model. Additionally, north Pacific SST anomalies, in response to AMO, are known to induce secondary circulation anomalies over equatorial western Pacific which can also impact the low-level convergence over the monsoon domain. Such responses seem to be weak during the summer monsoon season in both observations and model experiments. Finally, we discuss the delayed Pacific response to AMO forcing. It is seen that AMO-ISM strongest association exists when AMO leads ISM by 8 years. Such delayed association is consistent with the development of strong extra-tropical-tropical SST gradient between north Pacific and equatorial Pacific. In fact, the decadal variability of ISM is significantly correlated to the strength of the SST gradient. This delayed Pacific response is not markedly different from the concurrent response in model experiments. The pacemaker experiment where the model is forced with observed SST over the entire Atlantic, shows strong concurrent and delayed SST gradient. Separate experiments with prescribed forcing over tropical north Atlantic and extratropical north Atlantic suggest the meridional SST gradient can be largely explained by AMO forcing arising from tropical north Atlantic.

Pacemaker experiments failed to simulate realistic Indian Ocean SST anomalies associated with AMO forcing. Proper representation of Indian Ocean SST might improve the simulated low-level winds over the ISM domain. The ISM response in the simulations is primarily a result of Atlantic forced Pacific variability and associated anomalies in Walker circulation. Further work should be carried to account for the monsoon variability coming from Indian Ocean anomalies in response to AMO. While model experiments suggest tropical Atlantic as the key driver to the observed teleconnection, future works should also investigate the role of extratropical air-sea interaction over the north Atlantic in the AMO induced Pacific variability.

Thesis summary

In this thesis, the AMO-ISM relationship is explored using observational datasets, long climate model simulations from CMIP5/PMIP3 archive, and simple model experiments. It highlights the central role played by the atmospheric teleconnection processes through two dominant pathways. The AMO-induced stationary wave response across Eurasia has a significant bearing on ISM multi-decadal variability. Extratropical SST anomalies associated with AMO warm phase/cold phase trigger equivalent barotropic response over North Atlantic. Such circulation structure can trigger downstream Rossby waves with significant anomalies over central Asia. An idealized model experiment with a dry linear baroclinic model is able to capture this teleconnection pattern. Resulting circulation anomalies over central Asia impacts ISM through anomalous meridional tropospheric temperature gradient and easterly shear. Change in this teleconnection pathway has played a central role in the recent out-of-phase AMO-ISM relationship. Anomalous high latitude warming over North Atlantic Ocean altered the stationary wave response in the recent AMO warm phase causing a weakening in ISM. However, the exact mechanism through which the central Asian circulation anomalies interact with ISM in intraseasonal timescale needs more investigation. Also, there exists a large disagreement in the simulated stationary wave response across the state-of-art GCMs. More work needs to be done to understand the limitations of the simulated response. AMO-induced Pacific Ocean variability is rather robust in the GCMs. Sensitivity experiments with an intermediate complexity GCM highlights the key aspects of this teleconnection pathway. Anomalous Walker circulation resulting from AMO induced equatorial Pacific Ocean variability is the primary mode of AMO-ISM teleconnection. On the other hand, model simulations show significant seasonality in the North Pacific response to AMO and might not play any significant role in the observed teleconnection. The strongest AMO-ISM correlation is observed when AMO leads ISM by almost a decade which is consistent with the development of a strong meridional gradient in SST over the Pacific Ocean. Model simulations capture the lagged response and indicate that significant forcing might arise from the tropical North Atlantic SST anomalies.

While this thesis brings out the essential atmospheric teleconnection mechanisms in the observed AMO-ISM relationship, it also highlights the need for a better representation of these processes in GCMs for a better projection of future AMO-ISM link. Future work should also include understanding the North Atlantic wave activity for different regimes of atmospheric variability over the Euro-Atlantic sector. Having insights into how AMO modulates the statistics of these activities would be crucial to our understanding of the AMO-ISM relationship. Also, how such wave activity impacts the monsoon intraseasonal variability remains an open area of research. This has serious implications for the decadal prediction of ISM. While the Pacific Ocean pathway is robust in the GCMs, they have limitations in simulating the lagged response. Also, the relative roles of tropical and extratropical air-sea interaction over the North Atlantic in driving the Pacific pathway need to be understood through idealized model experiments with the state-of-the-art GCMs.

Adler RF, Huffman GJ, Chang A, et al (2003) The version-2 global precipitation climatology project (GPCP) monthly precipitation analysis (1979-present). J Hydrometeorol 4:. https://doi.org/10.1175/1525-7541(2003)004<1147:TVGPCP>2.0.CO;2

Agnihotri R, Dutta K, Bhushan R, Somayajulu BLK (2002) Evidence for solar forcing on the Indian monsoon during the last millennium. Earth Planet Sci Lett 198:. https://doi.org/10.1016/S0012-821X(02)00530-7

Ahmad A, Li S, Luo F, Gao Y (2022) The unstable connection between Atlantic Multidecadal Oscillation and Indian Summer Monsoon in CESM-LE. Clim Dyn 58:1525–1537. https://doi.org/10.1007/s00382-021-05976-6

Álvarez-García F, Latif M, Biastoch A (2008) On Multidecadal and Quasi-Decadal North Atlantic Variability. J Clim 21:3433–3452. https://doi.org/10.1175/2007JCLI1800.1

Ashok K, Soraisam B, Tejavath CT, Cubasch U (2022) Summer monsoon over northeastern India during the last millennium. International Journal of Climatology 42:. https://doi.org/10.1002/joc.7332

B Ratna S, J Osborn T, Joshi M, et al (2019) Identifying teleconnections and multidecadal variability of East Asian surface temperature during the last millennium in CMIP5 simulations. Climate of the Past 15:. https://doi.org/10.5194/cp-15-1825-2019

Baines PG, Folland CK (2007) Evidence for a rapid global climate shift across the late 1960s. J Clim 20:. https://doi.org/10.1175/JCLI4177.1

Bellomo K, Murphy LN, Cane MA, et al (2018) Historical forcings as main drivers of the Atlantic multidecadal variability in the CESM large ensemble. Clim Dyn 50:3687–3698. https://doi.org/10.1007/S00382-017-3834-3/FIGURES/6

Bellucci A, Mariotti A, Gualdi S (2017) The Role of Forcings in the Twentieth-Century North Atlantic Multidecadal Variability: The 1940–75 North Atlantic Cooling Case Study. J Clim 30:7317–7337. https://doi.org/10.1175/JCLI-D-16-0301.1

Berkelhammer M, Sinha A, Mudelsee M, et al (2010) Persistent multidecadal power of the Indian Summer Monsoon. Earth Planet Sci Lett 290:. https://doi.org/10.1016/j.epsl.2009.12.017

Beverley JD, Woolnough SJ, Baker LH, et al (2019) The northern hemisphere circumglobal teleconnection in a seasonal forecast model and its relationship to European summer forecast skill. Clim Dyn 52:. https://doi.org/10.1007/s00382-018-4371-4

Beverley JD, Woolnough SJ, Baker LH, et al (2021) Dynamical mechanisms linking Indian monsoon precipitation and the circumglobal teleconnection. Clim Dyn 57:2615–2636. https://doi.org/10.1007/s00382-021-05825-6

Bhattacharyya S, Narasimha R (2005) Possible association between Indian monsoon rainfall and solar activity. Geophys Res Lett 32:. https://doi.org/10.1029/2004GL021044

Bjerknes J (1964) Atlantic Air-Sea Interaction. In: Landsberg HE, Van Mieghem JBT-A in G (eds). Elsevier, pp 1–82

Bollasina MA, Ming Y, Ramaswamy V (2011) Anthropogenic aerosols and the weakening of the south asian summer monsoon. Science (1979) 334:. https://doi.org/10.1126/science.1204994

Booth BBB, Dunstone NJ, Halloran PR, et al (2012) Aerosols implicated as a prime driver of twentieth-century North Atlantic climate variability. Nature 2012 484:7393 484:228–232. https://doi.org/10.1038/nature10946

Borah PJ, Venugopal V, Sukhatme J, et al (2020) Indian monsoon derailed by a North Atlantic wavetrain. Science (1979) 370:1335–1338. https://doi.org/10.1126/science.aay6043

Braconnot P, Harrison SP, Kageyama M, et al (2012) Evaluation of climate models using palaeoclimatic data. Nat Clim Chang 2

Branstator G (2002) Circumglobal teleconnections, the jet stream waveguide, and the North Atlantic Oscillation. J Clim 15:. https://doi.org/10.1175/1520-0442(2002)015<1893:CTTJSW>2.0.CO;2

Broccoli AJ, Dahl KA, Stouffer RJ (2006) Response of the ITCZ to Northern Hemisphere cooling. Geophys Res Lett 33:1702. https://doi.org/10.1029/2005GL024546

Burns SJ, Fleitmann D, Mudelsee M, et al (2002) A 780-year annually resolved record of Indian Ocean monsoon precipitation from a speleothem from south Oman. Journal of Geophysical Research: Atmospheres 107:. https://doi.org/10.1029/2001JD001281

Cane MA, Clement AC, Murphy LN, Bellomo K (2017) Low-Pass Filtering, Heat Flux, and Atlantic Multidecadal Variability. J Clim 30:7529–7553. https://doi.org/10.1175/JCLI-D-16-0810.1

Cen S, Chen W, Chen S, et al (2020) Potential impact of atmospheric heating over East Europe on the zonal shift in the South Asian high: the role of the Silk Road teleconnection. Sci Rep 10:1–10. https://doi.org/10.1038/s41598-020-63364-2

Chang CP, Harr P, Ju J (2001) Possible roles of atlantic circulation on the weakening Indian monsoon rainfall-ENSO relationship. J Clim 14:2376–2380. https://doi.org/10.1175/1520-0442(2001)014<2376:PROACO>2.0.CO;2

Clement A, Bellomo K, Murphy LN, et al (2015) The Atlantic Multidecadal Oscillation without a role for ocean circulation. Science (1979) 350:320–324. https://doi.org/10.1126/SCIENCE.AAB3980/SUPPL_FILE/AAB3980-CLEMENT-SM.PDF

Compo GP, Whitaker JS, Sardeshmukh PD, et al (2011) The Twentieth Century Reanalysis Project. Quarterly Journal of the Royal Meteorological Society 137

Dai A (2006) Precipitation characteristics in eighteen coupled climate models. J Clim 19:. https://doi.org/10.1175/JCLI3884.1

Danabasoglu G, Yeager SG, Kwon YO, et al (2012) Variability of the Atlantic Meridional Overturning Circulation in CCSM4. J Clim 25:5153–5172. https://doi.org/10.1175/JCLI-D-11-00463.1

Delworth TL, Mann ME (2000) Observed and simulated multidecadal variability in the Northern Hemisphere. Clim Dyn 16:. https://doi.org/10.1007/s003820000075

Deser C, Alexander MA, Xie SP, Phillips AS (2010) Sea surface temperature variability: Patterns and mechanisms. Ann Rev Mar Sci 2:. https://doi.org/10.1146/annurev-marine-120408-151453

Dijkstra HA, Te Raa L, Schmeits M, Gerrits J (2006) On the physics of the Atlantic Multidecadal Oscillation. Ocean Dyn 56:36–50. https://doi.org/10.1007/S10236-005-0043-0/FIGURES/12

Ding Q, Wang B (2005) Circumglobal teleconnection in the Northern Hemisphere summer. J Clim 18:3483–3505. https://doi.org/10.1175/JCLI3473.1

Ding Q, Wang B (2007) Intraseasonal teleconnection between the summer Eurasian wave train and the Indian Monsoon. J Clim 20:3751–3767. https://doi.org/10.1175/JCLI4221.1

Dong B, Sutton RT, Scaife AA (2006) Multidecadal modulation of El Niño–Southern Oscillation (ENSO) variance by Atlantic Ocean sea surface temperatures. Geophys Res Lett 33:8705. https://doi.org/10.1029/2006GL025766

Duchon CE (1979) Lanczos Filtering in One and Two Dimensions. Journal of applied meteorology 18:1016–1022. https://doi.org/10.1175/1520-0450(1979)018<1016:LFIOAT>2.0.CO;2

Dutta A, Neena JM (2022) Exploring the circum-global teleconnection—Indian summer monsoon interactions in the interannual and multidecadal timescales. Front Earth Sci (Lausanne) 10:1897. https://doi.org/10.3389/FEART.2022.973468/BIBTEX

Enfield DB, Mestas-Nuñez AM, Trimble PJ (2001) The Atlantic multidecadal oscillation and its relation to rainfall and river flows in the continental U.S. Geophys Res Lett 28:. https://doi.org/10.1029/2000GL012745

Enomoto T, Hoskins BJ, Matsuda Y (2003) The formation mechanism of the Bonin high in August. Quarterly Journal of the Royal Meteorological Society 129:. https://doi.org/10.1256/qj.01.211

Fadnavis S, Müller R, Chakraborty T, et al (2021) The role of tropical volcanic eruptions in exacerbating Indian droughts. Scientific Reports 2021 11:1 11:1–13. https://doi.org/10.1038/s41598-021-81566-0

Fan M, Schneider EK (2012) Observed decadal North Atlantic tripole SST variability. Part I: Weather noise forcing and coupled response. J Atmos Sci 69:35–50. https://doi.org/10.1175/JAS-D-11-018.1

Fang M, Li X, Chen HW, Chen D (2022) Arctic amplification modulated by Atlantic Multidecadal Oscillation and greenhouse forcing on multidecadal to century scales. Nature Communications 2022 13:1 13:1–8. https://doi.org/10.1038/s41467-022-29523-x

Feldstein SB (2000) The Timescale, Power Spectra, and Climate Noise Properties of Teleconnection Patterns. J Clim 13:4430–4440. https://doi.org/10.1175/1520-0442(2000)013

Feng S, Hu Q (2008) How the North Atlantic Multidecadal Oscillation may have influenced the Indian summer monsoon during the past two millennia. Geophys Res Lett 35:1–5. https://doi.org/10.1029/2007GL032484

Feudale L, Kucharski F (2013) A common mode of variability of African and Indian monsoon rainfall at decadal timescale. Clim Dyn 41:. https://doi.org/10.1007/s00382-013-1827-4

Folland CK, Knight J, Linderholm HW, et al (2009) The summer North Atlantic oscillation: Past, present, and future. J Clim 22:1082–1103. https://doi.org/10.1175/2008JCLI2459.1

Folland CK, Palmer TN, Parker DE (1986) Sahel rainfall and worldwide sea temperatures, 1901–85. Nature 1986 320:6063 320:602–607. https://doi.org/10.1038/320602a0

Frierson DMW, Hwang YT (2012) Extratropical Influence on ITCZ Shifts in Slab Ocean Simulations of Global Warming. J Clim 25:720–733. https://doi.org/10.1175/JCLI-D-11-00116.1

Gadgil S, Gadgil S (2006) The Indian monsoon, GDP and agriculture. Econ Polit Wkly

Gao M, Yang J, Gong D, et al (2019) Footprints of Atlantic multidecadal oscillation in the low-frequency variation of extreme high temperature in the Northern Hemisphere. J Clim 32:791–802. https://doi.org/10.1175/JCLI-D-18-0446.1

Gill AE (1980) Some simple solutions for heat-induced tropical circulation. Quarterly Journal of the Royal Meteorological Society 106:. https://doi.org/10.1002/qj.49710644905

Gong Z, Sun C, Li J, et al (2020) An inter-basin teleconnection from the North Atlantic to the subarctic North Pacific at multidecadal time scales. Clim Dyn 54:. https://doi.org/10.1007/s00382-019-05031-5

Goswami BN (2006) The Asian monsoon: Interdecadal variability. In: The Asian Monsoon. Springer Berlin Heidelberg, Berlin, Heidelberg, pp 295–327

Goswami BN, Chakraborty D, Rajesh P V., Mitra A (2022) Predictability of South-Asian monsoon rainfall beyond the legacy of Tropical Ocean Global Atmosphere program (TOGA). npj Climate and Atmospheric Science 2022 5:1 5:1–12. https://doi.org/10.1038/s41612-022-00281-3

Goswami BN, Kripalani RH, Borgaonkar HP, Preethi B (2016) Multi-Decadal Variability in Indian Summer Monsoon Rainfall Using Proxy Data. In: World Scientific Series on Asia-Pacific Weather and Climate

Goswami BN, Madhusoodanan MS, Neema CP, Sengupta D (2006) A physical mechanism for North Atlantic SST influence on the Indian summer monsoon. Geophys Res Lett 33:1–4. https://doi.org/10.1029/2005GL024803

Goswami BN, Xavier PK (2005) ENSO control on the south Asian monsoon through the length of the rainy season. Geophys Res Lett 32:. https://doi.org/10.1029/2005GL023216

Gray ST, Graumlich LJ, Betancourt JL, Pederson GT (2004) A tree-ring based reconstruction of the Atlantic Multidecadal Oscillation since 1567 A.D. Geophys Res Lett 31:. https://doi.org/10.1029/2004GL019932

Han Z, Luo F, Li S, et al (2016) Simulation by CMIP5 models of the atlantic multidecadal oscillation and its climate impacts. Adv Atmos Sci 33:. https://doi.org/10.1007/s00376-016-5270-4

Harris I, Osborn TJ, Jones P, Lister D (2020) Version 4 of the CRU TS monthly high-resolution gridded multivariate climate dataset. Sci Data 7:. https://doi.org/10.1038/s41597-020-0453-3

He S, Gao Y, Furevik T, et al (2018) Teleconnection between sea ice in the Barents Sea in June and the Silk Road, Pacific–Japan and East Asian rainfall patterns in August. Adv Atmos Sci 35:. https://doi.org/10.1007/s00376-017-7029-y

He S, Wang H, Li F, et al (2020) Solar-wind-magnetosphere energy influences the interannual variability of the northern-hemispheric winter climate. Natl Sci Rev 7:. https://doi.org/10.1093/nsr/nwz082

Hermanson L, Eade R, Robinson NH, et al (2014) Forecast cooling of the Atlantic subpolar gyre and associated impacts. Geophys Res Lett 41:5167–5174. https://doi.org/10.1002/2014GL060420

Hirahara S, Ishii M, Fukuda Y (2014) Centennial-scale sea surface temperature analysis and its uncertainty. J Clim 27:. https://doi.org/10.1175/JCLI-D-12-00837.1

Huang B, Banzon VF, Freeman E, et al (2015) Extended reconstructed sea surface temperature version 4 (ERSST.v4). Part I: Upgrades and intercomparisons. J Clim 28:. https://doi.org/10.1175/JCLI-D-14-00006.1

Huang X, Zhou T, Turner A, et al (2020) The recent decline and recovery of Indian summer monsoon rainfall: Relative roles of external forcing and internal variability. J Clim 33:. https://doi.org/10.1175/JCLI-D-19-0833.1

Hurrell JW, Kushnir Y, Ottersen G, Visbeck M (2003) An overview of the north atlantic oscillation. In: Geophysical Monograph Series

Johnson ZF, Chikamoto Y, Wang SYS, et al (2020) Pacific decadal oscillation remotely forced by the equatorial Pacific and the Atlantic Oceans. Clim Dyn 55:. https://doi.org/10.1007/s00382-020-05295-2

Joshi MK, Ha KJ (2019) Fidelity of CMIP5-simulated teleconnection between Atlantic multidecadal oscillation and Indian summer monsoon rainfall. Clim Dyn 52:. https://doi.org/10.1007/s00382-018-4376-z

Joshi MK, Kucharski F (2017) Impact of Interdecadal Pacific Oscillation on Indian summer monsoon rainfall: an assessment from CMIP5 climate models. Clim Dyn 48:. https://doi.org/10.1007/s00382-016-3210-8

Joshi MK, Pandey AC (2011) Trend and spectral analysis of rainfall over India during 1901-2000. Journal of Geophysical Research Atmospheres 116:. https://doi.org/10.1029/2010JD014966

Joshi MK, Rai A (2015) Combined interplay of the Atlantic multidecadal oscillation and the interdecadal Pacific oscillation on rainfall and its extremes over Indian subcontinent. Clim Dyn 44:. https://doi.org/10.1007/s00382-014-2333-z

Joshi MK, Rai A, Kulkarni A (2022) Global-scale interdecadal variability a skillful predictor at decadal-to-multidecadal timescales for Sahelian and Indian Monsoon Rainfall. NPJ Clim Atmos Sci 5:. https://doi.org/10.1038/s41612-021-00227-1

Kalnay E, Kanamitsu M, Kistler R, et al (1996) The NCEP/NCAR 40-year reanalysis project. Bull Am Meteorol Soc 77:. https://doi.org/10.1175/1520-0477(1996)077<0437:TNYRP>2.0.CO;2

Kang SM, Held IM, Frierson DMW, Zhao M (2008) The Response of the ITCZ to Extratropical Thermal Forcing: Idealized Slab-Ocean Experiments with a GCM. J Clim 21:3521–3532. https://doi.org/10.1175/2007JCLI2146.1

Katzenberger A, Schewe J, Pongratz J, Levermann A (2021) Robust increase of Indian monsoon rainfall and its variability under future warming in CMIP6 models. Earth Syst Dynam 12:367–386. https://doi.org/10.5194/esd-12-367-2021

Knight JR, Allan RJ, Folland CK, et al (2005) A signature of persistent natural thermohaline circulation cycles in observed climate. Geophys Res Lett 32:1–4. https://doi.org/10.1029/2005GL024233

Knight JR, Folland CK, Scaife AA (2006) Climate impacts of the Atlantic Multidecadal Oscillation. Geophys Res Lett 33:17706. https://doi.org/10.1029/2006GL026242

Knudsen MF, Jacobsen BH, Seidenkrantz MS, Olsen J (2014) Evidence for external forcing of the Atlantic Multidecadal Oscillation since termination of the Little Ice Age. Nature Communications 2014 5:1 5:1–8. https://doi.org/10.1038/ncomms4323

Kobayashi S, Ota Y, Harada Y, et al (2015) The JRA-55 reanalysis: General specifications and basic characteristics. Journal of the Meteorological Society of Japan 93:. https://doi.org/10.2151/jmsj.2015-001

Kosaka Y, Nakamura H, Watanabe M, Kimoto M (2009) Analysis on the dynamics of a wave-like teleconnection pattern along the summertime Asian jet based on a reanalysis dataset and climate model simulations. Journal of the Meteorological Society of Japan 87:561–580. https://doi.org/10.2151/jmsj.87.561

Kripalani RH, Kulkarni A, Singh S V. (1997) Association of the Indian summer monsoon with the northern hemisphere mid-latitude circulation. International Journal of Climatology 17:. https://doi.org/10.1002/(SICI)1097-0088(199708)17:10<1055::AID-JOC180>3.0.CO;2-3

Krishnamurthy L, Krishnamurthy V (2014) Influence of PDO on South Asian summer monsoon and monsoon-ENSO relation. Clim Dyn 42:. https://doi.org/10.1007/s00382-013-1856-z

Krishnamurthy L, Krishnamurthy V (2016) Teleconnections of Indian monsoon rainfall with AMO and Atlantic tripole. Clim Dyn 46:2269–2285. https://doi.org/10.1007/s00382-015-2701-3

Krishnamurthy V, Goswami BN (2000) Indian monsoon-ENSO relationship on interdecadal timescale. J Clim 13:. https://doi.org/10.1175/1520-0442(2000)013<0579:IMEROI>2.0.CO;2

Krishnan R, Kumar V, Sugi M, Yoshimura J (2009) Internal feedbacks from monsoon-midlatitude interactions during droughts in the Indian summer monsoon. J Atmos Sci 66:553–578. https://doi.org/10.1175/2008JAS2723.1

Krishnan R, Sugi M (2003) Pacific decadal oscillation and variability of the Indian summer monsoon rainfall. Clim Dyn 21:. https://doi.org/10.1007/s00382-003-0330-8

Kröger J, Kucharski F (2011) Sensitivity of ENSO characteristics to a new interactive flux correction scheme in a coupled GCM. Clim Dyn 36:119–137. https://doi.org/10.1007/S00382-010-0759-5/FIGURES/14

Kucharski F, Ikram F, Molteni F, et al (2016a) Atlantic forcing of Pacific decadal variability. Clim Dyn 46:2337–2351. https://doi.org/10.1007/s00382-015-2705-z

Kucharski F, Molteni F, King MP, et al (2013) On the Need of Intermediate Complexity General Circulation Models: A “SPEEDY” Example. Bull Am Meteorol Soc 94:25–30. https://doi.org/10.1175/BAMS-D-11-00238.1

Kucharski F, Parvin A, Rodriguez-Fonseca B, et al (2016b) The teleconnection of the tropical Atlantic to Indo-Pacific sea surface temperatures on inter-annual to centennial time scales: A review of recent findings. Atmosphere (Basel) 7:1–20. https://doi.org/10.3390/atmos7020029

Kushnir Y, Robinson WA, Bladé I, et al (2002) Atmospheric GCM response to extratropical SST anomalies: Synthesis and evaluation. J Clim 15:. https://doi.org/10.1175/1520-0442(2002)015<2233:AGRTES>2.0.CO;2

Li S, Perlwitz J, Quan X, Hoerling MP (2008) Modelling the influence of North Atlantic multidecadal warmth on the Indian summer rainfall. Geophys Res Lett 35:1–6. https://doi.org/10.1029/2007GL032901

Lin JS, Wu B, Zhou TJ (2016) Is the interdecadal circumglobal teleconnection pattern excited by the Atlantic multidecadal Oscillation? Atmospheric and Oceanic Science Letters 9:451–457. https://doi.org/10.1080/16742834.2016.1233800

Lin P, Yu Z, Lü J, et al (2019) Two regimes of Atlantic multidecadal oscillation: cross-basin dependent or Atlantic-intrinsic. Sci Bull (Beijing) 64:. https://doi.org/10.1016/j.scib.2018.12.027

Liu Z, Alexander M (2007) Atmospheric bridge, oceanic tunnel, and global climatic teleconnections. Reviews of Geophysics 45:1–34. https://doi.org/10.1029/2005RG000172

Lu R, Dong B, Ding H (2006) Impact of the Atlantic Multidecadal Oscillation on the Asian summer monsoon. Geophys Res Lett 33:. https://doi.org/10.1029/2006GL027655

Lu RY, Oh JH, Kim BJ (2002) A teleconnection pattern in upper-level meridional wind over the North African and Eurasian continent in summer. Tellus, Series A: Dynamic Meteorology and Oceanography 54:44–55. https://doi.org/10.1034/j.1600-0870.2002.00248.x

Luo F, Li S, Furevik T (2011) The connection between the Atlantic Multidecadal Oscillation and the Indian Summer Monsoon in Bergen Climate Model Version 2.0. Journal of Geophysical Research Atmospheres 116:1–9. https://doi.org/10.1029/2011JD015848

Luo F, Li S, Gao Y, et al (2018a) The connection between the Atlantic multidecadal oscillation and the Indian summer monsoon in CMIP5 models. Clim Dyn 51:3023–3039. https://doi.org/10.1007/s00382-017-4062-6

Luo F, Li S, Gao Y, et al (2018b) The connection between the Atlantic Multidecadal Oscillation and the Indian Summer Monsoon since the Industrial Revolution is intrinsic to the climate system. Environmental Research Letters 13:. https://doi.org/10.1088/1748-9326/aade11

Luo FF, Li S, Furevik T (2018c) Weaker connection between the Atlantic Multidecadal Oscillation and Indian summer rainfall since the mid-1990s. Atmospheric and Oceanic Science Letters 11:37–43. https://doi.org/10.1080/16742834.2018.1394779

Lyu K, Yu JY (2017) Climate impacts of the Atlantic Multidecadal Oscillation simulated in the CMIP5 models: A re-evaluation based on a revised index. Geophys Res Lett 44:3867–3876. https://doi.org/10.1002/2017GL072681

Madec G (2008) NEMO ocean engine, Technical Note, IPSL

Malik A, Brönnimann S, Stickler A, et al (2017) Decadal to multi-decadal scale variability of Indian summer monsoon rainfall in the coupled ocean-atmosphere-chemistry climate model SOCOL-MPIOM. Clim Dyn 49:3551–3572. https://doi.org/10.1007/s00382-017-3529-9

Mann ME, Steinman BA, Brouillette DJ, et al (2022) On the Estimation of Internal Climate Variability During the Preindustrial Past Millennium. Geophys Res Lett 49:e2021GL096596. https://doi.org/10.1029/2021GL096596

Mann ME, Steinman BA, Miller SK (2020) Absence of internal multidecadal and interdecadal oscillations in climate model simulations. Nature Communications 2020 11:1 11:1–9. https://doi.org/10.1038/s41467-019-13823-w

Mann ME, Zhang Z, Rutherford S, et al (2009) Global signatures and dynamical origins of the little ice age and medieval climate anomaly. Science (1979) 326:1256–1260. https://doi.org/10.1126/SCIENCE.1177303/SUPPL_FILE/MULTIPROXYSPATIAL09.ZIP

Mantua NJ, Hare SR, Zhang Y, et al (1997) A Pacific Interdecadal Climate Oscillation with Impacts on Salmon Production. Bull Am Meteorol Soc 78:. https://doi.org/10.1175/1520-0477(1997)078<1069:APICOW>2.0.CO;2

Menon A, Levermann A, Schewe J, et al (2013) Consistent increase in Indian monsoon rainfall and its variability across CMIP-5 models. Earth System Dynamics 4:287–300. https://doi.org/10.5194/esd-4-287-2013

Mohtadi M, Prange M, Steinke S (2016) Palaeoclimatic insights into forcing and response of monsoon rainfall. Nature 2016 533:7602 533:191–199. https://doi.org/10.1038/nature17450

Monerie PA, Robson J, Dong B, et al (2019) Effect of the Atlantic Multidecadal Variability on the Global Monsoon. Geophys Res Lett 46:. https://doi.org/10.1029/2018GL080903

Mooley DA, Parthasarathy B (1984) Fluctuations in All-India summer monsoon rainfall during 1871-1978. Clim Change 6:. https://doi.org/10.1007/BF00142477

Msadek R, Delworth TL, Rosati A, et al (2014) Predicting a Decadal Shift in North Atlantic Climate Variability Using the GFDL Forecast System. J Clim 27:6472–6496. https://doi.org/10.1175/JCLI-D-13-00476.1

Msadek R, Frankignoul C, Li LZX (2011) Mechanisms of the atmospheric response to North Atlantic multidecadal variability: A model study. Clim Dyn 36:. https://doi.org/10.1007/s00382-010-0958-0

Naidu PD, Ganeshram R, Bollasina MA, et al (2020) Coherent response of the Indian Monsoon Rainfall to Atlantic Multi-decadal Variability over the last 2000 years. Sci Rep 10:. https://doi.org/10.1038/s41598-020-58265-3

Nguyen H, Evans A, Lucas C, et al (2013) The Hadley Circulation in Reanalyses: Climatology, Variability, and Change. J Clim 26:3357–3376. https://doi.org/10.1175/JCLI-D-12-00224.1

Okumura YM, Deser C, Hu A, et al (2009) North Pacific climate response to freshwater forcing in the subarctic North Atlantic: Oceanic and atmospheric pathways. J Clim 22:. https://doi.org/10.1175/2008JCLI2511.1

Otterå OH, Bentsen M, Drange H, Suo L (2010) External forcing as a metronome for Atlantic multidecadal variability. Nature Geoscience 2010 3:10 3:688–694. https://doi.org/10.1038/ngeo955

Parker D, Folland C, Scaife A, et al (2007) Decadal to multidecadal variability and the climate change background. Journal of Geophysical Research Atmospheres 112:1–18. https://doi.org/10.1029/2007JD008411

Parthasarathy B, Kumar KR, Munot AA (1993) Homogeneous Indian Monsoon rainfall: Variability and prediction. Proceedings of the Indian Academy of Sciences - Earth and Planetary Sciences 102:121–155. https://doi.org/10.1007/BF02839187/METRICS

Parthasarathy B, Munot AA, Kothawale DR (1994) All-India monthly and seasonal rainfall series: 1871-1993. Theor Appl Climatol 49:217–224. https://doi.org/10.1007/BF00867461/METRICS

Parzen E (1962) On Estimation of a Probability Density Function and Mode. The Annals of Mathematical Statistics 33:. https://doi.org/10.1214/aoms/1177704472

Peings Y, Magnusdottir G (2014) Forcing of the wintertime atmospheric circulation by the multidecadal fluctuations of the North Atlantic ocean. Environmental Research Letters 9:. https://doi.org/10.1088/1748-9326/9/3/034018

Peings Y, Simpkins G, Magnusdottir G (2016) Multidecadal fluctuations of the North Atlantic Ocean and feedback on the winter climate in CMIP5 control simulations. Journal of Geophysical Research: Atmospheres 121:2571–2592. https://doi.org/10.1002/2015JD024107

Rajesh P V., Goswami BN (2020) Four-dimensional structure and sub-seasonal regulation of the Indian summer monsoon multi-decadal mode. Clim Dyn 55:2645–2666. https://doi.org/10.1007/S00382-020-05407-Y/FIGURES/14

Ratna SB, Osborn TJ, Joshi M, et al (2019) Identifying teleconnections and multidecadal variability of East Asian surface temperature during the last millennium in CMIP5 simulations. Climate of the Past 15:1825–1844. https://doi.org/10.5194/cp-15-1825-2019

Ratna SB, Osborn TJ, Joshi M, Luterbacher J (2020) The influence of atlantic variability on asian summer climate is sensitive to the pattern of the sea surface temperature anomaly. J Clim 33:. https://doi.org/10.1175/JCLI-D-20-0039.1

Rayner NA, Parker DE, Horton EB, et al (2003) Global analyses of sea surface temperature, sea ice, and night marine air temperature since the late nineteenth century. Journal of Geophysical Research: Atmospheres 108:. https://doi.org/10.1029/2002jd002670

Rodwell MJ, Hoskins BJ (1996) Monsoons and the dynamics of deserts. Quarterly Journal of the Royal Meteorological Society 122:1385–1404. https://doi.org/10.1256/smsqj.53407

Rosenblatt M (1956) Remarks on Some Nonparametric Estimates of a Density Function. The Annals of Mathematical Statistics 27:. https://doi.org/10.1214/aoms/1177728190

Roy I, Kripalani RH (2019a) The role of natural factors (part 2): Indian summer monsoon in climate change period—observation and CMIP5 models. Theor Appl Climatol. https://doi.org/10.1007/s00704-019-02864-2

Sabeerali CT, Ajayamohan RS, Bangalath HK, Chen N (2019) Atlantic Zonal Mode: An Emerging Source of Indian Summer Monsoon Variability in a Warming World. Geophys Res Lett 46:. https://doi.org/10.1029/2019GL082379

Sabeerali CT, Rao SA, Dhakate AR, et al (2015) Why ensemble mean projection of south Asian monsoon rainfall by CMIP5 models is not reliable? Clim Dyn 45:. https://doi.org/10.1007/s00382-014-2269-3

Saeed S, Müller WA, Hagemann S, Jacob D (2011) Circumglobal wave train and the summer monsoon over northwestern India and Pakistan: The explicit role of the surface heat low. Clim Dyn 37:. https://doi.org/10.1007/s00382-010-0888-x

Saeed S, Van Lipzig N, Müller WA, et al (2014) Influence of the circumglobal wave-train on European summer precipitation. Clim Dyn 43:503–515. https://doi.org/10.1007/S00382-013-1871-0/FIGURES/12

Sandeep N, Swapna P, Krishnan R, et al (2022) On the weakening association between South Asian Monsoon and Atlantic Multidecadal Oscillation. Clim Dyn. https://doi.org/10.1007/s00382-022-06224-1

Sankar S, Svendsen L, Gokulapalan B, et al (2016) The relationship between Indian summer monsoon rainfall and Atlantic multidecadal variability over the last 500 years. Tellus, Series A: Dynamic Meteorology and Oceanography 68:. https://doi.org/10.3402/tellusa.v68.31717

Sato N, Takahashi M (2006) Dynamical processes related to the appearance of quasi-stationary waves on the subtropical jet in the midsummer northern hemisphere. J Clim 19:. https://doi.org/10.1175/JCLI3697.1

Schlesinger ME, Ramankutty N (1994) An oscillation in the global climate system of period 65–70 years. Nature 367:723–726. https://doi.org/10.1038/367723a0

Schmidt GA, Jungclaus JH, Ammann CM, et al (2012) Climate forcing reconstructions for use in PMIP simulations of the Last Millennium (v1.1). Geosci Model Dev 5:185–191. https://doi.org/10.5194/gmd-5-185-2012

Sengupta A, Rajeevan M (2013) Uncertainty quantification and reliability analysis of CMIP5 projections for the Indian summer monsoon. Curr Sci 105:1692–1703

Seth A, Giannini A, Rojas M, et al (2019) Monsoon Responses to Climate Changes—Connecting Past, Present and Future. Current Climate Change Reports 2019 5:2 5:63–79. https://doi.org/10.1007/S40641-019-00125-Y

Shanahan TM, Overpeck JT, Anchukaitis KJ, et al (2009) Atlantic forcing of persistent drought in West Africa. Science (1979) 324:377–380. https://doi.org/10.1126/SCIENCE.1166352/SUPPL_FILE/SHANAHAN.SOM.PDF

Sinha A, Berkelhammer M, Stott L, et al (2011) The leading mode of Indian Summer Monsoon precipitation variability during the last millennium. Geophys Res Lett 38:. https://doi.org/10.1029/2011GL047713

Sinha A, Cannariato KG, Stott LD, et al (2007) A 900-year (600 to 1500 A.D.) record of the Indian summer monsoon precipitation from the core monsoon zone of India. Geophys Res Lett 34:. https://doi.org/10.1029/2007GL030431

Son JH, Seo KH, Son SW, Cha DH (2021) How Does Indian Monsoon Regulate the Northern Hemisphere Stationary Wave Pattern? Front Earth Sci (Lausanne) 8:1–10. https://doi.org/10.3389/feart.2020.599745

Srivastava AK, Rajeevan M, Kulkarni R (2002) Teleconnection of OLR and SST anomalies over Atlantic Ocean with Indian summer monsoon. Geophys Res Lett 29:125-1-125–4. https://doi.org/10.1029/2001gl013837

Stephan CC, Klingaman NP, Turner AG (2019) A mechanism for the recently increased interdecadal variability of the silk road pattern. J Clim 32:717–736. https://doi.org/10.1175/JCLI-D-18-0405.1

Sun C, Kucharski F, Li J, et al (2017) Western tropical Pacific multidecadal variability forced by the Atlantic multidecadal oscillation. Nat Commun 8:1–10. https://doi.org/10.1038/ncomms15998

Sun C, Li J, Kucharski F, et al (2019) Recent Acceleration of Arabian Sea Warming Induced by the Atlantic-Western Pacific Trans-basin Multidecadal Variability. Geophys Res Lett 46:1662–1671. https://doi.org/10.1029/2018GL081175

Sutton RT, Hodson DLR (2007) Climate Response to Basin-Scale Warming and Cooling of the North Atlantic Ocean. J Clim 20:891–907. https://doi.org/10.1175/JCLI4038.1

Sutton RT, Hodson DLR (2005) Ocean science: Atlantic Ocean forcing of North American and European summer climate. Science (1979) 309:. https://doi.org/10.1126/science.1109496

Svendsen L (2021) The Atlantic Multidecadal Oscillation and Indian summer monsoon variability: A revisit. Indian Summer Monsoon Variability: El Niño-Teleconnections and Beyond 353–374. https://doi.org/10.1016/B978-0-12-822402-1.00001-6

Syed FS, Yoo JH, Körnich H, Kucharski F (2012) Extratropical influences on the inter-annual variability of South-Asian monsoon. Clim Dyn 38:1661–1674. https://doi.org/10.1007/S00382-011-1059-4/FIGURES/11

Tejavath CT, Ashok K, Chakraborty S, Ramesh R (2019) A PMIP3 narrative of modulation of ENSO teleconnections to the Indian summer monsoon by background changes in the Last Millennium. Clim Dyn 53:. https://doi.org/10.1007/s00382-019-04718-z

Ting M, Kushnir Y, Seager R, Li C (2011) Robust features of Atlantic multi-decadal variability and its climate impacts. Geophys Res Lett 38:1–6. https://doi.org/10.1029/2011GL048712

Trenberth KE, Shea DJ (2006) Atlantic hurricanes and natural variability in 2005. Geophys Res Lett 33:. https://doi.org/10.1029/2006GL026894

Tung KK, Zhou J (2013) Using data to attribute episodes of warming and cooling in instrumental records. Proc Natl Acad Sci U S A 110:2058–2063. https://doi.org/10.1073/pnas.1212471110

Valcke S (2006) OASIS3 user guide (prism 2-5). PRISM-Support Initiative Report No 3

Vecchi GA, Delworth TL, Booth B (2017) Origins of Atlantic decadal swings. Nature 2017 548:7667 548:284–285. https://doi.org/10.1038/nature23538

Wang J, Yang B, Ljungqvist FC, et al (2017) Internal and external forcing of multidecadal Atlantic climate variability over the past 1,200 years. Nature Geoscience 2017 10:7 10:512–517. https://doi.org/10.1038/ngeo2962

Wang P, Clemens S, Beaufort L, et al (2005) Evolution and variability of the Asian monsoon system: state of the art and outstanding issues. Quat Sci Rev 24:595–629. https://doi.org/10.1016/J.QUASCIREV.2004.10.002

Wang X, Brown PM, Zhang Y, Song L (2011) Imprint of the Atlantic multidecadal oscillation on tree-ring widths in northeastern Asia since 1568. PLoS One 6:. https://doi.org/10.1371/JOURNAL.PONE.0022740

Wang X, Li J, Sun C, Liu T (2017) NAO and its relationship with the Northern Hemisphere mean surface temperature in CMIP5 simulations. J Geophys Res 122:. https://doi.org/10.1002/2016JD025979

Wang X, Lu R, Hong X (2021) Reduction of mid-summer rainfall in northern India after the late-1990s induced by the decadal change of the Silk Road pattern. Environmental Research Letters 16:. https://doi.org/10.1088/1748-9326/ac2cea

Wang Y, Li S, Lu D (2009) Seasonal response of Asian monsoonal climate to the Atlantic Multidecadal Oscillation. Journal of Geophysical Research Atmospheres 114:. https://doi.org/10.1029/2008JD010929

Watanabe M (2004) Asian Jet Waveguide and a Downstream Extension of the North Atlantic Oscillation. J Clim 17:4674–4691. https://doi.org/10.1175/JCLI-3228.1

Watanabe M, Kimoto M (2000) Atmosphere-ocean thermal coupling in the North Atlantic: A positive feedback. Quarterly Journal of the Royal Meteorological Society 126:3343–3369. https://doi.org/10.1002/QJ.49712657017

Watanabe T, Yamazaki K (2014) The upper-level circulation anomaly over Central Asia and its relationship to the Asian monsoon and mid-latitude wave train in early summer. Clim Dyn 42:2477–2489. https://doi.org/10.1007/s00382-013-1888-4

Webster PJ, Yang S (1992) Monsoon and Enso: Selectively Interactive Systems. Quarterly Journal of the Royal Meteorological Society 118:. https://doi.org/10.1002/qj.49711850705

Welch P (1967) The use of fast Fourier transform for the estimation of power spectra: A method based on time averaging over short, modified periodograms. IEEE Transactions on Audio and Electroacoustics 15:70–73. https://doi.org/10.1109/TAU.1967.1161901

Wills RCJ, Armour KC, Battisti DS, Hartmann DL (2019) Ocean–Atmosphere Dynamical Coupling Fundamental to the Atlantic Multidecadal Oscillation. J Clim 32:251–272. https://doi.org/10.1175/JCLI-D-18-0269.1

Wu B, Lin J, Zhou T (2016) Interdecadal circumglobal teleconnection pattern during boreal summer. Atmospheric Science Letters 17:446–452. https://doi.org/10.1002/asl.677

Wu B, Zhou T, Li C, et al (2019) Improved decadal prediction of Northern-Hemisphere summer land temperature. Clim Dyn 53:. https://doi.org/10.1007/s00382-019-04658-8

Wu L, Liu Z (2005) North Atlantic decadal variability: Air-sea coupling, oceanic memory, and potential Northern Hemisphere resonance. J Clim 18:. https://doi.org/10.1175/JCLI-3264.1

Xavier PK, Marzin C, Goswami BN (2007) An objective definition of the Indian summer monsoon season and a new perspective on the ENSO-monsoon relationship. Quarterly Journal of the Royal Meteorological Society 133:. https://doi.org/10.1002/qj.45

Yang YM, An S Il, Wang B, Park JH (2020) A global-scale multidecadal variability driven by Atlantic multidecadal oscillation. Natl Sci Rev 7:. https://doi.org/10.1093/nsr/nwz216

Yasui S, Watanabe M (2010) Forcing processes of the summertime circumglobal teleconnection pattern in a dry AGCM. J Clim 23:. https://doi.org/10.1175/2009JCLI3323.1

Yeager SG, Robson JI (2017) Recent Progress in Understanding and Predicting Atlantic Decadal Climate Variability. Curr Clim Change Rep 3:112–127. https://doi.org/10.1007/S40641-017-0064-Z/FIGURES/1

Yeh SW, Wang X, Wang C, Dewitte B (2015) On the relationship between the North Pacific climate variability and the central Pacific El Niño. J Clim 28:. https://doi.org/10.1175/JCLI-D-14-00137.1

Zhang R (2017) On the persistence and coherence of subpolar sea surface temperature and salinity anomalies associated with the Atlantic multidecadal variability. Geophys Res Lett 44:7865–7875. https://doi.org/10.1002/2017GL074342

Zhang R, Delworth TL (2007) Impact of the Atlantic Multidecadal Oscillation on North Pacific climate variability. Geophys Res Lett 34:2–7. https://doi.org/10.1029/2007GL031601

Zhang R, Delworth TL (2006) Impact of Atlantic multidecadal oscillations on India/Sahel rainfall and Atlantic hurricanes. Geophys Res Lett 33:. https://doi.org/10.1029/2006GL026267

Zhang R, Sutton R, Danabasoglu G, et al (2019) A Review of the Role of the Atlantic Meridional Overturning Circulation in Atlantic Multidecadal Variability and Associated Climate Impacts. Reviews of Geophysics 57

Zhou T, Brönnimann S, Griesser T, et al (2010) A reconstructed dynamic Indian monsoon index extended back to 1880. Clim Dyn 34:. https://doi.org/10.1007/s00382-009-0552-5

List of publications

1. *Arijeet Dutta* and Neena Joseph Mani," Exploring the circum-global teleconnection–Indian summer monsoon interactions in the interannual and multidecadal timescales." *Frontiers in Earth Science*: 1897. https://doi.org/10.3389/feart.2022.973468

2. *Arijeet Dutta*, Rahul Sivankutty and Neena Joseph Mani," Investigating the Atlantic-monsoon teleconnection pathways in PMIP3 Last Millennium Simulations", 12 March 2023, *PREPRINT* (Version 1) available at Research Square https://doi.org/10.21203/rs.3.rs-2641807/v1 *Under minor revision at Climate Dynamics*

3. *Arijeet Dutta* and Neena Joseph Mani," Possible role of north Atlantic vorticity anomalies in the observed relationship between the Atlantic multi-decadal oscillation and Indian summer monsoon" *In preparation*

4. *Arijeet Dutta* and Neena Joseph Mani," Exploring the role of Pacific Ocean feedbacks in the observed relationship between the Atlantic multi-decadal oscillation and Indian summer monsoon in a simplified coupled GCM" *In preparation*